Field Guides

Fire and water: Volcanology, geomorphology, and hydrogeology of the Cascade Range, central Oregon

Katharine V. Cashman, Natalia I. Deligne, Marshall W. Gannett, Gordon E. Grant and Anne Jefferson

Field Guides 2009;15;539-582
doi: 10.1130/2009.fld015(26)

Notes

The Geological Society of America
Field Guide 15
2009

Fire and water: Volcanology, geomorphology, and hydrogeology of the Cascade Range, central Oregon

Katharine V. Cashman
Natalia I. Deligne
Department of Geological Sciences, University of Oregon, Eugene, Oregon 97403, USA

Marshall W. Gannett
U.S. Geological Survey, Oregon Water Science Center, Portland, Oregon 97201, USA

Gordon E. Grant
Pacific Northwest Research Station, U.S. Department of Agriculture (USDA), Forest Service, Corvallis, Oregon 97331, USA

Anne Jefferson
Department of Geography and Earth Sciences, University of North Carolina at Charlotte, Charlotte, North Carolina 28223, USA

ABSTRACT

This field trip guide explores the interactions among the geologic evolution, hydrology, and fluvial geomorphology of the central Oregon Cascade Range. Key topics include the geologic control of hydrologic regimes on both the wet and dry sides of the Cascade Range crest, groundwater dynamics and interaction between surface and groundwater in young volcanic arcs, and interactions between rivers and lava flows. As we trace the Willamette and McKenzie Rivers back to source springs high in the young volcanic rocks of the Cascade Range, there is abundant evidence for the large permeability of young lava flows, as manifested in streams that dewater into lava flows, lava-dammed lakes in closed basins, and rivers that emerge from single springs. These dynamics contrast sharply with the older, lower permeability Western Cascades terrane and associated runoff-dominated fluvial systems. On the east side of the Cascades we encounter similar hydrologic characteristics resulting in complex interactions between surface water and groundwater as we follow the Deschutes River downstream to its confluence with the Crooked River. Here, deep canyons have cut through most of the permeable part of the geologic section, have been invaded by multiple large intracanyon lava flows, and are the locus of substantial regional groundwater discharge. The groundwater and surface-water interaction in the Deschutes Basin is further complicated by surface-water diversions and an extensive network of leaking irrigation canals. Our west-to-east transect offers an unparalleled opportunity to examine the co-evolution of the geology and hydrology of an active volcanic arc.

Cashman, K.V., Deligne, N.I., Gannett, M.W., Grant, G.E., and Jefferson, A., 2009. Fire and water: Volcanology, geomorphology, and hydrogeology of the Cascade Range, central Oregon, *in* O'Connor, J.E., Dorsey, R.J., and Madin, I.P., eds., Volcanoes to Vineyards: Geologic Field Trips through the Dynamic Landscape of the Pacific Northwest: Geological Society of America Field Guide 15, p. 539–582, doi: 10.1130/2009.fld015(26).

INTRODUCTION AND TRIP OVERVIEW

The Cascade Range of Oregon is the result of ~40 million years of evolution of an active volcanic arc located on the leading edge of a continental plate downwind of an enormous source of moisture—the Pacific Ocean. The focus of our trip will be the interplay among these factors, particularly as expressed in the recent (Quaternary) history and styles of volcanism associated with the convergent plate margin just offshore, the flow paths and volumes of groundwater systems located within the range, and the geomorphic evolution of rivers that have developed on both sides of the Cascade Range crest.

This is very much a "West- and East-side story." The north-trending Cascade Range is perpendicular to the path of the prevailing westerly winds, creating a strong orographic lift and rain shadow effect. Precipitation on the windward western slopes of the Cascades ranges from 2000 to over 4000 mm per year. On the leeward east side, precipitation drops tenfold to around 300 mm per year, resulting in one of the steepest precipitation gradients in the United States. The topography, hydrogeology, vegetation, and landscape evolution reflect this sharp contrast in precipitation and provide a unique natural laboratory for examining both geologic and climatic controls on landscape development.

Our trip will begin in Portland and proceed south through the Willamette Valley toward the headwaters of the Willamette River (Fig. 1). As we travel south on Interstate 5, to the west (right) across the broad valley floor rises the Oregon Coast Range, an uplifted and dissected continental shelf of early Tertiary age. To the east (left), one can see the foothills of the Western Cascades, and, if the day is clear, an occasional glimpse of the large stratovolcanoes along the crest of the High Cascades. Along the way, we will cross several large rivers draining the Coast and Cascade Ranges.

At Eugene, we will turn east and follow the McKenzie River, a major tributary of the Willamette River. The McKenzie River and its tributaries, Lost Creek and White Branch, will lead us to the crest of the Cascade Range at McKenzie Pass. The stops on Day 1 are intended to display aspects of the regional geology, climatology, and landscape history, including the striking contrast between the Western and High Cascades geology, topography and dissection patterns, features and styles of Holocene lava flows, westside Cascade Range spring systems, and various erosional processes, including glacial erosion and mass movements. We will spend the night at the H.J. Andrews Experimental Forest, a National Science Foundation (NSF)–funded Long-Term Ecological Research site, which is surrounded by magnificent old-growth forest.

On the morning of the second day, we will continue along the McKenzie River to its source at Clear Lake, stopping to observe spectacular waterfalls, lava-filled canyons, and dry riverbeds. At Clear Lake, which owes its origin to a lava flow that dammed the river, we will board rowboats for the short crossing to the Great Spring, a high-volume cold spring emanating from the base of a late Holocene lava flow, and discuss different river and lava flow interactions. We will then drive over Santiam Pass, stopping to observe a range of young volcanic structures and styles and another very large spring and river system, the Metolius River.

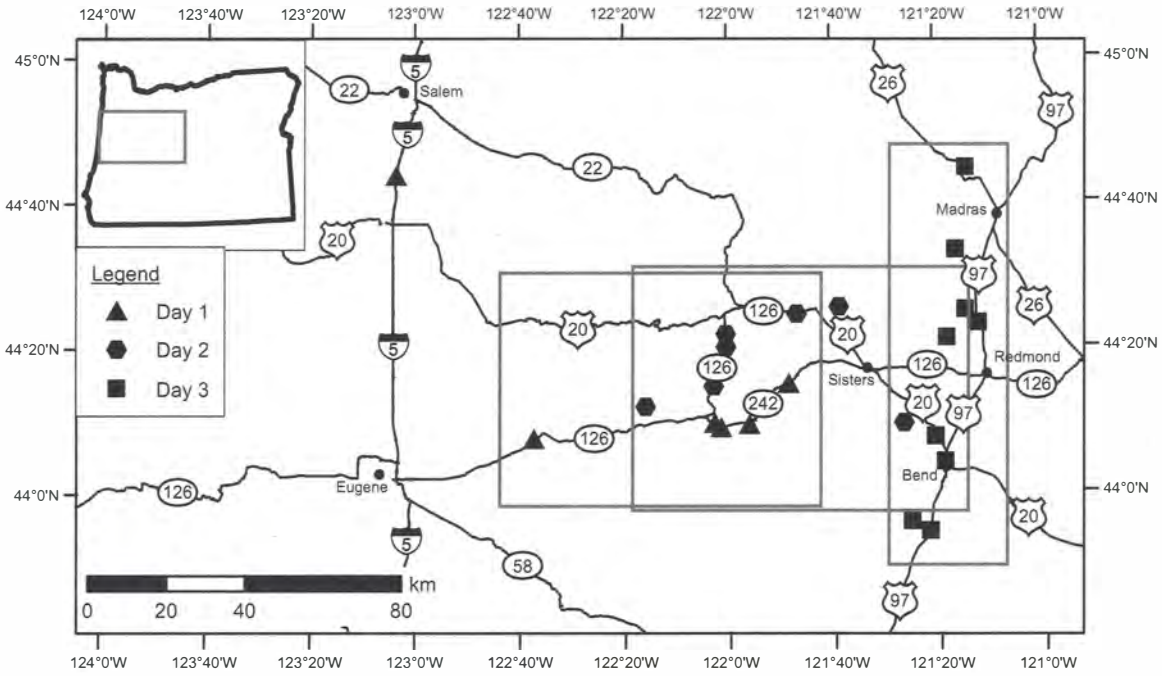

Figure 1. Map of northwestern Oregon showing field trip route and locations of individual stops for each day, plus areas covered by more detailed maps for each day of the field trip.

We will end the day at Bull Flat and Tumalo Dam, with an introduction to the east side story. Overnight will be in Bend, Oregon.

The third and final day of our trip will begin with a focus on lava and river interactions in the vicinity of Lava Butte, a Holocene cinder cone that was the source of lava flows that encroached on, and temporarily dammed, the Deschutes River. We will then travel north along the Deschutes River from Bend, where the river is hundreds of meters above the water table, to Lower Bridge, where the river is at the same elevation as the regional water table, and on to Pelton Dam, where the river has cut entirely through the permeable part of the geologic section and, hence, the regional groundwater flow system. This day will include a hike into the Crooked River canyon to observe the stratigraphy of diverse deposits of the Pliocene Cascade Range (the Deschutes Formation), Pleistocene intracanyon lava flows, and the springs through which the regional groundwater returns to the surface. Along the way we will consider the regional groundwater story in relation to the volcanic history and current issues and conflicts in water management associated with this groundwater system. Finally we will climb out of the Deschutes Basin, cross the Cascades on the lower slopes of Mount Hood, and return to Portland.

The discussion for last stop on the second day, Tumalo Dam, and discussions and figures for most stops on the third day are taken verbatim, or nearly so, from an earlier field trip guide by Dave Sherrod, Marshall Gannett, and Ken Lite (Sherrod et al., 2002).

A Brief Overview of the Geologic and Physiographic Setting of the Cascade Range

The Cascade Range extends from northern California to southern Canada. In central Oregon, the Cascade Range is 50–120 km wide, bounded on the west by the Willamette Valley and on the east by the Deschutes Basin. The Cascade volcanic arc has been active for ~40 million years due to the convergence of the Pacific and Juan de Fuca plates, although volcanism has not been continuous in either space or time throughout this period (Sherrod and Smith, 1990). In Oregon, the Cascade Range is commonly divided into two physiographic subprovinces—the Western Cascades and the High Cascades—which differ markedly in their degree of dissection, owing mainly to the near absence of Quaternary and Pliocene volcanoes in the Western Cascades. From the Three Sisters north to Mount Hood, the young (Quaternary to Pliocene) High Cascades occupy a structural graben formed by a northward-propagating rift (Sherrod et al., 2002), which has affected both the composition of the erupted magma and patterns of groundwater flow.

The Western Cascades are composed of a thick, mixed assemblage of mafic lava flows, mostly of andesitic composition, and ash-flow and ash-fall tuffs, with minor silicic intrusive bodies and stocks, which range in age from middle Eocene to early Pliocene (40–5 million years). Rocks along the western margin of the Western Cascades tend to be older and decrease in age toward the boundary with the High Cascades; some intracanyon lava flows from the High Cascades fill the upper valleys. Rocks have been locally altered by hydrothermal processes, particularly in the contact aureoles surrounding granitic stocks. The landscape has been covered repeatedly by montane glaciers, dissected by rivers, and is prone to frequent mass wasting by landslides, debris flows, and earthflows. Consequently, the topography is extremely rugged, ranging in elevation from 200 to 1800 m, with sharp dissected ridges, and steep slopes of 30° or more. Stream channels range from high-gradient bedrock channels to alluvial gravel to boulder-bed rivers.

In the Western Cascades, outcrops are commonly obscured by dense native coniferous forests of Douglas fir, western hemlock, and western red cedar. Trees in this region can grow to great height (>80 m) and age (>500 yr old) and are subject to episodic wildfires combined with, more recently, intensive logging on both public and private lands. At one point in the 1980s, timber harvested from the Willamette National Forest, which includes much of the Western Cascades, produced more than 20% of the nation's softwood timber. The legacy of this harvest remains in a distinct pattern of regenerating clearcuts of various sizes and shapes. Precipitation of up to 2500 mm/yr typically falls from November through April as both rain (below 400 m) and snow (above 1200 m), with the intervening elevations, which make up much of the landscape, constituting a "transitional snow zone."

Extending along the east margin of the Western Cascades is the modern volcanic arc of the High Cascades, a north-trending belt 30–50 km wide of upper Miocene to Holocene volcanic rocks. In central Oregon, the High Cascades form a broad ridge composed of a 2- to 3-km-thick sequence of lava flows that fill a graben formed in the older rocks (Sherrod and Smith, 1990; Sherrod et al., 2004). High Quaternary stratovolcanoes are constructed on top of the flows; they have rhyolitic to basaltic compositions and are composed of interlayered thin lava flows and pyroclastic deposits overlying cinder cones (Taylor, 1981). The location of the High Cascades at the western margin of the Basin and Range places it in a zone of crustal extension, which influences both its structural features and volcanic history. Most striking is the density of Quaternary volcanoes in the Oregon Cascade Range, with 1054 vents in 9500 km^2 (Hildreth, 2007). In the Sisters reach, which we will traverse, there are at least 466 Quaternary volcanoes, many with a pronounced N-S alignment of vents and most of which are mafic (basalt or basaltic andesite; Hildreth, 2007). Sherrod and Smith (1990) estimate an average mafic magma production rate in the central Oregon Cascades of 3–6 km^3 $m.y.^{-1}$ per linear km of arc during the Quaternary. Mafic activity has continued into post-glacial times, with 290 km^3 of magma erupted from the Cascade Range over the past 15 ka. Hildreth (2007) estimates that 21% of the erupted material forms mafic cones and shields, and that most of these edifices are within the Oregon Cascade Range.

The crest of the Oregon Cascade Range has an average altitude of 1500–2000 m, with several of the high volcanoes exceeding 3000 m. The conical morphology of the stratovolcanoes is best preserved on the younger edifices—Middle Sister, South Sister, and Mount Bachelor—as the older cones have been deeply

eroded by Pleistocene glaciation. The High Cascades has also been extensively and repeatedly glaciated by thick montane ice sheets but is relatively undissected by streams (drainage density is ~1–2 km/km^2; Grant, 1997) and generally preserves many primary volcanic features. Most winter precipitation falls as snow in this zone, with occasional summer thunderstorms contributing to the water budget. Forests east of the crest are a mix of alpine and subalpine firs that transition abruptly into a more open forest of ponderosa and lodgepole pine in response to the abrupt rainfall gradient just east of the crest. Much of the land is in public ownership and managed by the Forest Service and Bureau of Land Management for timber, grazing, and recreation. Of the High Cascades subprovince in central Oregon, 25% is in wilderness areas managed by the U.S. Forest Service. On the east side, the Pleistocene glacial record is better preserved and mapped than the west side, due to the lower rainfall (~300 mm/yr), more subdued topography, and limited opportunity for fluvial erosion (Scott, 1977; Scott and Gardner, 1992; Sherrod et al., 2004).

On the east the Oregon Cascade Range is bounded by the upper Deschutes Basin, a volcanic landscape dominated by a thick (>700 m) sequence of lava flows, pyroclastic and volcaniclastic deposits of Cascade Range origin, and fluvial gravels deposited between ~7 and 4 million years ago in a broad depositional basin (Smith, 1986a). These deposits extend east to uplands consisting of early Tertiary volcanic rocks of the John Day and Clarno Formations. Interspersed throughout are local eruptive centers of a wide variety of sizes, compositions, and eruptive styles. The most prominent eruptive center off the Cascade Range axis is Newberry Volcano, which forms the southeastern boundary of the Deschutes Basin. Lava flows from Newberry blanket a large portion of the central Deschutes Basin, and partially fill canyons of the ancestral Deschutes and Crooked Rivers. The volcanic eruptions that generated the Deschutes Formation culminated with the formation of a downfaulted depression along the axis of the Cascade Range in central Oregon (Allen, 1966; Smith et al., 1987). The Pleistocene deposits in this part of the range are largely restricted to this axial graben.

The basic feature controlling regional groundwater flow on the east side is the pronounced permeability contrast between the early Tertiary units and the Pliocene and younger deposits (Lite and Gannett, 2002). Deposits of the Mio-Pliocene Deschutes Formation are highly permeable and, along with the younger volcanic deposits, host a continuous regional groundwater system that extends from the Cascade Range to the depositional contact with the early Tertiary deposits in the eastern part of the basin. The High Cascades subprovince is the principal source of recharge to this regional aquifer system.

DAY 1. PORTLAND, OREGON TO H.J. ANDREWS EXPERIMENTAL FOREST (BLUE RIVER, OREGON)

Starting in Portland, the trip takes us south through the Willamette Valley to Eugene, before turning eastward into the Cascade Range (Fig. 2). We stop to observe and discuss geologic controls on the hydrologic regimes of the westward flowing tributaries of the Willamette River (Stop 1). We then turn east at Eugene, and drive into the Western Cascades along the McKenzie River, stopping to consider the hydrogeology of the McKenzie (Stop 2). Our lunch stop is at Limberlost Campground (Stop 3), a nice example of a High Cascades stream. We then visit "Lost Spring" (Stop 4), where we discuss the relation between groundwater and lava flows and then continue up the White Branch glaciated valley to the crest of the Cascades at McKenzie Pass (Stop 5), to discuss the volcanic history and dynamics and emplacement features of young lava flows. After the stop at McKenzie Pass, we return to our evening's quarters at the H.J. Andrews Experimental Forest, near Blue River.

In Transit: I-5 Corridor and the Willamette Valley

Heading south from Portland, we traverse the Willamette Valley, part of a broad structural low that extends from the Puget Sound lowland to just south of Eugene and has existed for at least 15 million years (O'Connor et al., 2001b). The valley is a broad alluvial plain, 30–50 km wide, and is flanked by the sedimentary rocks of the Coast Range to the west and the volcanic rocks of the Cascade Range to the east. The valley slopes gently to the north, with elevations ranging from 120 m at Eugene to 20 m at Portland. The hills that the road traverses south of Portland and near Salem represent incursions and faulting of lava flows from the east; the Salem Hills in particular are underlain by Miocene Columbia River Basalt flows that were erupted in eastern Washington and followed the path of the paleo–Columbia River toward the ocean prior to the construction and uplift of the High Cascades.

The Quaternary history of the Willamette Valley has been the subject of geological investigation for over 100 yr. It reflects a dramatic interplay between erosion and deposition from the Willamette River and its tributaries, and backwater flooding and lacustrine deposition from the catastrophic flooding of the Columbia River. As summarized in O'Connor et al. (2001b), the valley is floored and filled with Quaternary gravels brought down by tributaries draining the Cascade Range and, to a lesser extent, the Coast Range. This thick (100+ m) alluvium is capped by a thinner (10+ m) but areally extensive sequence of sand, silt, and clay of late Pleistocene age that was deposited during backflooding of the Willamette Valley by the immense Missoula floods coming down the Columbia River. Multiple episodes of outbreak flooding occurred as glacial Lake Missoula repeatedly filled and failed catastrophically, resulting in rhythmically bedded, fine-grained units draped over the older alluvium, into which the modern Willamette River is now incised. The flat valley floor is thus a constructional surface ~15,000 yr old. The Missoula flood deposits thin to the south and can be traced as far south as just north of Eugene. The total volume of these deposits is ~50 km^3, and the volume of water inundating the Willamette Valley during the largest floods was ~250 km^3, equivalent to 10 yr of the annual flow of the Willamette River at Salem (Jim O'Connor, 2009, oral commun.).

Directions from Portland to Stop 1

Follow Interstate 5 south to Salem. After passing through the Salem Hills we will enter the wide southern portion of the Willamette Valley. The Santiam rest stop is near MP 241; pull in here for a restroom stop and introduction to the Willamette Valley.

Stop 1. Santiam Rest Stop—Willamette Valley Overview

The Santiam River is one of the major west-flowing tributaries of the Willamette River (Fig. 3). Drainage area at the U.S. Geological Survey (USGS) gage (Santiam River at Jefferson) 5.7 km upstream is 4580 km^2; the confluence of the Santiam and the Willamette Rivers is ~8 km downstream from our location.

The pattern of streamflow in the Santiam and the other rivers draining the western margin of the Cascades is one of the story lines of this field trip: the geological control of hydrologic regimes in volcanic landscapes. This characteristic of Cascade streams was generally described by Russell (1905), Meinzer (1927), and Stearns (1929, 1931) but has been the subject of extensive work since then (Ingebritsen et al., 1992, 1994; Grant, 1997; Gannett et al., 2001, 2003; Tague and Grant, 2004; Jefferson et al., 2006, 2007, 2008).

Understanding the role of geology in hydrologic regimes first requires an appreciation of how annual variation in precipitation controls runoff. The first rains of the hydrologic year typically begin in mid- to late October, following a prolonged summer drought of three to four months. Early fall storms must therefore satisfy a pronounced soil deficit before any significant runoff occurs. Once this deficit has been satisfied and soils are hydrologically "wetted up"—a condition that normally occurs by early to mid-November—streamflow becomes more synchronized with precipitation, rising and falling in response to passage of frontal storms from the Pacific. At higher elevations (above ~1200 m), however, precipitation typically falls as snow, building the winter snowpack, so the upper elevations of westward-draining rivers do not normally contribute much to streamflow until the spring melt.

A pattern of repeated rising and falling streamflow during the winter is clearly visible in the hydrograph for the Little North Santiam, one of the tributaries of the Santiam that exclusively drains the Western Cascades landscape (Fig. 4). Some of these rises may be augmented by melting snow during rain; these "rain-on-snow" events are generally responsible for the largest floods in the Willamette Valley, such as occurred in December

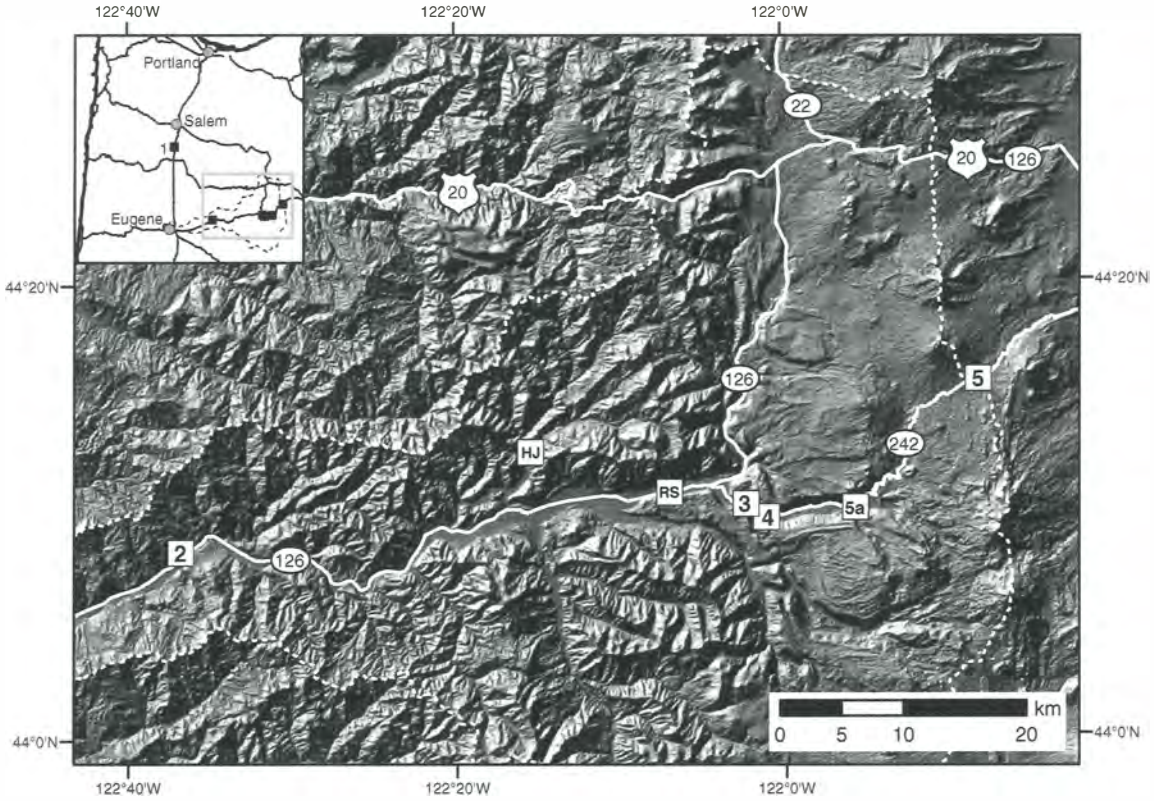

Figure 2. Overview map for Day 1, Stops 2 through 5 (squares). H.J. Andrews Experimental Forest (HJ) and McKenzie River Ranger Station (RS) are also indicated. Shaded relief map created from a 10 m digital elevation model (DEM) shows the striking contrast in morphology of the older, rugged Western Cascades and young High Cascades. The McKenzie River watershed is outlined with a dashed line.

1861, December 1964, and February 1996. As precipitation diminishes in the spring, there is a minor snowmelt rise in late April or May and then a distinct recession into very low flows that typically persist until the first fall rains begin the cycle anew. The steep, deeply dissected landscape and permeable soils of the Western Cascades respond quickly to precipitation recharge and have little storage (Tague and Grant, 2004). For this reason, the overarching pattern of flashy winter responses and very low summer flows is the characteristic signature of rivers draining Western Cascades landscapes.

Contrast this pattern with the hydrograph of the upper McKenzie River, which is located ~50 km southeast, and drains the High Cascades landscape (Fig. 4). This basin receives similar amounts of precipitation to the Little North Santiam, although more winter moisture falls as snow at its higher elevation. This snow-dominated system overlies the permeable volcanic rocks and relatively modest relief of the High Cascades subprovince, resulting in subsurface flow that buffers the hydrograph response. Major increases in streamflow are effectively limited to only the largest winter storms. A significant snowmelt peak occurs in the spring, the summer flow recession is much less pronounced, and high base flows are sustained throughout the summer, supported by discharge from volcanic aquifers (Jefferson et al., 2006).

Larger rivers, such as the Santiam and the Willamette, are hybrids of these two distinct flow regimes and demonstrate streamflow characteristics of the end members described above directly in proportion to the percentage of basin area that is in the High or Western Cascades (Tague and Grant, 2004). These trends are best illustrated by low flow regimes, including absolute flow volume (Fig. 5) and trajectories of longitudinal change in discharge with distance downstream (Fig. 6), which are both directly correlated with percent High Cascades rocks in the basin area. In essence, summer low flows come from young volcanic rocks in the High Cascades and winter peak flows are due

Figure 3. Willamette River Basin, Oregon, showing approximate location of High and Western Cascades subprovince boundary and major west-flowing tributaries. Geology from Walker and MacLeod (1991); figure from Tague and Grant (2004).

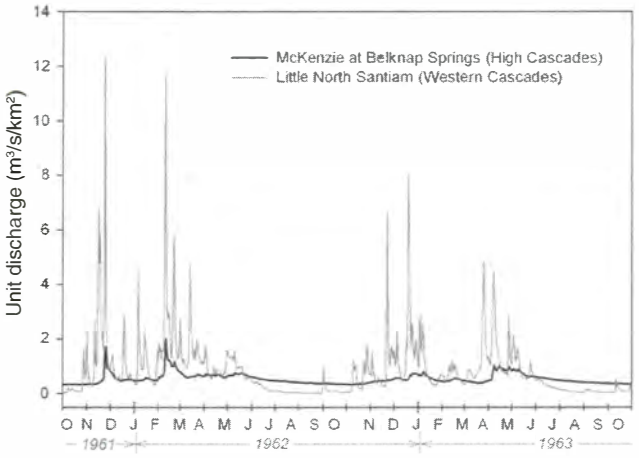

Figure 4. Daily streamflow hydrographs, normalized by drainage area, for a predominantly High Cascades (McKenzie River at Belknap Springs) and Western Cascades (Little North Santiam) river. Discharge data from U.S. Geological Survey streamflow data archive.

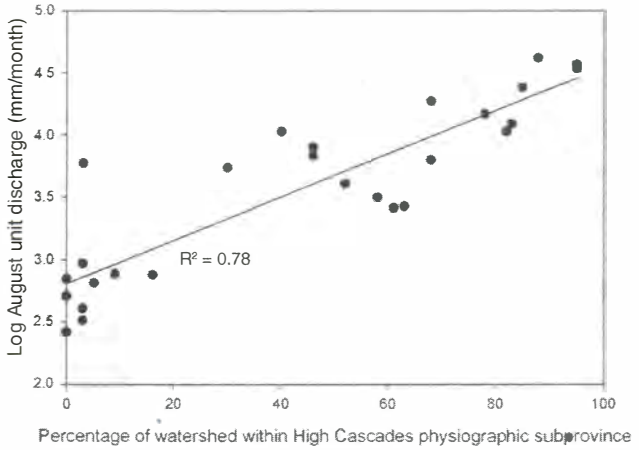

Figure 5. Mean August streamflow and percent High Cascades in contributing area for selected Willamette tributary basins (after Tague and Grant, 2004).

to runoff over older, less porous volcanic rocks in the Western Cascades. The Santiam River at Jefferson, just upstream of Stop 1, is ~15% High Cascades by area, with the North Fork Santiam (drainage area = 1990 km^2) at 28%, and the slightly larger South Fork (drainage area = 2590 km^2) at 5% (Fig. 6B). So the Santiam River is primarily a Western Cascades stream with some High Cascades influence. We'll contrast it to the McKenzie River at the next several stops.

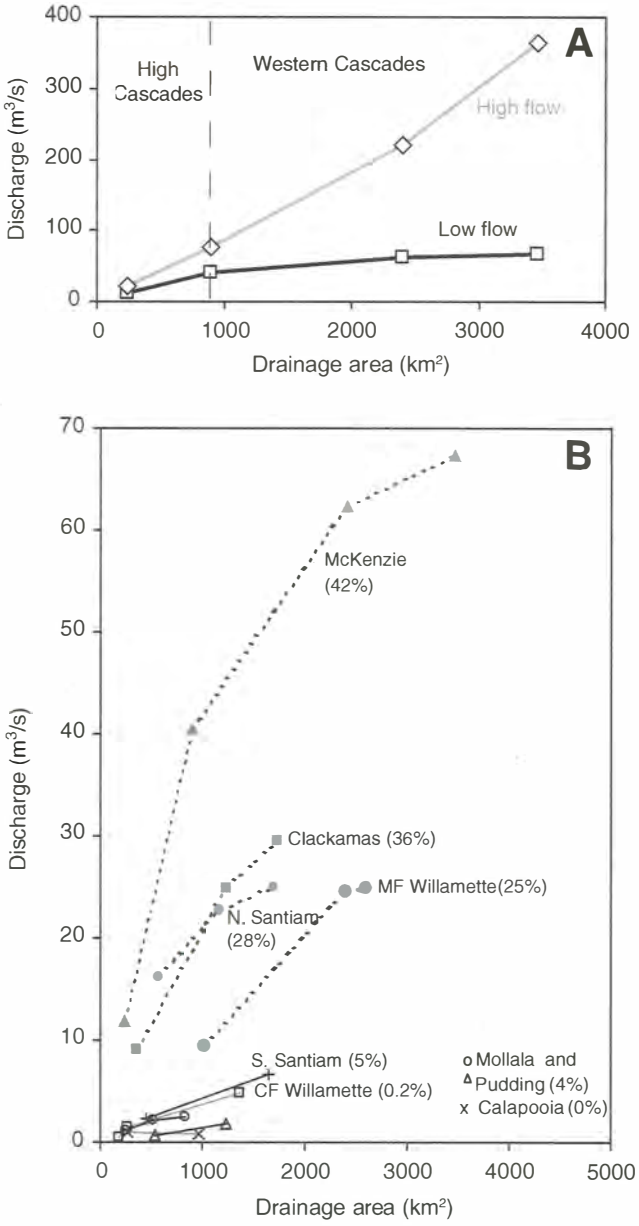

Figure 6. Discharge-drainage area relations showing impact of High Cascades contributions for (A) gages along the McKenzie River for high (1 March 1950) and low (1 September 1950) flow and (B) east-west–trending subbasins of the Willamette at low flow (1 September 1950). Percentages of High Cascades basin area shown in parentheses. Modified from Tague and Grant (2004).

Directions to Stop 2

Leave the rest stop and head south on Interstate 5. Follow I-5 south up the Willamette Valley, crossing the Santiam River immediately after leaving the rest stop. On the outskirts of Eugene, 44 mi to the south, we will cross the McKenzie River. Take Exit 194A (48 mi south of the rest stop) east onto I-105 and Oregon Highway 126 toward Springfield. Follow the highway for 6.4 mi to a stoplight at Main Street. Turn left and follow Highway 126 for 17.7 mi to Leaburg Dam. We will be traveling up the McKenzie River valley, and crossing the McKenzie River again at Hendricks Bridge State Wayside. After 13.8 mi we will cross a power canal, where water diverted from the McKenzie is transported almost 10 mi downstream to a hydroelectric generation facility. Leaburg Dam is just after mile marker 24; turn right into the parking area.

Stop 2. Leaburg Dam—Introduction to the West Side Story

The McKenzie River valley crosses the Western Cascades and extends to the High Cascades in its upper reaches (Fig. 2). At Leaburg Dam, the McKenzie River has a drainage area of 2637 km^2, of which 61% is classified as High Cascades (Tague and Grant, 2004). Contrast this with McKenzie River at Belknap Springs (40 km upstream), where the drainage area is only 374 km^2, of which 95% is in the High Cascades. The McKenzie at Leaburg Dam is a hybrid of flow regime types but more dominated by the High Cascades overall, particularly in summer. Comparison of the sources of water during low and high flow shows the relative contribution of water from the High and Western Cascades and highlights the importance of groundwater discharge during the summer (Fig. 7). As a result of the contrasting drainage mechanisms in the High and Western Cascades, the McKenzie River has a non-linear drainage-discharge relation, particularly during the summer dry season, when nearly two-thirds of the water in the McKenzie is derived from High Cascades aquifers (Fig. 6A). Over the next two days we will investigate the ways in which the geology of the High Cascades, which is dominated by Quaternary mafic lava flows, controls the hydrology of this region.

Directions to Stop 3

From the Leaburg Dam, follow Highway 126 past the Goodpasture covered bridge and through the town of Vida. Continue along Highway 126 past the towns of Finn Rock, Blue River, and McKenzie Bridge. In 28.6 mi you will see the McKenzie Bridge Ranger Station on the right. Turn into the parking lot; we'll stop briefly here to get an overview of the geography of the upper McKenzie. This is also a good place to purchase maps. Return to the vehicles and continue on Highway 126 for another 2.2 mi to the intersection with Oregon Highway 242, where we

will turn right (east) off of Highway 126 to climb toward McKenzie Pass through the White Branch valley. Here outcrops of till mark the most recent termination of the glacial tongue that carved out the White Branch valley (Fig. 8A). Follow Highway 242 for 2.2 mi; turn left at the sign for Limberlost Campground (Forest Road 220).

Stop 3. Limberlost—A High Cascades Stream

This scenic Forest Service campground is bordered by Lost Creek, a channel fed by both large springs and glaciers located on the western flanks of the Three Sisters volcano complex. The geomorphic form of the channel is typical for spring-dominated streams: a rectangular channel cross section, absence of bedforms and exposed gravel bars, lack of well-developed floodplain, mature vegetation down to the water level, and stable woody debris accumulations. These attributes reflect the extremely stable flow regime and lack of floods that characterize High Cascades streams.

Directions to Stop 4

Follow Highway 242 for another 1.4 mi; there will be a small meadow on the left. Turn in on a dirt track; park under the big tree.

Stop 4. Lost Spring—Groundwater System

"Lost Spring" (once called Lost Creek Spring) lies at the distal end of the White Branch valley, carved by glacial ice that accumulated and flowed from the vicinity of North and Middle Sister volcanoes. As noted by Lund (1977), the stream that enters the upper part of a valley usually has the same name as the stream that flows out the lower end. This is not the case here, where the stream name changes from the White Branch in the upper parts of the valley to Lost Creek in the lower. This change in name reflects the complex hydrology of the area and the flow of water largely through, rather than over, the young mafic lava flows that fill the valley. This valley, with its transient surface water flow, provides an elegant vignette of the hydrology of the High Cascades, where

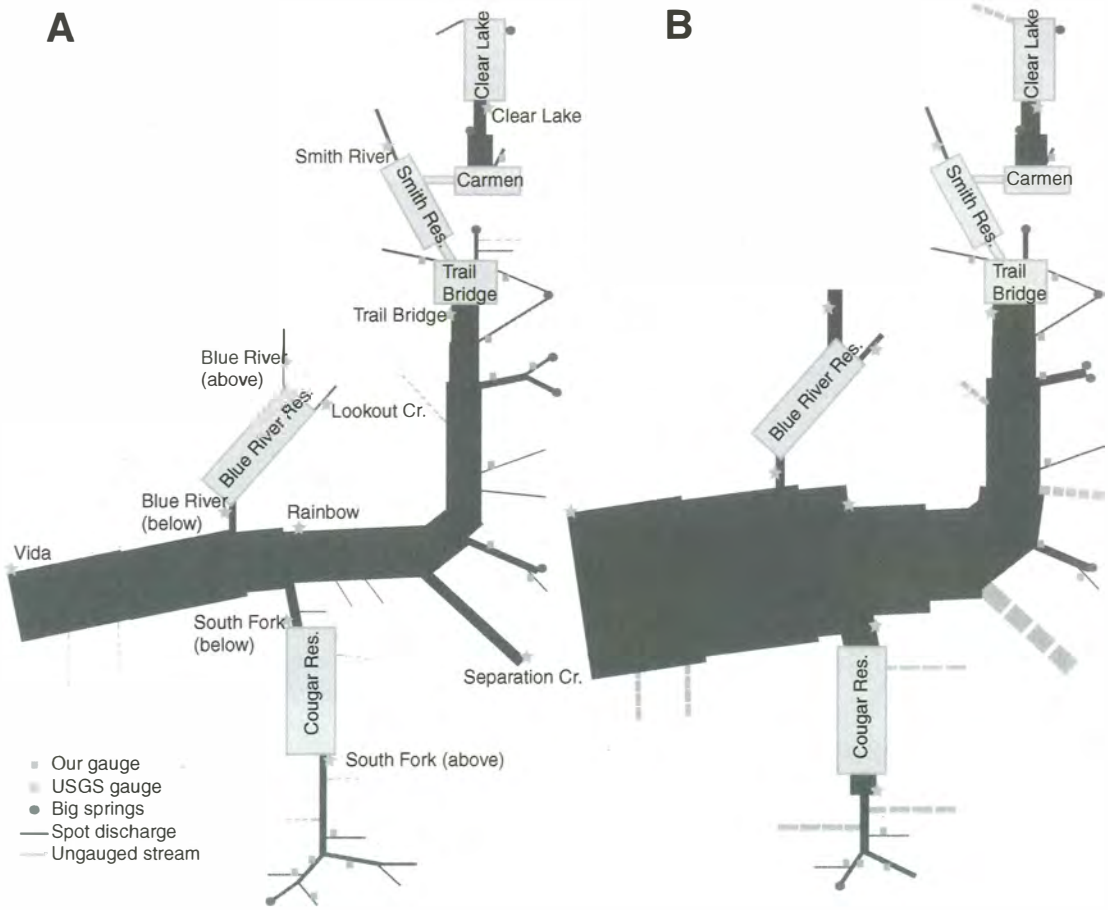

Figure 7. Sources of August and March flow in the McKenzie River. Discharges are schematically represented by thickness of each line. Distances are not to scale (after Jefferson et al., 2007).

young and highly permeable volcanic rocks form aquifers for subsurface transport of water from the high peaks to the valleys below.

Two young lava flows fill the White Branch valley. One lava flow originated at Sims Butte in the late Pleistocene (Fig. 9) and traveled nearly all the way down the White Branch valley. The younger lava flow originated at Collier Cone (ca. 1600 yr B.P.; Scott, 1990), just northwest of North Sister, and advanced west into the White Branch valley, partially covering the Sims Butte lava flow. The younger Collier Cone flow, in particular, developed a complex surface morphology because of multiple flow pulses (which created multiple levees) and interactions with the surrounding topography (Fig. 8B).

Lost Spring is actually a complex of small outlet springs emerging from the terminus of the Sims Butte lava flow (e.g., Stearns, 1929) and flows into a series of larger ponds. At a mean discharge of 6 m^3/s (212 ft^3/s), the spring complex has the largest discharge of any of the springs tributary to the McKenzie River, and also exhibits more seasonal fluctuations in discharge than other McKenzie springs. Like other springs that feed the upper McKenzie River, its estimated recharge area (114 km^2) is substantially

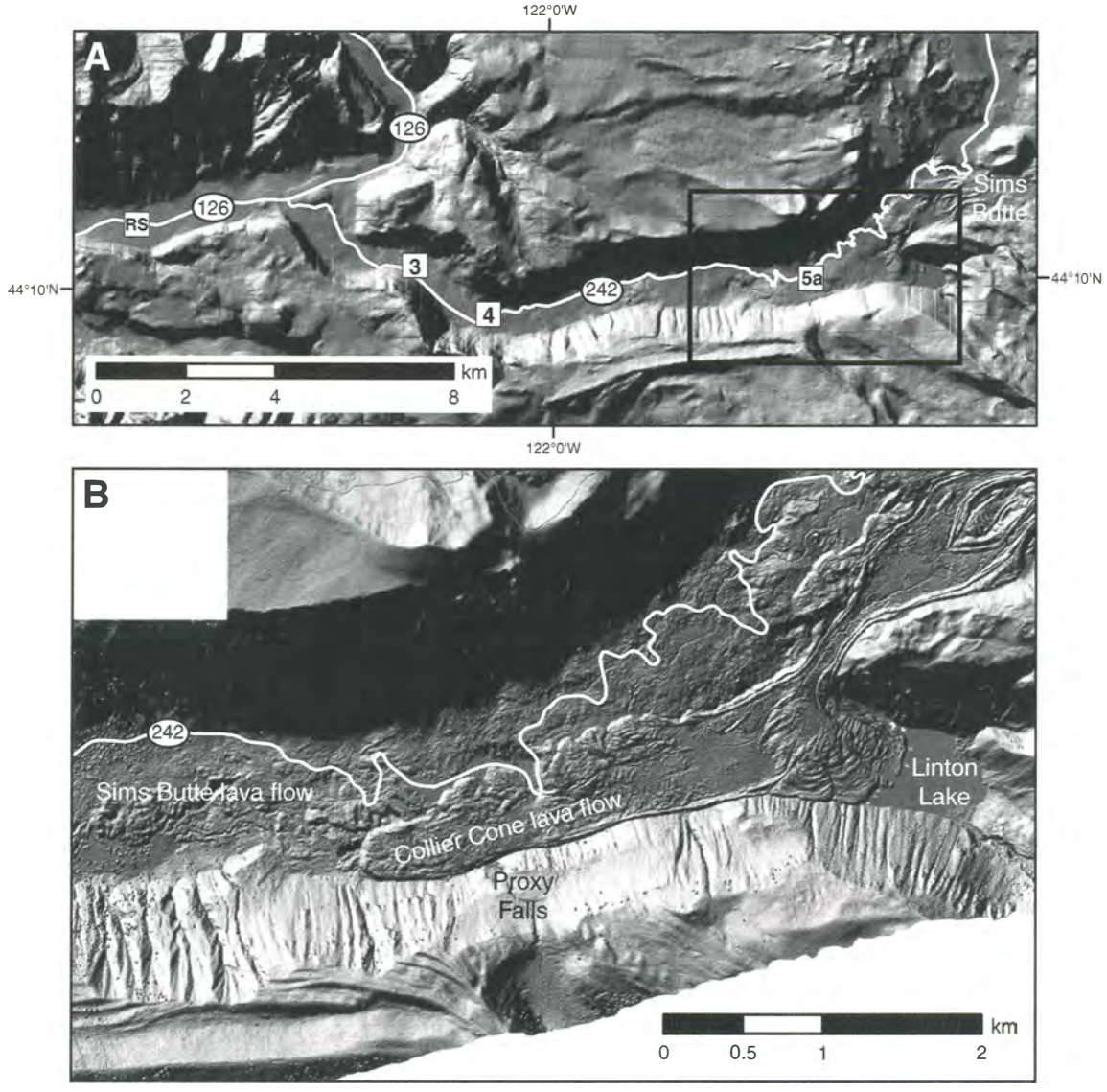

Figure 8. White Branch glacial trough. (A) Shaded relief map created from a 10 m digital elevation model of the entire White Branch valley shows stop locations and McKenzie River Ranger Station (squares), and location of (B), a light detection and ranging–generated shaded relief image showing the distal end of the Collier Cone flow (dashed line) and the lava dam that it formed to impound Linton Lake. Also shown are the locations of Proxy Falls and Highway 242.

different from its topographic watershed area (197 km^2), indicating that modern topography is not the main constraint on groundwater catchments (Jefferson et al., 2006). It also has the highest temperature (6.3 °C) of the cold springs in the area, the largest component of mantle-derived volatile constituents (as estimated from ^{3}He/^{4}He ratios) and the longest estimated transit time (54.5 yr; Jefferson et al., 2006). These data combine to suggest that the water emerging from Lost Spring is a mixture of deep-derived (warm) water rising along a fault zone 5 km upstream (Ingebritsen et al., 1994) and shallow-derived (cold) groundwater.

To the south of Lost Spring, a channel of White Branch may also contain water. The White Branch originates at the toe of Collier Glacier, on the northwest flank of Middle Sister and just south of Collier Cone. As Collier Glacier retreated in the twentieth century, a lake formed behind the terminal moraine and then breached catastrophically in July 1942, and again in 1954–1956. Peak discharge from the 1942 breach is estimated at 140 m^3/s (4944 ft^3/s) and formed a debris flow that traveled 7.5 km downstream to where the preexisting White Branch channel disappears into the Collier Cone lava flow (O'Connor et al., 2001a). Under current conditions, White Branch is ephemeral from Collier Glacier downstream to its junction with discharge from Lost Spring. Surface flow is discontinuous in the stream, and in some places there is no identifiable channel (e.g., 1 km upstream from Lost Spring). In places, the channel is well defined on the Collier Lava flow (e.g., north of Linton Lake, shown on Fig. 8B), and we interpret that channel as resulting from vigorous glacial meltwater discharge during the advanced glaciers of the Little Ice Age.

About 750 m up valley from Lost Spring, White Branch emerges from the Sims Butte lava flow in a seasonally fluctuating spring. Discharge in this spring ranges from 0 to 2 m^3/s (0–70 ft^3/s), peaking in March and late June and drying up from late summer to mid-winter. When White Branch Spring is discharging water, the water is the same temperature and oxygen isotopic composition as water in Lost Spring. We infer that the two springs discharge from the same aquifer, but that seasonal fluctuations in the water table result in perennial flow to Lost Spring and intermittent flow to White Branch Spring (Jefferson et al., 2006). Just downstream and to the south of the springs, White Branch Creek plunges over a small 3 m waterfall into a short slot canyon, before joining Lost Creek and flowing into the McKenzie River below Belknap Hot Springs.

In-Transit: White Branch Glacial Trough to McKenzie Pass

From Lost Spring, we follow Highway 242 up the White Branch along the Collier Cone lava flow (Fig. 8B). The lava flow

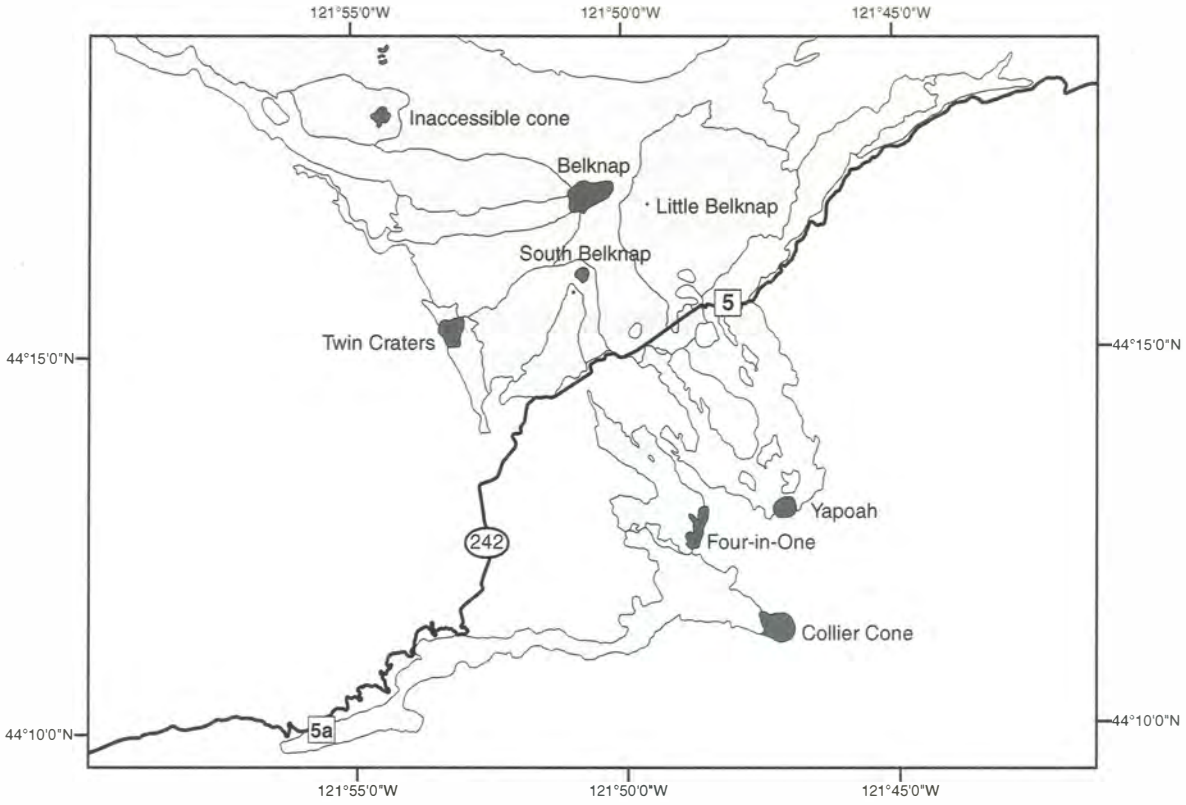

Figure 9. Post-glacial lava flows visible from McKenzie Pass. Stop numbers (squares), Young (<4000 ^{14}C yr B.P.) lava flows (dark gray) and older flows (light gray) are indicated. After Sherrod et al. (2004).

extends more than 13 km from its source at Collier Cone down the White Branch valley to form one of the longest Holocene lava flows in the Cascade Range of central Oregon. The lava flow created two lakes as it flowed down the valley and blocked streams: Spring Lake, northeast of Sims Butte, and Linton Lake, which is fed by both Obsidian and Linton Creeks. Obsidian Creek seasonally carries snowmelt runoff but is dry in the summer; Linton Creek is perennial and fed from springs to the west of Middle Sister. Linton Lake has no surface outlet. In July and August 2004, Linton Creek had an average discharge of 1.46 m^3/s (51 ft^3/s), and over that same period, lake levels dropped ~3 m. This drop is unlikely to be solely the result of evaporation, based on a comparison with the evaporation rate of Crater Lake, located at 1883 m elevation, which is 1.2 m/yr (Redmond, 1990). Linton Lake is at 1067 m in elevation, so the evaporation rate is probably higher than at Crater Lake, but not likely to exceed 3 m/yr. Thus, all of the water discharge lost from Linton Creek in the summer, plus some water stored in the lake, is recharging groundwater. Several small sinkholes that visibly and audibly drain lake water are present along the Collier lava margin. The water that flows out of Linton Lake probably mingles with both upstream water from White Branch and downstream water introduced at Proxy Falls to emerge from the distal end of the Sims Butte flow at Lost Spring.

Directions to Stop 5

Depart the parking area at Lost Spring, turn left, and follow Highway 242 up the White Branch valley. After 3.4 mi we pass the parking lot for the Proxy Falls trailhead, which is our alternative Stop 5 in the event of inclement weather or road closures (see below). From Proxy Falls, follow Highway 242 up the headwall of the valley, around the cone of Sims Butte, past the trail to Hand Lake (dammed by a lava flow from Twin Craters) and along young lava flows from Belknap Crater. In 13.2 mi you will see Dee Wright Observatory, a small stone viewing shelter and associated restrooms, on your left. Park here.

Stop 5. Dee Wright Observatory—McKenzie Pass and the High Cascades

Dee Wright Observatory is located at an elevation of 1581 m at the summit of McKenzie Pass. This stone structure was constructed by the Civilian Conservation Corps in 1935 and named for the foreman who oversaw the project. From the top of the Observatory we will (if the day is clear) have a spectacular view of Pleistocene to Holocene volcanoes of the central Oregon Cascades. Table 1 lists features visible from this location. The most prominent peaks include North and Middle Sister to the south and Belknap Crater, Mount Washington, and Mount Jefferson to the north. Also evident are numerous older mafic composite volcanoes and cinder cones, as well as the young cinder cones to the south (Four-in-One Cone and Yapoah Crater) and Belknap Crater to the north, which are the source of the young lava flows that surround us (Fig. 9).

Dee Wright Observatory is built on a basaltic andesite lava flow from Yapoah Crater, one of the young cinder cones at the base of North Sister (the other is Collier Cone, the source of the lava flow that we traced up the White Branch valley). Although this eruption has not been dated directly, tephra deposits from Yapoah Crater immediately overlie silicic ash produced during the eruptions of Rock Mesa and the Devils Hill Chain, near South Sister (~2300–2000 ^{14}C yr B.P.; Scott, 1987). The Yapoah lava flow turns to the east at the pass and travels another 8 km toward the town of Sisters. Near the vent, lava flows from Yapoah are overlain by tephra from Four-in-One Cone, a NNE-trending chain of small cinder cones produced by an eruption ca. 2000 ^{14}C yr B.P. (Scott,

TABLE 1. VIEW OF CENTRAL OREGON VOLCANOES FROM DEE WRIGHT OBSERVATORY, MCKENZIE PASS

Azimuth (°)	Feature	Description
1	Mount Jefferson	Andesitic and dacitic stratovolcano
7	Cache Mountain	Glaciated basaltic andesite shield (0.88 Ma)
11	Bald Peter	Glaciated remnant of basaltic andesite shield (2.2 Ma)
20	Dugout Butte	Glaciated basaltic shield forested foreground
30	Green Ridge	East-bounding graben fault (5–7.5 Ma)
40	Black Butte	Basaltic andesite shield volcano (1.42 Ma)
82	Black Crater	Basaltic andesite shield volcano (ca. 50 ka?)
105–155	Matthieu Lakes Fissure	Basaltic andesite–andesite (11–75 ka)
167	Yapoah Crater	Basaltic andesite ca. 2000 yr B.P.
168	North Sister	Basaltic andesite shield volcano
171	Collier Cone	Basaltic andesite ca. 1600 yr B.P.
174	Middle Sister	Stratovolcano of variable age and composition
178	Little Brother	Basaltic shield volcano (coeval or older than North Sister)
188	Four-in-One cones	Basaltic andesite and andesite ca. 2000 yr B.P.
195	Huckleberry Butte	Glaciated basalt
197	The Husband	Eroded core of basaltic andesite shield volcano (<0.42 Ma)
218	Condon Butte	Basaltic andesite shield
235	Horsepasture Mountain	Western Cascades
256	Scott Mountain	Basaltic shield volcano
282	South Belknap cone	Basaltic andesite flank vent, 1800–1500 yr B.P.
309	Belknap Crater	Basaltic andesite and andesite shield volcano; 2635–1500 yr B.P.
321	Little Belknap	Basaltic andesite flank vent, 2900 yr B.P.
340	Mount Washington	Glaciated basaltic andesite shield volcano

Note: Descriptive data from U.S. Geological Survey (USGS) Cascade Volcano Observatory, Conrey et al. (2002), Sherrod et al. (2004), Schmidt and Grunder (2009)

1990). The tephra deposit has a maximum thickness of >2 m immediately east of the cones and thins rapidly to the east. Two small cones that lie along the same trend to the SSW of Four-in-One Cone are surrounded by basaltic andesite flows from Collier Cone (1600 ^{14}C yr B.P.). The eruption that produced Collier Cone also produced a thick (>2.5 m, 1 km east of the vent) tephra blanket, although its full extent is not known.

Collier Cone, Yapoah Crater, and Four-in-One Cone are monogenetic cones, that is, cones produced by a single eruption. A classic example of a monogenetic cone is Parícutin Volcano, Mexico (the volcano that erupted in a cornfield), which was active from 1943 to 1952 (e.g., Luhr and Simkin, 1993). Monogenetic eruptions are assumed to be fed by a single batch of magma (although see Strong and Wolff, 2003; Johnson et al., 2008) and typically persist for months to years. Strombolian explosions produce abundant bombs and scoria clasts, which accumulate close to the vent to form cinder (scoria) cones. At the same time, lava flows emerge from the base of the cone. Sufficiently high mass eruption rates may generate violent strombolian eruptions, which are characterized by high (6–8 km) ash columns that produce widespread tephra deposits (e.g., Walker, 1973; Pioli et al., 2008). The relative proportions of cone-forming scoria, lava, and tephra reflect the relative fluxes of gas and melt (and crystals). All of the young scoria cones in the McKenzie Pass region produced tephra blankets in addition to lava flows, indicating relatively high mass eruption rates.

Like Parícutin, Collier Cone, Yapoah Crater, and Four-in-One Cone erupted magma of basaltic andesite composition (Fig. 10), with genetic affinities to magma produced at North Sister (e.g., Conrey et al., 2002; Schmidt and Grunder, 2009). However, although basaltic andesite magmas from Collier Cone, Yapoah Crater, and Four-in-One Cone are similar, they are not identical in composition, suggesting that each batch of magma had a slightly different source. Additionally, all three show surprising variability in composition; Collier Cone lavas, for example, show extensive heterogeneities in both major elements and phenocryst content (Schick, 1994). Variations in SiO_2 are similar to those observed during the 1943–1952 eruption of Parícutin, Mexico, which have been interpreted to reflect assimilation of silicic upper crustal rocks in shallow dikes and sills (Wilcox, 1954). Silicic xenoliths present in tephra and lava deposits from both Collier Cone and Four-in-One Cone (Taylor, 1965; Schick, 1994) may explain much of the chemical variation observed in these two eruptive sequences (Fig. 10B).

To the west and northwest of Dee Wright Observatory are lava flows from Belknap Crater (Figs. 9 and 11) that cover 88 km^2 and are described by Williams (1976) as "one of the largest and most impressive sheets of recent lava anywhere in the United States." Unlike Collier Cone, Yapoah Crater, and Four-in-One Cone to the south, Belknap is composed of lavas that are primarily basaltic in composition and slightly enriched in K_2O (Fig. 10), continuing a trend noted by Schmidt and Grunder (2009) of a general decrease in SiO_2 in younger lavas from North Sister to McKenzie Pass (Fig. 12). Belknap also differs in being a mafic shield volcano formed by numerous eruptions from the same vent. The oldest exposed Belknap lavas lie to the northeast and have not been dated. Lava flows from South Belknap have an age of 2635 ± 50 ^{14}C yr B.P. (Licciardi et al., 1999) and form numerous interfingering small channels and flows with blocky surfaces. Overlying lava flows from Little Belknap have been dated at 2883 ^{14}C yr B.P. (Taylor, 1968, 1990), a date that seems too old for the young morphology and stratigraphic relationship with Belknap Crater (Sherrod et al., 2004). An eruption of Belknap ca. 1500 ^{14}C yr B.P. sent flows 15 km west into the McKenzie River

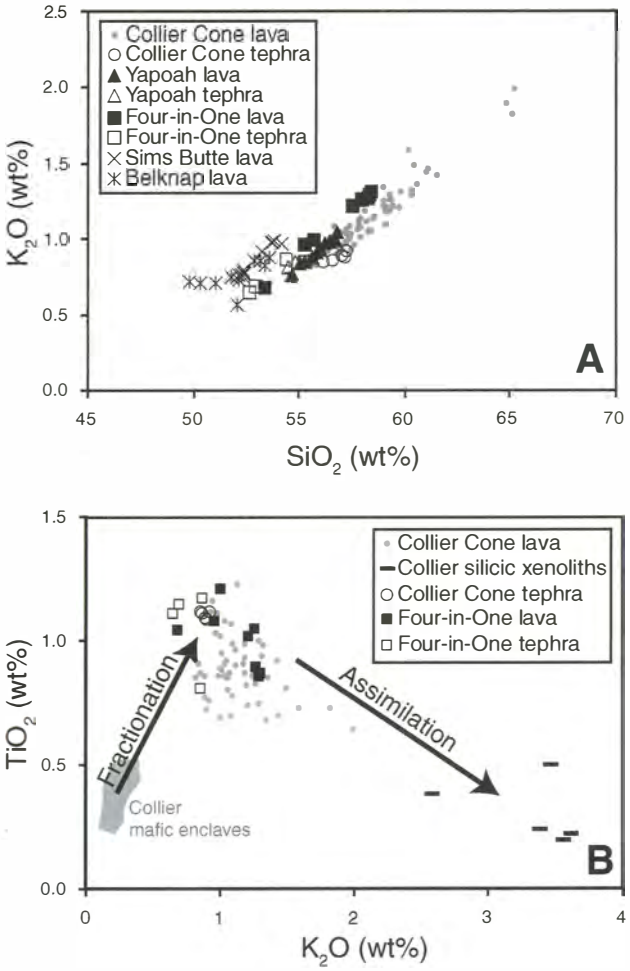

Figure 10. Composition of McKenzie Pass Holocene lavas. (A) A plot of wt% K_2O versus wt% SiO_2. Note the range in compositions of the young cinder cones north of North Sister (Collier Cone, Yapoah, Four-in-One) and the contrast with the basaltic lavas erupted from Belknap and Sims Butte. (B) A plot of wt% K_2O versus wt% TiO_2 for tephra, lava, xenoliths, and mafic enclaves from Collier Cone and Four-in-One Cone. Note that the tephra samples are less evolved than corresponding lava and that lava samples from both eruptions appear to have experienced varying degrees of assimilation of underlying silicic material. Data from Schick (1994), Conrey et al. (2002), and D. McKay (2009, personal commun.).

valley (see Day 2, Stop 8). Together these eruptions have created a shield-like edifice cored by a scoria cone. The lava flows have surface morphologies that range from blocky to pāhoehoe, with the latter flows from Little Belknap creating islands (kipukas) of older lavas within the younger (Fig. 11).

The permeable surfaces of the Holocene lava flows on the Cascade Range crest facilitate rapid infiltration and recharge to the groundwater flow system. Although average precipitation in this area exceeds 2500 mm annually (mostly as snow), there are no streams and no evidence of fluvial incision. Instead, this volume of water percolates into the permeable lava to re-emerge as spring flow, such as at Lost Spring, farther downstream. Jefferson et al. (2006) calculated the volume of mobile groundwater stored in the upper McKenzie River area as 4 km^3, based on a mean transit time of 7.2 yr and a total discharge of 17.1 m^3/s from seven major springs. Aquifer thickness may range from 30 to 120 m, derived from dividing aquifer volume by an effective porosity of 15% (following Ingebritsen et al., 1994). Thermal profiles in boreholes near Santiam Pass are isothermal for the uppermost several hundred meters, as a result of groundwater fluxes (Saar and Manga, 2004). Near the surface, hydraulic conductivity is ~10^{-3} m/s (Manga, 1996; Jefferson et al., 2006); hydraulic conductivity decreases rapidly with depth, such that at 500 m it is estimated to be ~10^{-6} m/s (Saar and Manga, 2004).

Absence of fluvial incision in this young terrane raises the question of how long it takes for rivers to become established in a constructional volcanic landscape. To initiate fluvial incision, vertical infiltration through highly porous lava flows must evolve toward integrated development of surface flow paths. A fundamental question is whether surface flow develops from the top down (development of an impermeable surface layer through soil and clay formation) or bottom up (infilling of pores by translocation of fines and bulk weathering). An additional question includes the role of glaciers in jumpstarting drainage development both by incising canyons and by producing large quantities of rock flour that can reduce landscape permeability. Initial data suggest that timescales of 10^5 to 10^6 years are required for maximum soil development and measurable increase in surface drainage density.

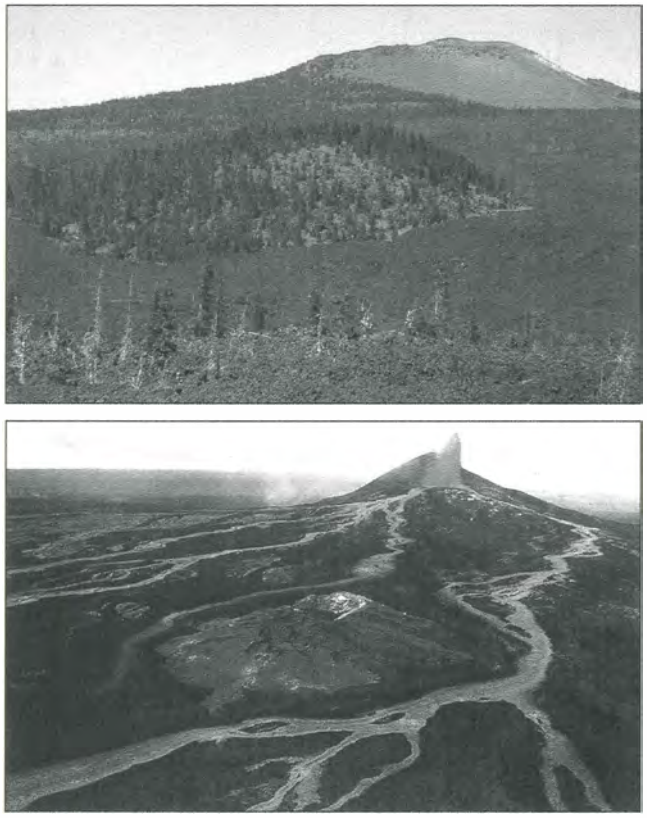

Figure 11. (A) Photograph of Belknap Crater (the cinder cone on the horizon) and pāhoehoe lava flows from Little Belknap (foreground), which surround an older cone to form a kipuka. (B) Photograph of Pu'u 'Ō'ō, Kilauea Volcano, Hawaii, showing the formation of a kipuka of older material surrounded by active lava channels (U.S. Geological Survey photo by J.D. Griggs, 1986).

Stop 5a. Proxy Falls—Traversing the Collier Cone Lava Flow

Note: this is an alternate to Stop 5, if McKenzie Pass is not open to traffic or if the weather is particularly inclement.

Starting from the Proxy Falls parking lot, 8.9 mi from the junction with Highway 126, we will hike 0.6 km to Proxy Falls. The trail crosses the ca. 1600 yr B.P. Collier Cone lava flow and the (typically dry) surface channel of the White Branch watercourse that has been carved into the flow (Fig. 8B). The light detection and ranging (LiDAR) image shows that here, at its distal end, the Collier Cone lava flow is confined on its south side by the steep walls of the glacial valley. In contrast, the north side has lobate structures that formed as the flow spread laterally.

The hydrology of the Proxy Falls area is described in detail by Lund (1977). He notes that Proxy Falls consists of several waterfalls with different sources. Upper Proxy Falls originates in

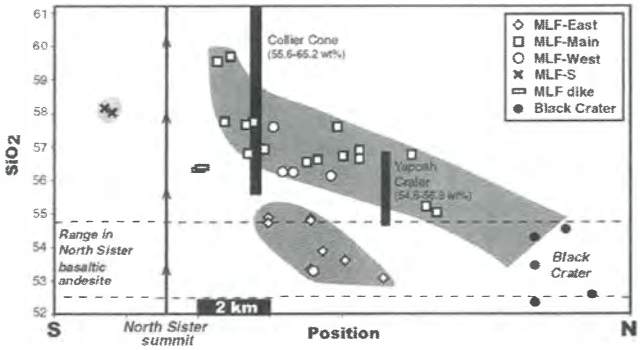

Figure 12. Illustration of the compositional variation of younger mafic lavas south of McKenzie Pass as a function of the distance from North Sister (from Schmidt and Grunder, 2009). This variation is interpreted to reflect the influence of a well-developed magma storage region beneath North Sister. MLF—Matthieu Lakes Fissure.

springs emerging from an older lava flow ~200 m above the valley floor. These springs feed streams that flow down two ravines and join at Upper Proxy Falls. Lower Proxy Falls is fed by Proxy Creek, which traverses a glacially carved hanging valley. Below the falls, Proxy Creek continues along the southern edge of the Collier Cone until the end, when it flows on top of the Sims Butte lava and loses much of its water to the underlying lava flow. All of the waters from this system, Linton Lake, and the White Branch ultimately emerge in the Lost Spring to form Lost Creek (Stop 4).

Directions to the H.J. Andrews Experimental Forest (End of Day 1)

Retrace the route west from Dee Wright Observatory, following Highway 242 for 22.1 mi to its intersection with Highway 126. Turn left (west) on Highway 126 and follow it 15.3 mi, passing though the town of McKenzie Bridge. Turn right (north) at the "Blue River Reservoir" sign onto Forest Road 15. Drive up the hill and away from the McKenzie River, following the edge of Blue River Reservoir. After 3.8 mi you will cross the Lookout Creek Bridge. Just past the bridge, turn right onto Forest Road 130 at the Andrews Forest Headquarters sign. Park in the parking lot.

DAY 2. H.J. ANDREWS EXPERIMENTAL FOREST (BLUE RIVER, OREGON) TO BEND, OREGON

Day 2 of the field trip will focus primarily on changes to patterns of water flow through the upper McKenzie River caused by the incursion of lava flows (Fig. 13). However, first we start the day by contrasting the morphology of a typical Western Cascades stream (Lookout Creek at the Andrews, Stop 6) with the morphology of rivers dominated by High Cascades streamflow regimes at Olallie Creek (Stop 7). We then travel up the McKenzie to Carmen Reservoir (Stops 8 and 9), where we examine the seasonally occupied channel of the McKenzie where the river traverses a lava flow from Belknap Crater. We then continue up the McKenzie to its headwaters in Clear Lake, a lava-dammed, spring-fed lake that we will explore using rowboats (Stop 10). After leaving Clear Lake we travel along the west side of the young basaltic Sand Mountain volcanic chain before crossing the chain to head east over Santiam Pass (Stop 11). Here we see tuyas formed during the last glaciation, have a good view of the glacially sculpted cone of Mount Washington, and look down on Blue Lake crater, the product of another recent eruption. From the Blue Lake–Suttle Lake valley, the trip descends the flank of the High Cascades, crossing glacial outwash deposits and Quaternary lava to the base of Black

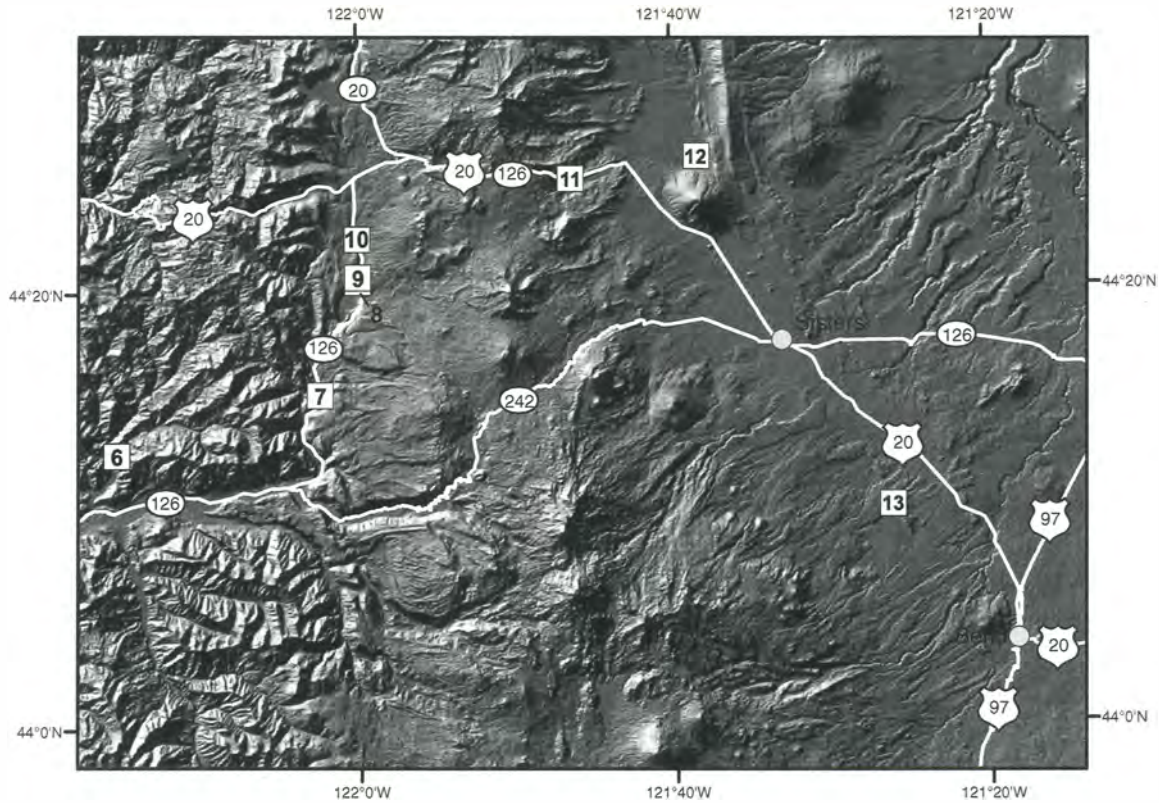

Figure 13. Overview map of Day 2, Stops 6 through 13 (squares). Shaded relief map created from a 10 m digital elevation model shows notable features including the Three Sisters volcanoes in the southern central part of the image, the pronounced Green Ridge fault, and symmetrical Black Butte cone to the north, and the broad lava plains to the east.

Butte, a large symmetrical cone prominent on the landscape. At Stop 12, on the north base of Black Butte, is the headwaters spring of the Metolius River, a major spring-fed stream tributary to the Deschutes River. Also prominent on the landscape at this location is Green Ridge, the escarpment of the eastern bounding fault of the graben in which this part of the High Cascades resides. From Black Butte the trip continues southeast along the Sisters Fault Zone, a 5–15 km zone of nearly 50 mapped faults (Sherrod et al., 2002, 2004) that extends from Green Ridge to the north side of Newberry Volcano. The final stop of Day 2 (Stop 13) examines Quaternary and Tertiary deposits on either side of the Tumalo fault, a principal strand of the fault zone, at the location of a dam and reservoir that never held water.

Stop 6. Lookout Creek—A Typical Western Cascades Stream

Lookout Creek near the main H.J. Andrews administration site is a classic Western Cascades stream, with a drainage area of 64 km^2. Characteristic features of this Western Cascades stream include: (1) a planform morphology dominated by coarse-grained lateral and marginal bars of flood origin, now colonized by broadleaf alders, cottonwoods, and willows; (2) a well-defined floodplain of mixed fluvial and debris-flow origin, now colonized by old-growth Douglas fir forest; (3) a well-defined channel morphology of step-pool sequences; and (4) marginal and occasionally channel-spanning, large, woody debris accumulations.

Channel and valley floor morphology, processes, and changes in this reach have been extensively studied and described (e.g., Grant et al., 1990; Grant and Swanson, 1995; Nakamura and Swanson, 1993; Swanson and Jones, 2002; Faustini, 2001; Dreher, 2004), and reveal interactions among fluvial processes, debris flows from upstream tributaries, growth and disturbance of riparian vegetation, and dynamics of large woody debris. In particular, this reach has been affected by repeated debris flows generated during major storms in 1964 and 1996. These debris flows entered the Lookout Creek channel ~2 km upstream, transitioned into bedload-laden floods that mobilized large woody debris accumulations, stripped mature and old-growth riparian forests, and deposited large coarse cobble bars that now support a young forest of alders and conifers. Stratigraphy of older deposits on which the current old-growth forest now grows reveals a similar origin. These reaches undergo a decades-long sequence of morphologic changes following large floods that is driven both by fluvial reworking of flood deposits and morphologic adjustments around large pieces of wood that fall in from the adjacent forest stand (Fig. 14).

In-Transit: Fluvial Incision and Hydrology along the Western Cascades-High Cascades Boundary

The Western Cascades–High Cascades boundary is traversed by several ridge-capping lavas resulting from topographic inversion and illustrating the persistent effects of erosion-resistant lava flows on landscape form. These lava flows can also be used to estimate incision rates across this boundary. Lookout Ridge, which separates Lookout Creek from the McKenzie River, is capped by 6–8 Ma lavas from the ancestral High Cascades (Conrey et al., 2002). These ridge-capping lavas probably originated as intracanyon lava flows and therefore mark the course of the ancestral McKenzie River. The elevation difference between the summit of Lookout Ridge (1341 m) and the modern McKenzie River at the town of McKenzie Bridge (396 m) yields an average incision rate of 0.12–0.16 mm/yr. Similar calculations for Foley Ridge (634 m), a 0.6–0.8 Ma intracanyon flow on the south side of the McKenzie River near the ranger station (454 m) indicate incision at 0.23–0.3 mm/yr. These rates bracket estimates for the Middle Santiam River of 0.14 mm/yr over the past 5 Ma (Conrey et al., 2002), and rates for the Western Cascades of 0.28–0.33 mm/yr from 3.3 to 2 Ma and 0.14–0.17 mm/yr since 2 Ma (Sherrod, 1986).

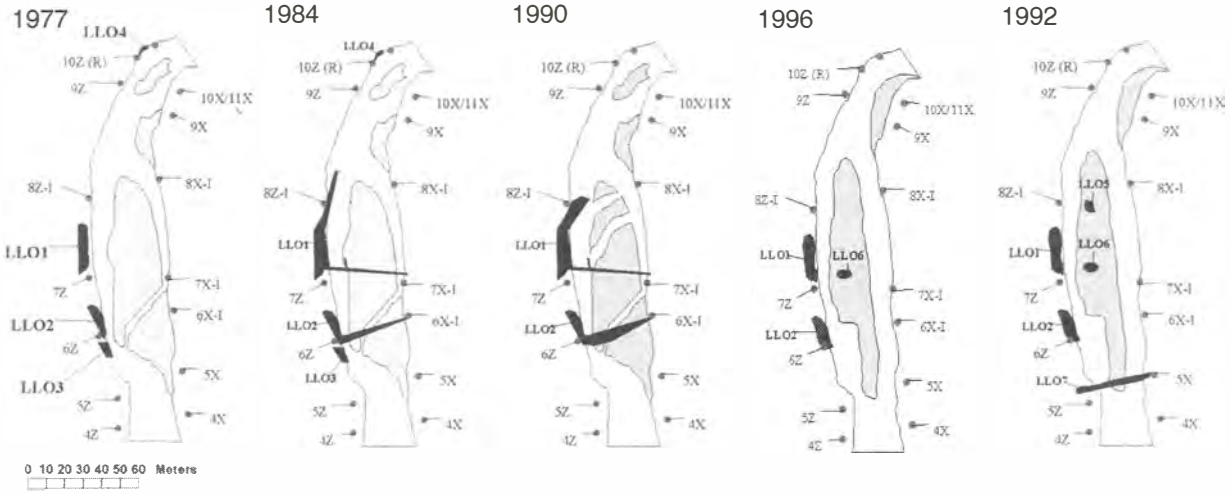

Figure 14. Changes in wood accumulation (black) and gravel bars (gray) in Lower Lookout Creek between 1977 and 2002. Numbers denote surveyed cross-section locations. Figure from Dreher (2004).

Just beyond the turnoff for Highway 242, site of yesterday's Stops 4 and 5, the McKenzie River (and Highway 126) makes an abrupt turn to the north. From here to its headwaters, the McKenzie River flows along the western graben boundary between the High Cascades and the Western Cascades. Within the graben, there has been nearly 3 km of subsidence over the past 5 million years (Conrey et al., 2002).

Along the graben-bounding fault zone, there are several hot springs discharging into the McKenzie River or its tributaries, including the privately-owned Belknap Hot Spring, and Bigelow Hot Spring on Deer Creek, which is submerged during high flows of the McKenzie River. The thermal waters are inferred to recharge near the Cascade crest, move in flow paths several km deep, and emerge along faults, which interrupt the downgradient flow of water (Ingebritsen et al., 1994). The waters discharge at temperatures of 46–79 °C, are enriched in Na, Ca, and Cl, and contain a magmatic signature in their helium isotopes. Discharge at individual hot springs ranges from 5 to 24 L/s. Total discharge of geothermal water in the Central Oregon Cascades is less than 0.2% of annual groundwater recharge but represents 148 MW of heat discharge (Ingebritsen et al., 1994). To date there has been no development for geothermal energy production, but numerous exploratory wells have been drilled.

The deep-flowing thermal water captures most of the geothermal heat and magmatic gases migrating upward through the west slope of the High Cascades (Fig. 15). As a result, water flowing from the large nonthermal springs is close to the temperature at the mean recharge elevation inferred from stable isotopes, has low total dissolved solids, and a helium isotope ratio close to that of the atmosphere.

Directions to Stop 7

Exit the Andrews Forest Headquarters and turn left onto Forest Road 15. Follow the Blue River Reservoir 3.8 mi to Highway 126. Turn left and follow the highway for ~18 mi to Olallie Campground. Park at the northern end of the campground.

Stop 7. Olallie Creek—Geomorphology of Western and High Cascades Streams

This stop offers an excellent opportunity to contrast the morphology of Western and High Cascades streams. Channel-flanking unvegetated gravel bars, large boulders, well-developed step-pool sequences, and woody debris pieces and accumulations that indicate fluvial transport are all features characteristic of Western Cascades streams (Stop 6). Contrast this with the Olallie Creek channel here, a spring-fed High Cascades stream characterized by: (1) a planform morphology with few emergent gravel bars and dominated by stable wood accumulations, as indicated by moss growth and nurse logs; (2) mature conifers at the channel margin and absence of well-defined floodplain and broadleaf species; (3) a chaotic and poorly defined channel unit structure; and (4) stable, channel-spanning wood accumulations with little evidence of fluvial transport. High Cascades channels reflect the near-constant flow regimes, absence of flooding, and limited sediment and wood transport.

LiDAR imagery suggests that the path of Olallie Creek is controlled by the position of lava flow margins, and the creek is fed by springs <800 m apart at the heads of two tributary channels. The north spring discharges 1.7 m^3/s of constantly 4.5 °C water that cascades down a steep slope of lava from Scott Mountain, while the south spring emerges from under a talus pile, discharging 2.3 m^3/s at a constant 5.1 °C (Jefferson et al., 2006). Both springs discharge more water than falls as precipitation in their watersheds, showing that groundwater flowpaths cross modern topographic divides (Jefferson et al., 2006). Flowpaths are inferred to follow lava geometries that were influenced by now-obscured paleotopography. Using water temperature and hydrogen and oxygen stable isotopes, Jefferson et al. (2006) showed that the two springs feeding Olallie Creek receive groundwater from different source areas, with the south spring recharging at lower elevations than the north spring. Olallie Creek and its springs illustrate the dominant influence of constructional volcanic topography on pathways of both groundwater and surface water.

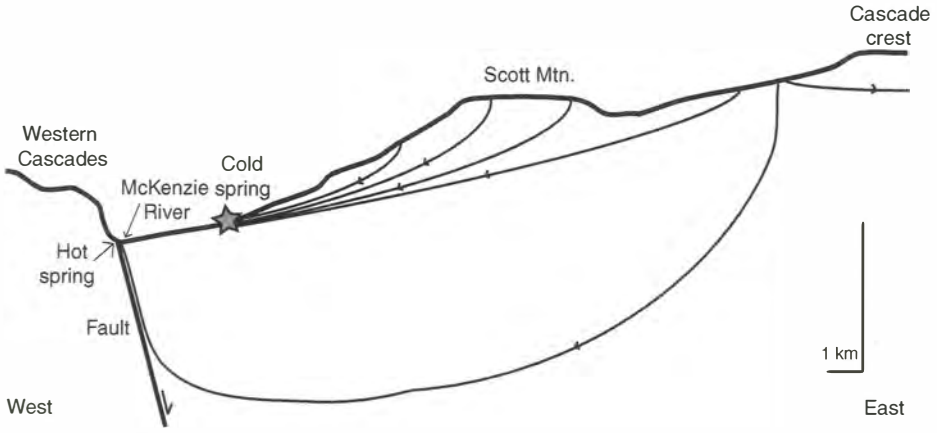

Figure 15. Cross section showing conceptual groundwater flow paths from the Cascade crest to the Western Cascades. Hot springs occur where deep groundwater flow paths are interrupted by faults (Ingebritsen et al., 1994), while cold springs are the result of shallower flow paths. From Jefferson et al. (2006).

Directions to Stop 8

Exit the campground and turn left (north) on Highway 126. Follow the highway for 7 mi to Forest Road 750, where you will turn left and follow the road around the northern end of Carmen Lake. Park at the trailhead at the end of the road.

Stop 8. Carmen Reservoir—Where the McKenzie River Goes Underground

Carmen Reservoir is part of a water diversion and power generation complex operated by the Eugene Water and Electric Board (EWEB). In 1958, EWEB was issued a license by the Federal Energy Regulatory Commission to establish and operate the hydroelectric system (described below), which became operational in 1963. EWEB recently renewed the license for another 50 yr.

The McKenzie River begins at Clear Lake and flows for 2.5 km before entering Carmen Reservoir. Water is then diverted to Smith Reservoir via an underground, 3469-m-long, 3.9-m-diameter tunnel to join water from the Smith River. The combined water is then run through a second tunnel (2217 m long by 4.1 m in diameter) to Trail Bridge Reservoir. In this second tunnel, power is generated with a maximum power output of 118 MW. At Trail Bridge Reservoir, water is returned to the McKenzie River, with flow rates closely controlled to mimic natural conditions (Figs. 7 and 16).

Although there is no surface river flow directly south of Carmen Reservoir, this is not solely a function of the Carmen-Smith Diversion. Stearns (1929, p. 176) noted that at this location in September 1926 the McKenzie River "flows only in the spring … during the rest of the year the water sinks into the permeable lava in the valley floor." Stearns noted that the McKenzie River flows underground between modern Carmen Reservoir and "Tamolitch Pool" (the "Lower Falls" in Stearns, 1929), where it re-emerges after flowing either beneath or through a young lava flow attributed to a ca. 1500 yr B.P. eruption from Belknap Crater (Taylor, 1965; Sherrod et al., 2004; Fig. 17). The diversion has decreased the amount of water traveling through this stretch by about one-half: the discharge rate at Tamolitch Pool in October 2003 was 4.1 m^3/s (Jefferson et al., 2006), which is roughly half the 9.9 m^3/s discharge estimated by Stearns (1929).

At this stop, we hike down the McKenzie River trail, beginning at the southwestern margin of Carmen Reservoir and following the trail for 0.8 km to a footbridge over the dry McKenzie River channel. Note that despite the lack of surface flow and the young age of the lava, the channel is well defined and composed of large angular boulders. Farther downstream, boulders within the channel are imbricated. Both channel creation and boulder imbrication require substantially larger flows than observed historically in this stretch of the McKenzie River. The valley itself was glacially carved, and several of the unusual morphologic features in this area, including the steep cliffs and the amphitheater immediately north of Tamolitch spring, reflect this origin.

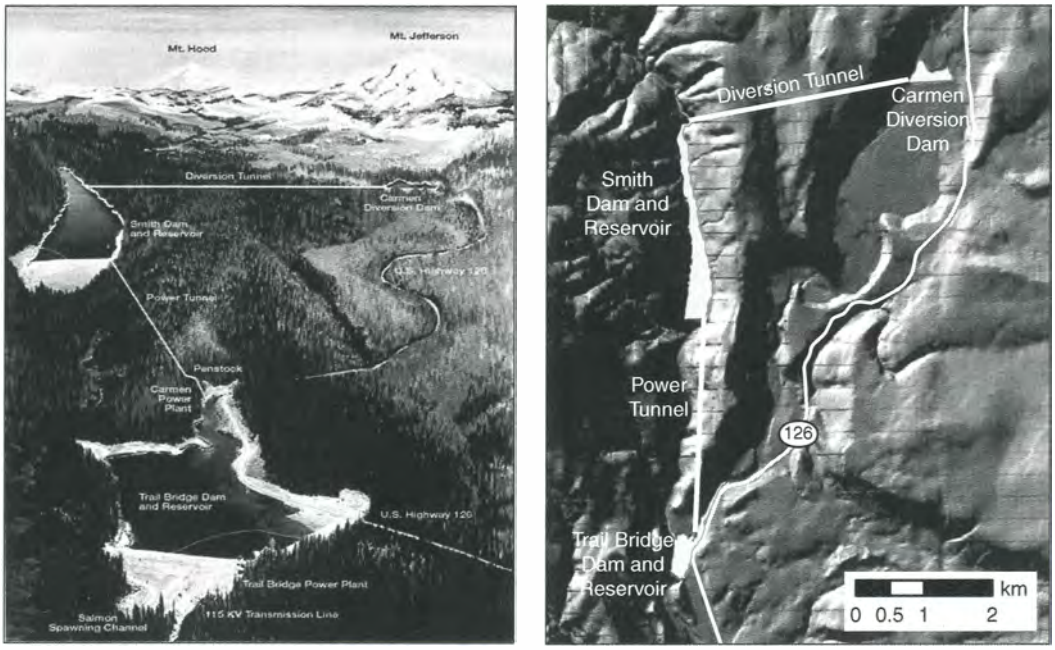

Figure 16. The Carmen Smith Project on the Upper McKenzie River in (A) illustration from Eugene Water Electric Board and (B) map view in shaded relief. Water is collected at Carmen Reservoir and transferred to the Smith River drainage and then back to the McKenzie River drainage at Trailbridge Reservoir for the purpose of power generation.

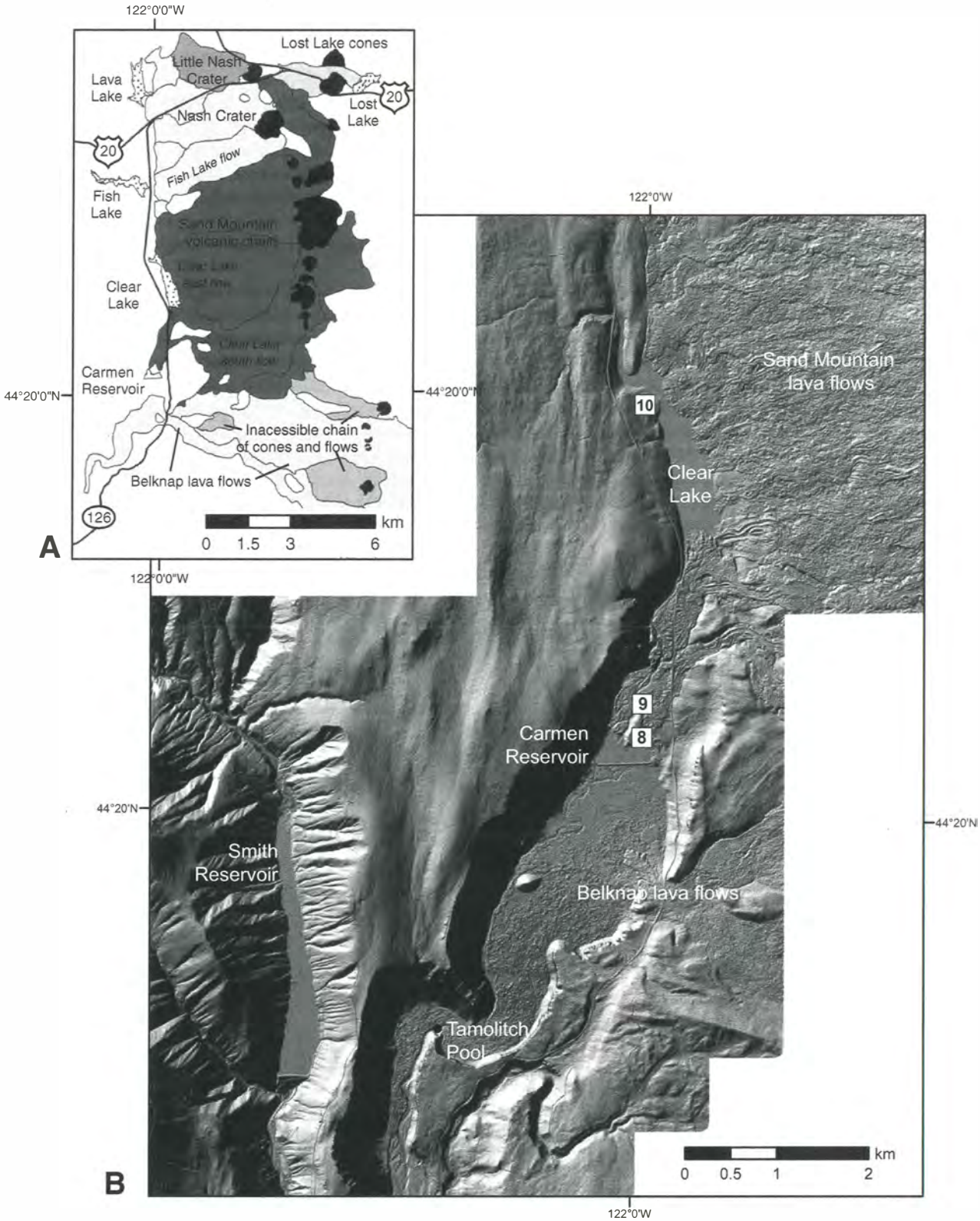

Figure 17. (A) Young lava flows (<4000 ^{14}C yr B.P.) that entered the McKenzie River Valley. Modern lakes and reservoirs are shown in light gray. Geology from Sherrod et al. (2004). (B) Light detection and ranging (LiDAR) of upper McKenzie River, with stop locations (squares) and Tamolitch pool (black dot) shown.

Directions to Stop 9

Retrace your route around the northern end of Carmen Lake and follow Forest Road 750 to Highway 126. Turn left and in less than 0.1 mi, turn left into Koosah Falls and Ice Cap Campground. Follow the road to the day use area in the campground, where we will park and walk to Koosah Falls.

Stop 9. Koosah Falls—Water Flow over and through Young Lava

Koosah Falls is the lower of two waterfalls along the McKenzie River between Clear Lake and Carmen Reservoir; the upper is Sahalie Falls. The river along this stretch flows from Clear Lake, along the graben structure that defines the uppermost McKenzie River valley, and over two lava flow lobes to form Sahalie and Koosah Falls (Fig. 18A). These flow lobes are part of the lava flow complex responsible for damming Clear Lake (e.g., Taylor, 1981; see Stop 10).

Koosah Falls and nearby Ice Cap Spring illustrate the multiple surface and subsurface flow paths of water through the young volcanic terrains. Although water flows over a young lava flow at this location, there is also evidence for additional flow of water through the lava flows in this part of the McKenzie River. Between Clear Lake and Carmen Reservoir, a distance of only ~3 km, ~6 m^3/s of flow is added to the river. Much of this water is discharged directly into the channel, as illustrated just below Koosah Falls, where springs discharge along flow boundaries within the valley walls. Ice Cap Spring, on the other side of the Koosah Falls parking area, demonstrates that flow paths and discharge areas can be strongly controlled by local lava topography. Ice Cap Spring, appropriately named for its 4.7 °C temperature, feeds a 0.35 m^3/s creek that parallels the McKenzie River for 400 m before entering Carmen Reservoir.

Directions to Stop 10

Leave the Koosah Falls–Ice Cap Campground parking lot and drive 1.9 mi to the entrance to the Clear Lake Resort on the right. Turn right into the resort and follow the road down the hill to the parking lot by the lake. In front of you is the restaurant providing rowboats required to access Stop 10.

Stop 10. Clear Lake—The Source of the McKenzie River

Clear Lake, the highest permanent source of the McKenzie River, is bordered by lava flows on the northern, eastern, and southern margins, and bounded by a fault along the western margin of the lake (Fig. 17). The lava flows on the northern and southern margins have considerable soil development and are covered with old-growth forest, while the lava flow on the eastern margin has relatively little soil development and sparse vegetation cover. Clear Lake's name stems from its remarkable clarity, stemming from the inability of most organisms to grow in the 4.0 °C spring water feeding the lake (Jefferson et al., 2006). Roughly 10% of

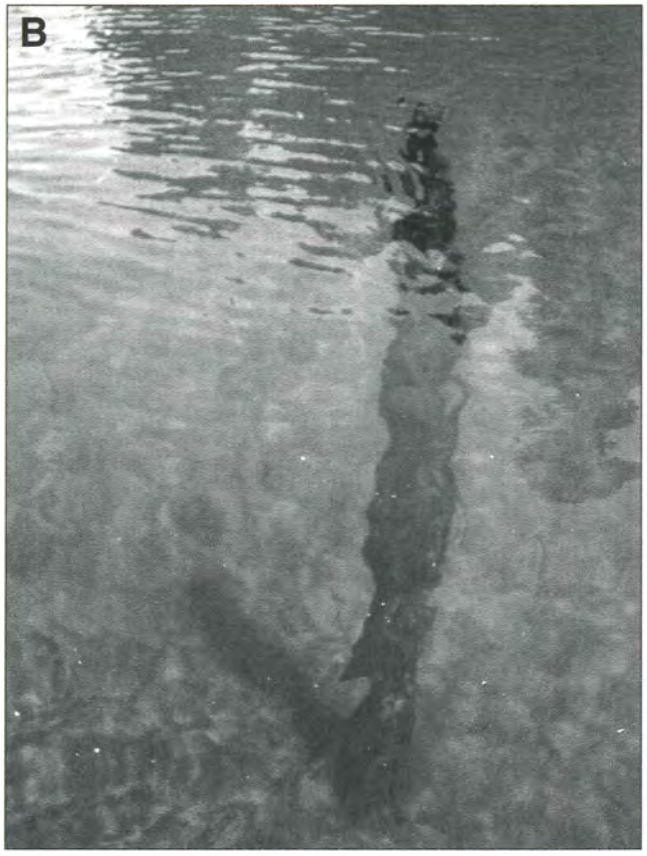

Figure 18. (A) Photograph of Koosah Falls, formed where the McKenzie River plunges over the lowermost of the lava flow lobes associated with the flow that dammed Clear Lake. Note the well-developed columnar joints within the lava flow and the obvious water seep from the base of the flow on the far canyon wall. (B) Photograph of a "ghost tree" that was drowned when Clear Lake was dammed. A similar tree has an age of 2700–3000 ^{14}C yr B.P. (Sherrod et al., 2004).

the water comes from the Great Spring situated along the northeastern margin of the lake (Fig. 19); the rest comes from small springs along the edges and bottom of the lake. There is seasonal runoff into Clear Lake from Ikenick and Fish Lake Creeks from the north and a small, unnamed creek from the west.

Clear Lake formed when lava flows entered and dammed the ancestral McKenzie River. Trees drowned by creation of the lake can still be seen in the shallower waters at the north end, preserved by the cold spring-fed water (Fig. 18B). The first scientific investigation of Clear Lake was by Stearns (1929), who evaluated the suitability of this and other areas in the McKenzie watershed as dam and reservoir sites. Stearns (1929) noted the remarkable clarity of the water, the drowned trees, and the striking difference between the lava flows on the eastern and the southern (damming) margins. He concluded that the trees were drowned when the southern flow was emplaced, and that the eastern flow was emplaced more recently. Stearns's observation that the lake is leaky, with clear evidence of water flow through the damming flow, led him to conclude that Clear Lake was an unsuitable dam or reservoir site.

Subsequently Taylor (1965) linked the Clear Lake lava flows to the Sand Mountain volcanic chain vents. He traced the flows exposed on the north shore of Clear Lake to the base of the north Sand Mountain cone and the basalt at Koosah Falls to the southern end of the Sand Mountain chain. Taylor (1965) grouped the flows that bound the eastern and southern shores of the lake as the "Clear Lake flow." However, subsequent geochemical analyses show that two flows differ substantially in composition (Conrey et al., 2002; Fig. 20). The sparsely vegetated flows on the

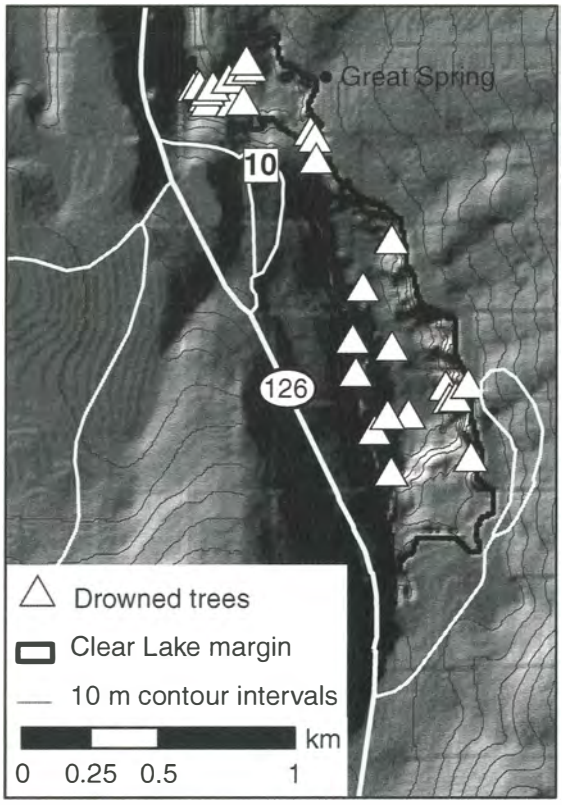

Figure 19. Topographic map of Clear Lake area including bathymetry mapped in the summer of 2008. Stop number indicates parking area; drowned tree locations (open triangles) and Great Spring (black dot) are also shown.

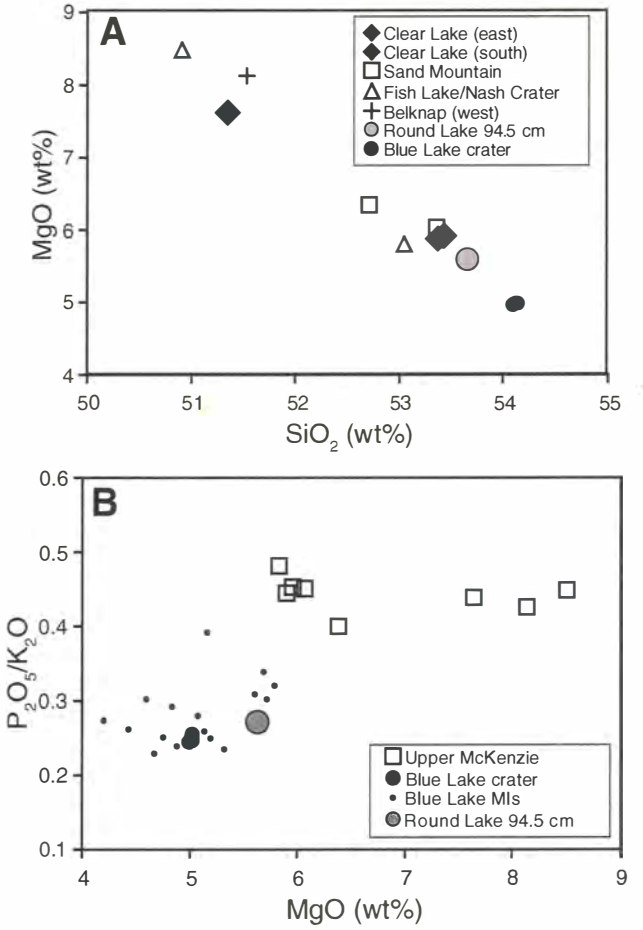

Figure 20. Geochemistry of Holocene flows from the upper McKenzie River and Santiam Pass areas. (A) A plot of wt% MgO versus wt% SiO_2 for lavas from Holocene vents in the upper McKenzie River (Sand Mountain chain, Fish Lake–Nash Crater, and the distal end of a flow from Belknap Crater). For comparison are shown lava samples from the southern and eastern side of Clear Lake, and tephra from Blue Lake crater. Note that young flows from the eastern margin of Clear Lake have compositions that are similar to those of the Sand Mountain chain, consistent with these being the sources of the lava flows (e.g., Taylor, 1990). (B) Comparison of bulk rock P_2O_5/K_2O compositions from upper McKenzie lavas (Fish Lake, Nash Crater, Sand Mountain chain, and Clear Lake lava flows), tephra and melt inclusion (MI) analysis from Blue Lake crater, and an ash layer from a Round Lake core. Because both P_2O_5 and K_2O are expected to act as incompatible elements except for late crystallization (as seen in the melt inclusion compositions), this ratio provides a useful fingerprint to distinguish the different magma types. Data from Conrey et al. (2002) and E. Johnson and D. McKay (2009, personal commun.).

east side of the lake are similar in composition to Sand Mountain (~53.4 wt% SiO_2, 5.9 wt% MgO) while the southern (damming) flow is substantially more mafic (51.3 wt% SiO_2; 7.6 wt% MgO). Placed in a larger context, the mafic composition of the damming flow is similar (although not identical) to early lavas from the northern end of the Sand Mountain chain (e.g., early Fish Lake lava), while the eastern flows are similar in composition to other lava samples from the southern Sand Mountain cone (Conrey et al., 2002).

Radiocarbon ages of ~2700–3000 yr B.P. obtained from a piece of a submerged tree at the southeast end of the lake (R. Conrey, 2009, oral commun.) correspond to dates obtained from charcoal fragments beneath the young lava flows on the lake's eastern shore, and have thus been used to date both the lake formation and part of the eruptive activity of the Sand Mountain chain (Champion, 1980; Taylor, 1965, 1990). Re-analysis of the submerged tree by anisotropy of magnetic susceptibility (AMS) yielded a radiocarbon age of 2750 ± 45 ^{14}C yr B.P. (2848 ± 69 cal. yr B.P.; Licciardi et al., 1999). Although considered by Taylor (1990) to be part of the same eruptive episode, no dates have been obtained for the damming flow.

Bathymetry measurements of Clear Lake made in September 2008 (Fig. 19) show that the lake is separated into two regions: a smaller northern region with a maximum depth of 18.5 m, and a large southern region with a maximum depth of 54 m. The two parts of the lake are separated by a bottleneck that has a maximum depth of 3 m. Drowned trees located during the same survey show that prior to inundation, the western slope was tree-covered to the valley floor (Fig. 19). The southern (damming) lava flow appears to correlate topographically with a submerged plateau at the southern end of the lake. However, there are standing trees on this platform, which indicate that this platform was not submerged prior to the last damming event. This observation, together with the more extensive vegetation cover and distinct composition of the damming flow, suggests that this flow may be substantially older than the accepted ca. 3000 yr B.P. age.

Clear Lake also provides a good opportunity to consider how the hydrology of this volcanic landscape is likely to change under conditions of climate warming (Fig. 21). Recent work suggests that Western and High Cascades streams are likely to respond quite differently (Tague and Grant, 2009). Both downscaled energy-balance models and empirical observations document that Cascade Range snow packs are diminishing and melting on the order of one to three weeks earlier, and will continue to do so in the future as the climate warms (Mote, 2003; Mote et al., 2005; Nolin and Daly, 2006; Jefferson et al., 2008; Tague et al., 2008). The consequences of reduced snow packs and earlier melting on streamflow will likely have different consequences in the Western and High Cascades. Simulations of effects of future climate on streamflow using RHESSys (Regional Hydro-Ecologic Simulation System), a distributed-parameter, spatially explicit, hydrologic model, reveal that Western Cascades streams will recede earlier in the year to minimum streamflow levels similar to those currently observed in summer months (Fig. 21B; from Tague and Grant, 2009). These low flows are remarkably similar from year to year under all climatic conditions, because they are constrained by an absence of significant groundwater storage. High Cascades streams, in contrast, will lose snowmelt peaks and also recede earlier, but because of large groundwater storage flux, will continue to recede throughout the summer (Fig. 21A). These results suggest that High Cascades streams will have higher winter flows than in the past but will also lose a larger proportion of their summer discharge than Western Cascades streams under conditions of climate warming.

In-Transit: Clear Lake to Santiam Pass

From Clear Lake we will drive north along the west side of the Sand Mountain chain of cinder cones to the extension of the chain at Nash and Little Nash cones and associated flows (Fig. 17). The volcanic history of the Sand Mountain region is described by Taylor (1965, 1990), who summarized the eruption history as including at least three distinct episodes: (1) early eruptions (ca. 3850 ^{14}C yr B.P.) from Nash Crater produced lava flows that traveled to the north and west and blocked drainages to create Fish Lake and Lava Lake; (2) eruptions that produced Sand Mountain and an extensive ash fall deposit (dated at ca. 3440 ^{14}C yr B.P.); and (3) eruptions along the southern segment that included the younger flows into Clear Lake (dated at ~2700–3000 ^{14}C yr B.P.). A lake core from Round Lake, north of Highway 22 and ~12 km east of the Sand Mountain chain, preserves ~0.75 m of tephra with geochemical similarities to Sand Mountain and is probably

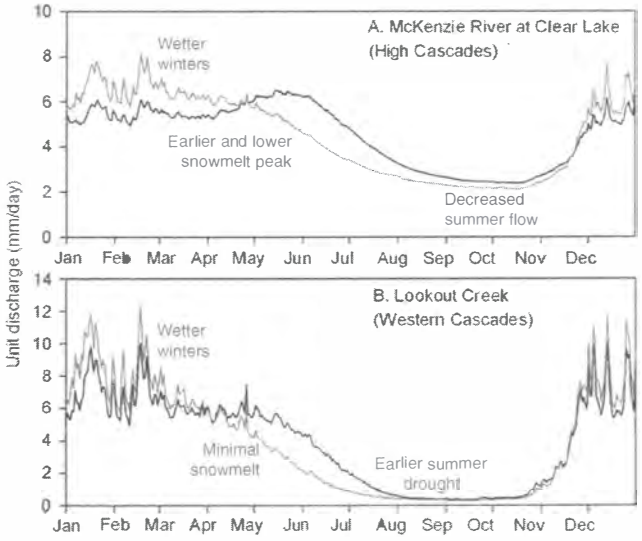

Figure 21. Modeled estimates of annual hydrograph and sensitivity to climate warming for (A) McKenzie River at Clear Lake and (B) Lookout Creek. Mean unit discharge is computed by averaging RHESSys (Regional Hydro-Ecologic Simulation System) estimates of daily streamflow (normalized by drainage area) for each day of year for 30 yr climate record. Black lines show estimated streamflow using baseline meteorologic data, and gray lines show estimated streamflow given a 1.5 °C warming. Modified from Tague and Grant (2009).

the same ash fall that was noted by Taylor (1965) and D. McKay (2008, personal commun.). Additionally, charcoal overlain by scoriaceous ash from Nash Crater has an age of 2590 ^{14}C yr B.P.; this ash is overlain, in turn, by scoria from Little Nash Crater (Sherrod et al., 2004). Thus it appears that the Sand Mountain chain has been intermittently active over a time period of at least 1500 yr during the past 4000 yr.

Between Fish Lake and Lava Lake, Highway 126 joins Highway 20 and then Highway 22, which travels east over Santiam Pass. Before reaching the pass, you will travel along the edge of Lost Lake, a shallow closed-basin lake with sinkholes in the lake bed. Lake levels fluctuate by >1 m, with the highest water during spring snowmelt and the lowest water levels at the end of the summer. Water draining from Lost Lake via the subsurface is inferred to re-emerge in Clear Lake (Jefferson and Grant, 2003).

Highway 22 crosses the northeastern Sand Mountain chain at Lost Lake and then bends south around Hogg Rock, one of two andesitic tuyas (the other is Hayrick Butte, to the south) that resulted from Pleistocene volcanism in this area. Hogg Rock has an age of 0.08 Ma (Hill and Priest, 1992), correlative with the onset of Wisconsin age glaciation. The spectacular exposure of glassy fine-scale columnar joints in the Hogg Rock roadcut is an example of an ice-contact morphology, where the columnar joints have formed by rapid cooling of the lava at the ice (water) interface (e.g., Lescinsky and Fink, 2000).

Directions to Stop 11

Exit Clear Lake Resort, turn right (north), and continue along Highway 126 for 3.4 mi to the junction with U.S. Highway 20. You will pass Fish Lake (now only seasonally wet) on your left, which was dammed by a lava flow from Nash Crater. Turn east on Highway 20 and continue for another 3.2 mi to the junction with Oregon Highway 22 (Santiam Junction). Continue east on Highway 20, passing south of the Lost Lake chain of cones and then around the western margin of Hogg Rock (4 mi from Santiam Junction). Cross Santiam Pass after 1.9 mi and continue another 3.9 mi to the Mount Washington and Blue Lake Crater overlook, on the right.

Stop 11. Mount Washington Overlook and Blue Lake Crater

This stop consists of two parts: first, a photo stop with a spectacular view of Mount Washington and second, an overlook of Blue Lake crater, another form of lava-water interaction.

Mount Washington is a mafic shield volcano composed of basaltic lava flows, accumulations of palagonitic tuff (evidence of subglacial eruption), and a central micronorite plug (Hughes and Taylor, 1986; Taylor, 1990; Conrey et al., 2002). No isotopic ages have been published for Mount Washington, but all samples have normal polarity magnetization, which, when considered with the geomorphology, indicate that Mount Washington is younger than 0.78 Ma.

Blue Lake crater sits east of the Cascade crest and is filled by a lake ~0.8 km long, 0.5 km wide, and >90 m deep. The lake is cold (2.5 °C at a depth of >10 m below the surface) and fed by springs. Its low temperature and low productivity contrast sharply with nearby Suttle Lake, which is shallow, warm, eutrophic, and glacial in origin (Johnson et al., 1985).

The geology of Blue Lake crater is described by Taylor (1965) as a series of three overlapping explosion craters that are rimmed by an agglutinate ridge covered with bombs (both juvenile and from older underlying lavas). It is commonly referred to as a maar in that it is a low-relief volcanic crater that is cut into the country rock below the general ground level (e.g., Fisher and Schmincke, 1984). Unlike most maars, however, which show evidence of extensive interaction with external water, Blue Lake crater deposits are dominated by vesicular scoria that appear to be the products of a magmatic (strombolian to violent strombolian) eruption. Tephra deposits reach a maximum depth near the vent of >5 m, and can be traced more than 6 km to the east-northeast (Fig. 22). The entire deposit volume estimated from the isopachs is $>\sim 4 \times 10^7$ m^3. The deposits are dominated by lapilli-sized scoria, with only the earliest erupted material enriched in fine particles, as might be expected, if meteoric water played an important role in the eruption process. Other evidence for magma as the primary driving force includes the high measured volatile content of olivine-hosted melt inclusions in the tephra (Fig. 23) and the near-absence of lithic (wall rock) fragments in the deposit, except for some late-stage bombs. The melt inclusion data are notable in that they show abundant H_2O and CO_2 and indicate a deep (magmatic, 230–320 MPa) rather than shallow (phreatomagmatic) source for the erupted material. The absence of associated lava flows may reflect the deep magma source and/or limited eruption duration; explosion craters may be the result of late-stage groundwater interaction.

Age constraints for Blue Lake crater are summarized by Sherrod et al. (2004). They include a maximum age of 3440 ± 250 ^{14}C yr B.P. reported by Taylor (1965) for a tree limb located at the interface between tephra from Blue Lake crater and underlying Sand Mountain ash, and a minimum age of 1330 ± 140 ^{14}C yr B.P. for charred forest litter beneath cinders from a chain of spatter cones 6 km SSW of (and on the same trend as) Blue Lake crater. Sherrod et al. (2004) prefer the latter date for Blue Lake crater because of both petrographic similarities in the erupted magma and the alignment of the vents. However, a core recently obtained from Round Lake, 3.6 km northwest of Blue Lake (Fig. 22), has a thin (~1 cm) mafic ash layer at a depth of 94.5 cm that is geochemically similar to Blue Lake crater tephra (Fig. 20B). If this correlation is correct, we can constrain the minimum age of Blue Lake crater to 1860 ± 25 ^{14}C yr B.P. using age constraints from organic material overlying Blue Lake crater ash in the core (C. Long, 2009, personal commun.).

Directions to Stop 12

Follow Highway 20 for 6.3 mi to Forest Service Road 1419 (McAllister Road); there should be a sign to Camp Sherman. Turn

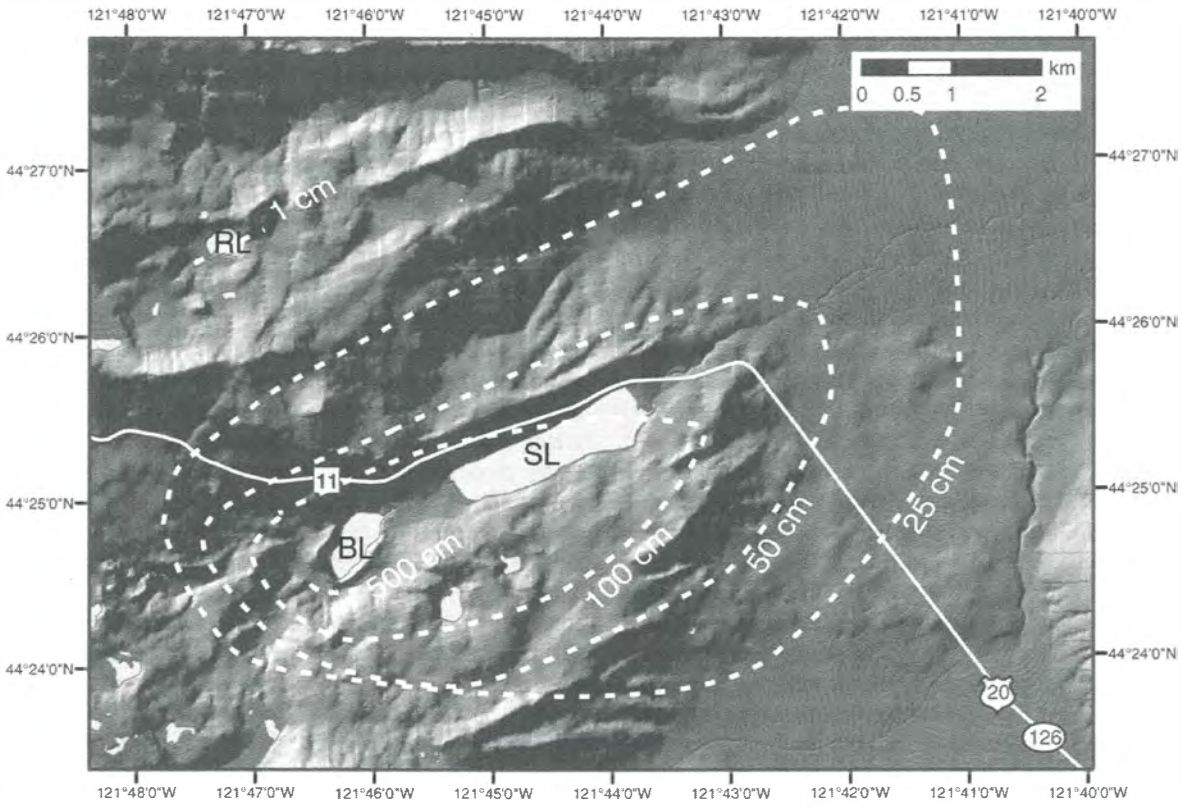

Figure 22. Isopach map showing the thickness of the tephra deposits (in cm) produced by the eruption of Blue Lake crater (BL). Isopachs are placed on shaded hillside digital elevation model that shows the elongated shape of Blue Lake crater and the location of nearby Suttle Lake (SL), which occupies a glacial trough. Also shown is the location of Round Lake (RL). Figure modified from Sherrod et al. (2004) with additional data from E. Johnson and D. McKay.

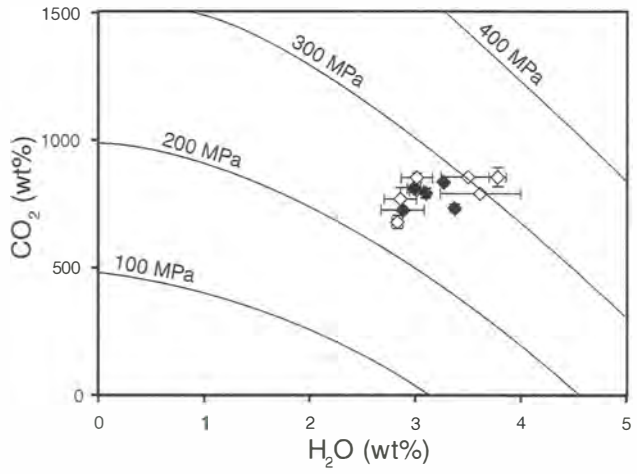

Figure 23. Volatile content of olivine-hosted melt inclusions from Blue Lake Crater tephra deposit. Open and closed symbols represent samples from the top and bottom of the deposit, respectively, and show that the entire eruption was driven by magma that derived from pressures of 220–320 MPa (~9–13 km). From E. Johnson, 2009, personal commun.

north on Road 1419 (McAllister Road) and go ~2.7 mi to Forest Service Road 14 (Metolius River Road). The turnoff to the Head of the Metolius parking lot will be ~1.6 mi on the left and is signed.

Stop 12. Metolius River Headwater Spring

The Metolius River emerges from the base of Black Butte and flows north along the base of Green Ridge for roughly 30 km until it turns east and flows another 30 km to join the Deschutes River (Fig. 24). The catchment of the Metolius River includes ~50 km of the axis of the Cascade Range. Mean annual discharge of the Metolius River (42 m^3/s) accounts for roughly one-third of the mean annual discharge of the upper Deschutes Basin (124 m^3/s) as measured at the gage near Madras.

The Metolius River is largely spring fed, as indicated by the remarkably constant discharge (Fig. 25). Most of the groundwater discharging to the stream emerges from springs along the main stem or lower parts of Cascade Range tributaries, and mostly within 20 km of the headwaters along the west side of Green Ridge. Measurements of flow at the headwaters spring range from 2.8 to 3.6 m^3/s.

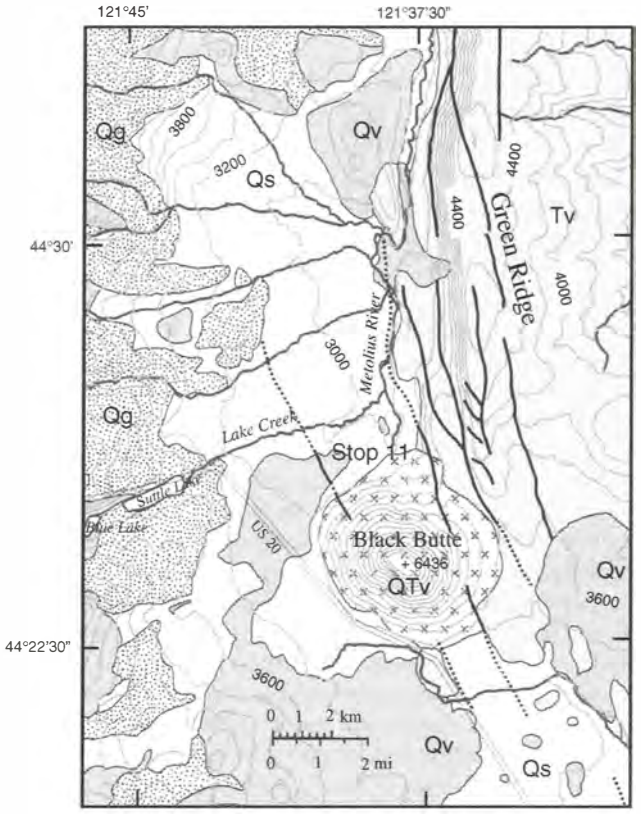

Figure 24. Generalized geology of the Black Butte–Green Ridge area. Key to map symbols: Qs—Quaternary glacial outwash and alluvium; Qg—Quaternary glacial drift; Qv—Quaternary volcanic deposits; QTv—Quaternary–Tertiary volcanic vents; Tv—Tertiary volcanic deposits; fault traces dotted where buried or inferred. Topographic contours and spot elevations in feet; geology from Sherrod and Smith (2000).

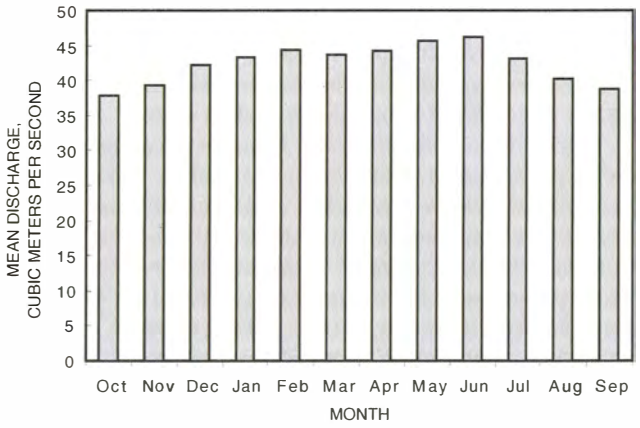

Figure 25. Mean monthly discharge of the Metolius River near Grandview (U.S. Geological Survey [USGS] gage number 14091500) for 1922–2008 from USGS streamflow data archive.

James et al. (2000) included the Metolius River headwaters spring in their analysis of groundwater flow in the Deschutes Basin using temperature, stable isotopes, and noble gases. The temperature of the headwater spring is ~8.2 °C (Table 2). The near-surface groundwater temperature at the mean recharge elevation inferred from oxygen isotope data (2200 m) is closer to 3 °C, indicating that the headwaters spring contains considerable geothermal heat. If one uses an average flow rate (3.1 m^3/s) and a conservative 4 °C rise in temperature along its flow path, the groundwater discharging at the Metolius headwater spring represents a geothermal heat output of ~50 MW. Blackwell et al. (1982) and Ingebritsen et al. (1994) describe a geothermal heat flux of over 100 mW/m^2 in the High Cascades. To pick up 50 MW, the groundwater discharging at the Metolius headwater spring would need to intercept all of the geothermal heat over an area of 400–500 km^2. The entire upper Metolius Basin encompasses ~1160 km^2. A 400 to 500 m^2 contributing area for the headwater spring is consistent with topography and surface drainage patterns in the Metolius and adjacent basins. A mass balance by Gannett and Lite (2004) indicates that there is a flux of ~23 m^3/s flowing to the Metolius River drainage from adjacent basins. The near-zero surface heat flux observed in the High Cascades (Ingebritsen et al., 1994) suggests that regional groundwater is indeed intercepting most of the geothermal heat flux.

Groundwater discharging at the Metolius headwater spring not only picks up geothermal heat along its flow path, but magmatic volatiles as well. Analysis of carbon and helium isotope data by James et al. (1999, 2000) indicates that the Metolius headwater spring contains a component of magmatic CO_2 and helium.

The age of water can be roughly calculated from mass balance considerations (Gannett et al., 2003). Assuming a 400 km^2 contributing area, a mean aquifer thickness of 300 m (consistent with estimates by Gannett and Lite, 2004), a porosity of 10%,

TABLE 2. TEMPERATURE, ALTITUDE, DISCHARGE, AND ISOTOPIC DATA FOR SELECTED SPRINGS IN THE UPPER DESCHUTES BASIN (FROM JAMES ET AL., 2000)

Spring name	Elevation (m)	Elevation (ft)	Temperature (°C)	Discharge (m^3/s)	$\delta^{18}O$ (‰)	$\delta^{13}C$ (‰)	^{14}C (pmc)	^{3}H (TU)
Browns Creek	1332	4369	3.8	1.1	−13.9	−16.4	115.3	6.9
Cultus River	1356	4448	3.4	1.8	−14.1	−15.8	113.9	9.0
Fall River	1286	4219	6.1	4.2	−14.2	−11.8	110.9	—
Lower Opal Springs	597	1959	12.0	6.8	−15.3	−12.7	60.0	0.8
Metolius River	920	3018	8.2	3.1	−14.7	−11.5	61.3	4.0
North Davis Creek	1323	4340	3.4	—	−14.1	−15.8	114.0	—
Quinn River	1354	4442	3.4	0.7	−13.7	−16.5	112.3	8.1
Snow Creek	1378	4521	5.5	0.8	−14.1	−12.9	111.1	—
Spring River	1268	4160	8.0	3.5	−14.6	−11.5	67.5	—

and an average discharge of 3.1 m^3/s, mean residence time would be ~120 yr. James et al. (2000) report a tritium content of 4.0 TU (Table 2), however, indicating that the Metolius headwater spring contains at least some component of modern water.

Black Butte, from which the Metolius River emerges, is described by Sherrod et al. (2004) as "a mildly eroded, steep sided lava cone whose pyroclastic center remains unexposed." Lavas of Black Butte are basaltic andesite with 5%–10% 1–2 mm plagioclase phenocrysts, and 3%–5%, 1 mm olivine phenocrysts. The potassium-argon age of the lava 1 km NE of the summit is 1.43 ± 0.33 Ma (whole rock) (Hill and Priest, 1992). Lavas of Black Butte exhibit reversed-polarity magnetization. The relatively pristine morphology of Black Butte stands in stark contrast to the glacially ravaged appearance of younger volcanic centers to the west, the difference owing to protection from glaciation by the rain shadow effect of the High Cascades.

Black Butte sits at the south end of Green Ridge, the eastern escarpment of the north-trending, 30-km-wide by 50-km-long High Cascades graben (e.g., Conrey et al., 2002). Formation of the graben commenced ca. 5.4 Ma, and since then the northern part of the upper Deschutes Basin has been effectively cut off from High Cascades volcanic centers (Smith et al., 1987; Sherrod et al., 2004). Green Ridge is capped by lava with an age of ca. 5 Ma. Displacement continued into early Pleistocene time, as lavas of Black Butte are offset by structures related to Green Ridge. Total offset exceeds 1 km based on drill-hole data at Santiam Pass (Hill and Priest, 1992; Sherrod et al., 2004).

The channel morphology of the upper part of the Metolius River should look familiar, as it is similar to the morphology of the spring-fed streams that we have seen on the west side. As on the west side, east side spring-fed streams are characterized by a constant flow throughout the year, so that they lack geomorphic features associated with either high flow events or substantial variations in flow, such as gravel bars and cut banks. Streams are usually close to bank full because seasonal stage variations are minimal, commonly on the order of a few to several centimeters. Vegetation typically extends right to the edge of the water, and flows required to mobilize large woody debris are lacking, so trees tend to stay in the stream and become covered with moss and grass. The hydrology and geomorphology of spring-fed channels in the Deschutes Basin is described by Peter Whiting and colleagues (Whiting and Stamm, 1995; Whiting and Moog, 2001).

Directions to Stop 13

Return to U.S. Highway 20 and head east 15.2 mi, through the town of Sisters, to Gist Road. Turn right on Gist Road and go 1.2 mi to Plainview Road. Turn left on Plainview road and go 0.3 mi to Sisemore Road. Turn right on Sisemore Road and proceed ~4.6 mi to the point where Sisemore Road crosses Tumalo Dam. The shoulder is narrow near the dam so it is best to proceed another couple hundred meters to the intersection with Couch Market Road where the road is wide enough to park.

Stop 13. Bull Flat and Tumalo Dam

Note: The Stop 13 description is adapted from Sherrod et al. (2002).

Our travel southeast from Sisters has generally followed the Sisters fault zone, which comprises nearly 50 mapped faults across a breadth of 5–15 km. Total length of the zone is 60 km; our stop here is about midway along it. This stop is at the most prominent strand, the Tumalo fault, which extends nearly continuously for 47 km. The Tumalo fault has displaced Pliocene lava flows of the Deschutes Formation by at least 60–70 m of normal separation at Tumalo Dam. Quaternary lava flows younger than 0.78 Ma in the same area have escarpments of only 6–10 m.

At Stop 13 we can see the geomorphic and stratigraphic contrast across the Tumalo fault (Fig. 26). On the northeast (upthrown) side are Pliocene strata of the Deschutes Formation. They are chiefly basaltic andesite lava flows. An andesitic ignimbrite (62% SiO_2; Smith, 1986a) is interlayered in the Deschutes sequence and visible in the roadcut at the east dam abutment. The Deschutes Formation units exposed here are probably ~4–5 Ma in age, although no isotopic ages have been reported from this area. Offset of at least 70 m is indicated by height of the Deschutes Formation ridge northeast of the fault and the absence of Deschutes Formation strata at the ground surface southwest of the fault. Cross sections by Taylor and Ferns (1994) suggest that the Deschutes Formation is buried by 50 m of volcaniclastic deposits in the downthrown block, in which case dip separation is 120 m.

On the southwest (downthrown) side is alluvium that floors Bull Flat, a treeless basin upstream from the dam. Middle Pleistocene pyroclastic-flow deposits are exposed locally where banked against the Deschutes Formation strata of the upthrown block or where the alluvium is thin on the floor of Bull Flat. It is likely that the ca. 0.6 Ma Desert Spring Tuff has been displaced several meters here, because no outcrops of the tuff are found on the downthrown side but are present on the upthrown block of the Tumalo fault near the dam. Displacement of younger pyroclastic-flow deposits is difficult to quantify because the pyroclastic flows may have overtopped topographic barriers and been deposited across a wide altitude range.

Bull Flat is an alluvial basin that likely has received sedimentary and volcanic deposits during at least the past million years. The water-table altitude is ~840 m in this area, and depths to water in wells average ~150 m. Neither the depth nor lithology of the subsurface fill is known. Rate of stream incision across the Tumalo fault in this area has kept pace with rate of uplift, however, because the distribution of all pyroclastic flows 0.6 Ma and younger suggests they escaped through channels cut through the upthrown block.

The west dam abutment is a Cascade Range basaltic andesite lava flow. Topographic escarpments only 6–10 m high mark the trace of the Tumalo fault across this flow. It possesses normal-polarity, thermal-remanent magnetization and is thought to be younger than 0.78 Ma. The lava flow is overlain upslope by the 0.2 Ma Shevlin Park Tuff.

The story of Tumalo Dam and its reservoir is one of broken promises and unfulfilled dreams, like many that surround

land-grab development of the arid west. In the 1890s, homesteaders were lured to this area by promises of free land and abundant water for irrigation (Winch, 1984–1985). By 1913, however, the private developers had gone bankrupt, and the promised water and delivery canals had not materialized. The State of Oregon stepped in to fulfill promises made to homesteaders and the federal government. Tumalo Dam was part of the attempt to provide the promised irrigation water.

The dam, constructed in 1914, is a 22-m-tall earth-fill structure with a steel-reinforced concrete core. The outlet was a 2.5 m × 2.5 m, concrete-lined tunnel 123 m long. Flow through the outlet was to be controlled from the small house at the end of the dam. The reservoir was to cover 447 ha and impound 24.7×10^6 m^3 of water. The dam was completed and the sluice gates closed on 5 December 1914.

Prior to construction, geologists expressed concern about the permeability of strata bounding the reservoir. These concerns were confirmed early in the winter of 1915 as the reservoir, at only a fraction of its capacity, saw its water level falling 0.2 m per day. When runoff increased in March and April and the water level started to rise, large sinkholes developed along the eastern margin of the reservoir not far south of the dam (perhaps along the Tumalo fault). The largest sinkhole was 9 m × 15 m across and 3–8 m deep, swallowing water at an estimated rate of 5.7 m^3/s. Attempts to seal the reservoir failed, and Tumalo Dam was never used. An excellent history of the Tumalo project is provided by Winch (1984–1985).

The Sisters fault zone is roughly on trend with a pronounced groundwater gradient (high–head-gradient zone) that characterizes the Deschutes Basin northwest from Bend for 60 km to Suttle Lake in the Cascade Range (Fig. 27). The fault zone and groundwater gradient are displaced from each other by roughly 10 km, however, with the groundwater gradient lying closer to the topographic slope of the Cascade Range. There is no evidence that the Sisters fault zone has a measurable effect on the distribution of groundwater. This observation is unsurprising stratigraphically because the upper Miocene and lower Pliocene strata of the Deschutes Formation on the upthrown side of faults along the zone are similar in permeability to upper Pliocene and Pleistocene deposits along the downthrown side. Thus, permeability contrasts across the faults likely are few. Groundwater damming would occur only if these faults had created substantial gouge, or if fault offsets occurred rapidly enough or were sufficiently great to create numerous or extensive closed basins.

Directions to Bend Oregon (End of Day 2)

From Tumalo Dam follow Sisemore road 0.2 mi south to Couch Market Road. Follow Couch Market Road east 3.5 mi to U.S. Highway 20. Turn right and follow U.S. 20 ~8 mi into Bend.

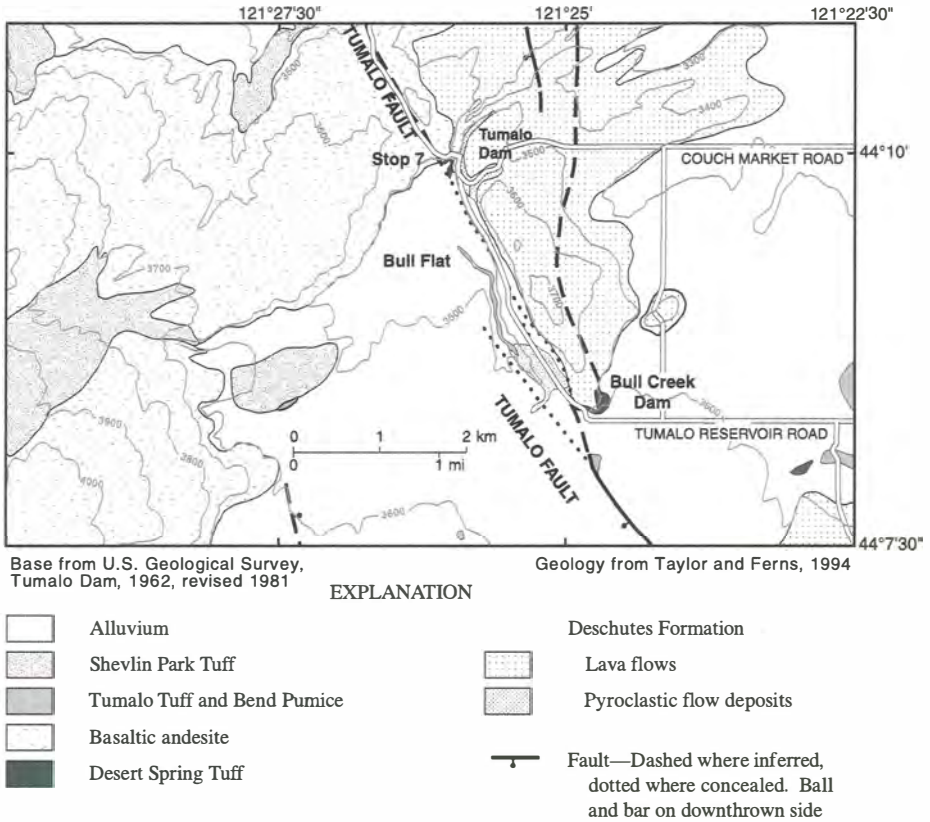

Figure 26. Geology of the Bull Flat–Tumalo Dam area. Illustration from Sherrod et al. (2002).

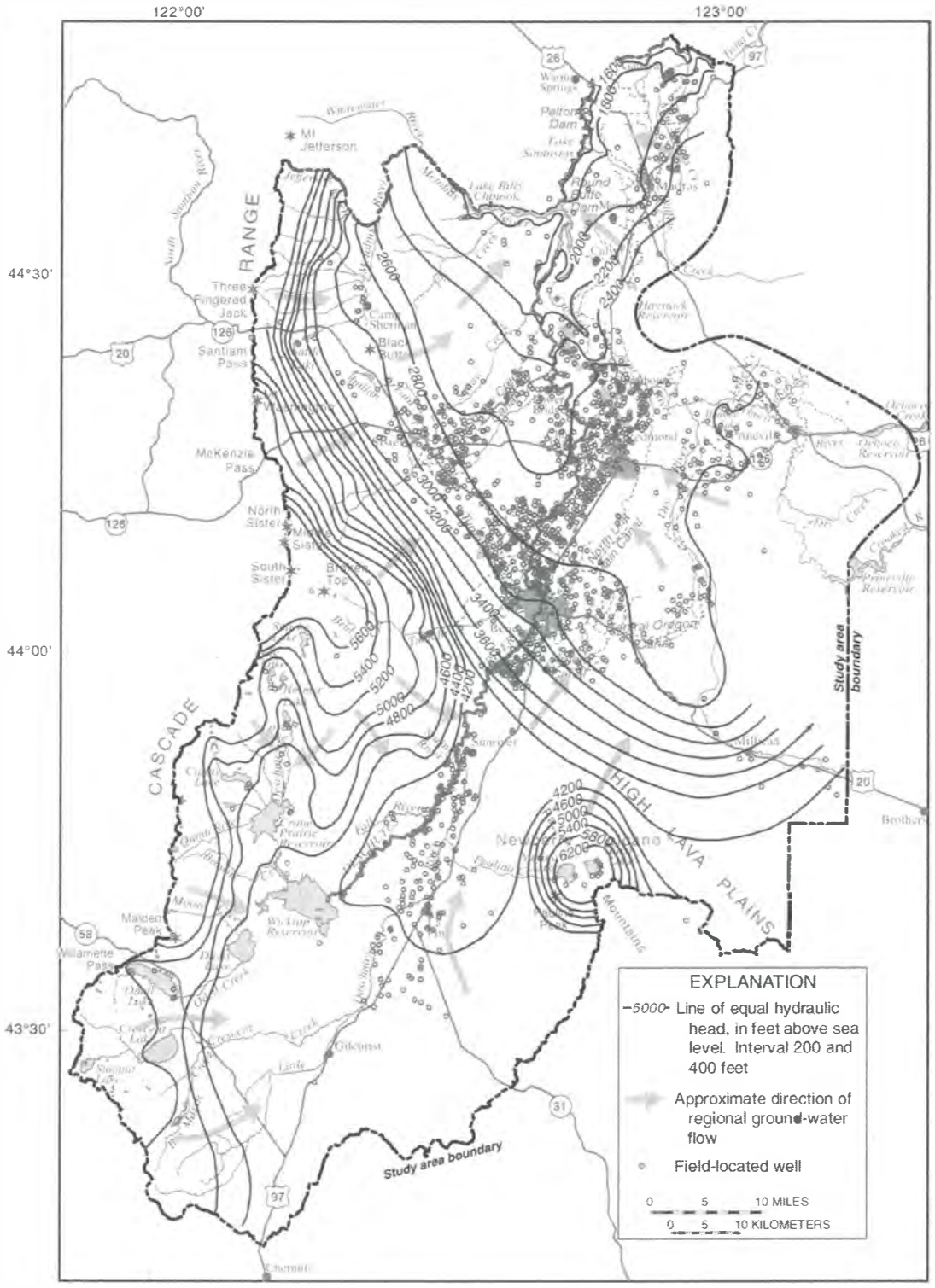

Figure 27. Generalized lines of equal hydraulic head and groundwater flow directions in the upper Deschutes Basin. From Gannett et al. (2001).

DAY 3. BEND, OREGON TO PORTLAND, OREGON

Note: All but the first paragraph of the Day 3 overview is adapted from Sherrod et al. (2002).

The third day of the trip covers the upper Deschutes Basin from Lava Butte to the point where the Deschutes River has incised down to early Tertiary deposits near the town of Warm Springs. The first stop is Lava Butte, one of many cinder cones dotting the northwest rift zone of Newberry Volcano (Stop 14). Lava Butte sits near the northern end of a sediment-filled graben (the La Pine subbasin) that separates Newberry Volcano from the Cascade Range in this area. Flows from Lava Butte displaced the Deschutes River westward against older deposits resulting in a series of waterfalls including Benham Falls (Stop 15). North of Lava Butte, the route continues on the surface of lava flows from Newberry Volcano, crossing the southern end of the Sisters Fault zone as it descends into the Bend area (Stops 15 and 16).

The traverse from Bend to Madras (Fig. 28) is within a broad valley dominated by a gently northward-sloping surface with scattered low hills. Many of the hills consist of cinder cones, small shield volcanoes, and silicic domes, mainly of the upper Miocene to Pliocene Deschutes Formation. Several small canyons form a northeast-trending topographic grain on the west side of the valley, exposing lava flows, ash-flow tuff, and sedimentary strata deposited as a result of volcanic eruptions during Deschutes time. We will drive down one of these canyons (Buckhorn) on our way to Lower Bridge (Stop 18).

The central and eastern surface in the southern part of the valley is flat and covered predominately with Pleistocene lava flows originating from Newberry volcano, which forms part of the southeast basin margin. Some of the lava flows from Newberry volcano traveled tens of km and entered the ancestral Deschutes and Crooked Rivers as intracanyon flows (Stop 19). Remnants of these lava flows form conspicuous benches within the canyons of the Deschutes and Crooked Rivers in the northern part of the valley. The eastern boundary of the valley consists of hills of mainly silicic rocks of the Oligocene to Miocene John Day Formation.

The modern Deschutes and Crooked Rivers form shallow incised drainages in the southern part of the valley but have carved narrow deep canyons in the northern half. These deep canyons expose much of the strata of the Deschutes Formation, including lava flows, ash-flow tuffs, debris-flow deposits, and fluvial silt, sand, and gravel deposits. Our hike down into the Crooked River canyon (Stop 20) will be an opportunity to examine some of those deposits in detail. By ~7 km downstream from Round Butte Dam, the Deschutes River has cut through the entire thickness of the Deschutes Formation, exposing the underlying Simtustus Formation and Prineville Basalt (Stop 21). Approximately 8 km downstream from that point, at about the location of the regulator dam, the river has cut down to the John Day Formation (Optional Stop 22).

The broad flat area between the Deschutes River canyon and Madras, known as the Agency Plains, is underlain by Deschutes Formation lava flows (the basalt of Tetherow Butte). These

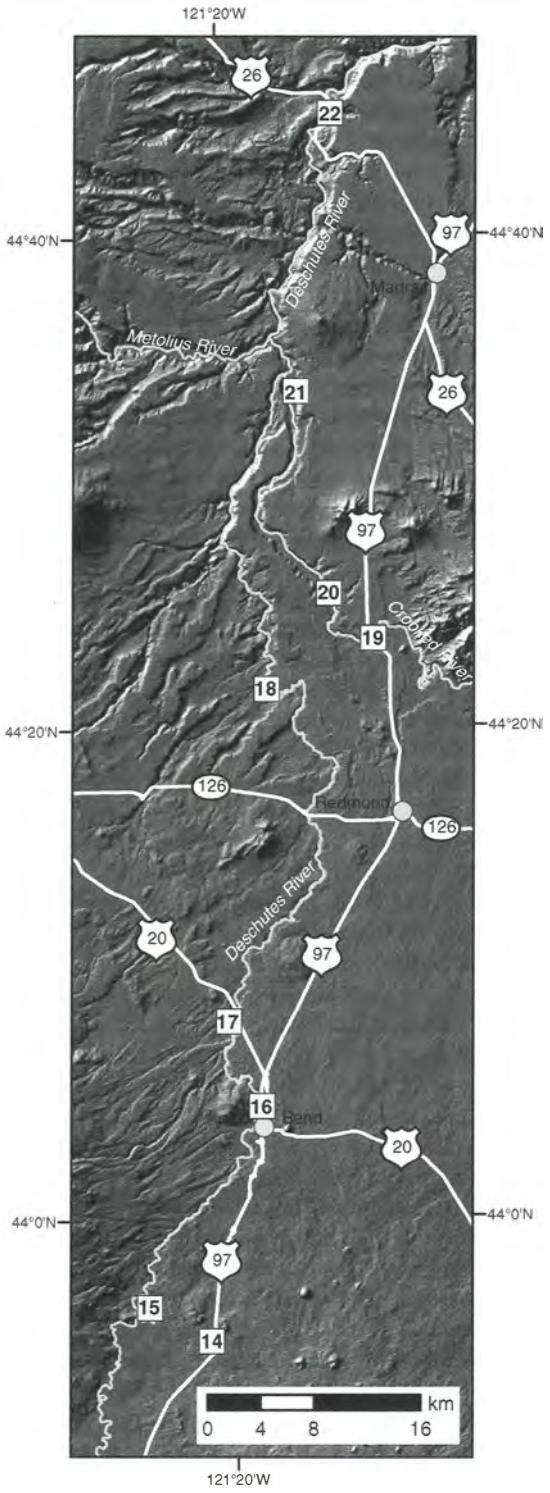

Figure 28. Overview map of Day 3, Stops 14 through 22 (squares). Shaded relief map created from a 10 m digital elevation model shows notable features including the cinder cones and young flows of Newberry Volcano to the southwest and the evolution of the Deschutes River valley from south to north.

flows cover only the west side of the Agency Plains. The eastern side, including Madras, is underlain by fine-grained sedimentary deposits of the Deschutes Formation shed mainly from the uplands to the east.

Groundwater Flow from Bend to Madras

Throughout the area between Black Butte and Madras, groundwater flows generally northward through sediment and lava of the Deschutes Formation toward the confluence of the Deschutes and Crooked Rivers. The overlying Pleistocene lava flows from Newberry volcano and pyroclastic deposits from the Bend highlands are largely unsaturated. The area around Bend extending north to Tumalo is characterized by a large vertical head gradient indicating strong downward vertical flow. Shallow wells in the area may have static water levels less than 30 m below the land surface, whereas nearby deep wells may have depths to water exceeding 200 m. The presence of the shallow water table and strong downward vertical gradient is attributed to local, and at least partly artificial, recharge from canal and stream leakage. Such areas of artificial recharge and anomalously shallow saturated zones are far less common to the north around Redmond. The water table slopes gently northward from Bend (Fig. 27) toward the Deschutes-Crooked Rivers confluence area with a gradient of ~3.8 m/km. The stream gradient, however, is somewhat steeper, averaging 6.2 m/km between Bend and Lower Bridge. As a consequence, the canyons of the Deschutes and Crooked Rivers intersect the regional water table several km north of Redmond.

The Deschutes River intersects the regional water table at about Lower Bridge (Fig. 27; river mile 134), and the Crooked River intersects the regional water table at about Trail Crossing (river mile 20.6), ~2.1 km northeast of the U.S. Highway 97 bridge. Downstream from these sites, the altitudes of the streams are below that of the regional water table, and groundwater flows toward, and discharges to, the streams, resulting in substantial increases in streamflow. Between the points where the Deschutes and Crooked Rivers intersect the regional water table and the point where the Deschutes River intersects the John Day Formation, the combined streams gain ~63 m^3/s from groundwater inflow (Gannett et al., 2001).

North of the Pelton re-regulation dam (at river mile 100), the Deschutes Formation thins against the underlying units and pinches out by about river mile 87. Below this point, the Deschutes River gains little, if any, flow from groundwater discharge, and the modest increases in flow that do occur are due to tributary inflow.

Directions from Bend to Stop 14

Follow Highway 97 south out of Bend (toward Klamath Falls) ~11 mi to the entrance to Lava Lands Visitor's Center on the west side of the highway. If the road is open, proceed up to the parking lot at the top of the cinder cone.

Stop 14. Top of Lava Butte

Note: From Sherrod et al. (2002).

A couple hundred large and small volcanoes and nearly two-thirds of the upper Deschutes Basin may be seen from the splendid vista atop Lava Butte. A simplified compass wheel shows the declination and distance to many features visible from the lookout on a clear day (Fig. 29).

Newberry Volcano is a large mafic shield volcano that lies south of Bend, Oregon, at the western end of the High Lava Plains. Lava Butte lies at the distal end of Newberry Volcano's northwest rift zone, which was active most recently between ~5900 and 6400 ^{14}C yr B.P. (MacLeod et al., 1995). A radiocarbon age of 6160 ± 70 ^{14}C yr B.P. was obtained from charcoal collected beneath Lava Butte's tephra plume where exposed in a highway roadcut northeast of the butte (Chitwood et al., 1977). The tephra immediately overlies silicic tephra from the eruption of Mount Mazama that created Crater Lake (dated at 6845 ^{14}C yr B.P.). Most of these Holocene northwest rift zone vents lie along a single fissure; resulting flows form a nearly continuous band of young lava that stretches 31 km from the north rim of the caldera to the Deschutes River and comprises ~0.7 km^3 of lava (Jensen, 2006). However the flows are variable in composition, ranging from the basalt of the Sugarpine

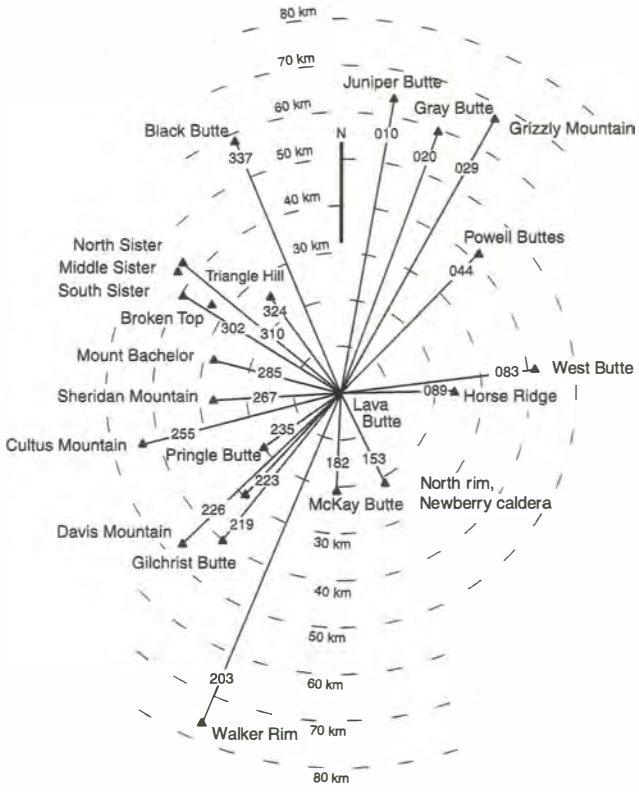

Figure 29. Compass wheel showing direction and distance to some geographic features visible from the top of Lava Butte. From Sherrod et al. (2002).

vents (which lie to the southwest of the rift zone) to the basaltic andesites and andesites of Lava Butte and Mokst Butte (MacLeod et al., 1995; Jensen, 2006), which suggests that they may not be the result of a single eruption. The large cones of Mokst Butte and Lava Butte also produced extensive lava flows and limited tephra sheets, suggesting that components of both eruptions were violent strombolian in eruptive style.

Lava flows of the northwest rift zone merge with lava flows from the Cascade Range to form the northern limit of the La Pine subbasin today and probably for a substantial part of the subbasin's history. Emplacement of the Lava Butte flow diverted the Deschutes River, forcing the river to establish a new channel along the west margin of the lava flow.

The topographic gradient increases abruptly north of the contact between the lava of Newberry Volcano and the Cascade Range, from relatively flat in the sediment-filled basin south of here to prominently northward sloping to the north. The stream gradient reflects this topographic change. The Deschutes River drops a mere 0.48 m/km along the 71 km reach between Wickiup Reservoir and Benham Falls. North of Benham Falls the gradient steepens to 8.7 m/km along the 18.5 km reach to Bend.

The slope of the water table also increases north of Benham Falls, but to a greater degree. The water table is roughly 3 m below the land surface in much of the La Pine subbasin. Starting at Sunriver 8 km south of Lava Butte, the water table slopes northward so steeply that at Bend the depth to water is 170–200 m below land surface. Near the river at Benham Falls, the water table is at an altitude of ~1260 m and 1.5–5 m below land surface (Fig. 27). In downtown Bend, the water table is at an altitude of 940 m, and land surface is 1110 m.

Directions to Stop 15

From the Lava Lands Visitor's Center, take Forest Service Road 9702 (Crawford Road) 4 mi west to the Benham Falls Picnic Area parking lot.

Stop 15. Benham Falls—Incursion of the Lava Butte Flow into the Deschutes River

Lava flows from Lava Butte entered the Deschutes River in several places, most of which are now marked by the rapids that attract rafting trips along this stretch of the Deschutes. Jensen (2006) provides a detailed reconstruction of the pre-eruption Deschutes channel, the syneruptive and posteruptive extent of a lava-dammed lake (Lake Benham), and a reconstruction of the gradual creation of the present-day river channel through this area, which we summarize here (Fig. 30).

The lava flow lobe that entered the Deschutes River south of Benham Falls dammed the river to create Lake Benham (Fig.

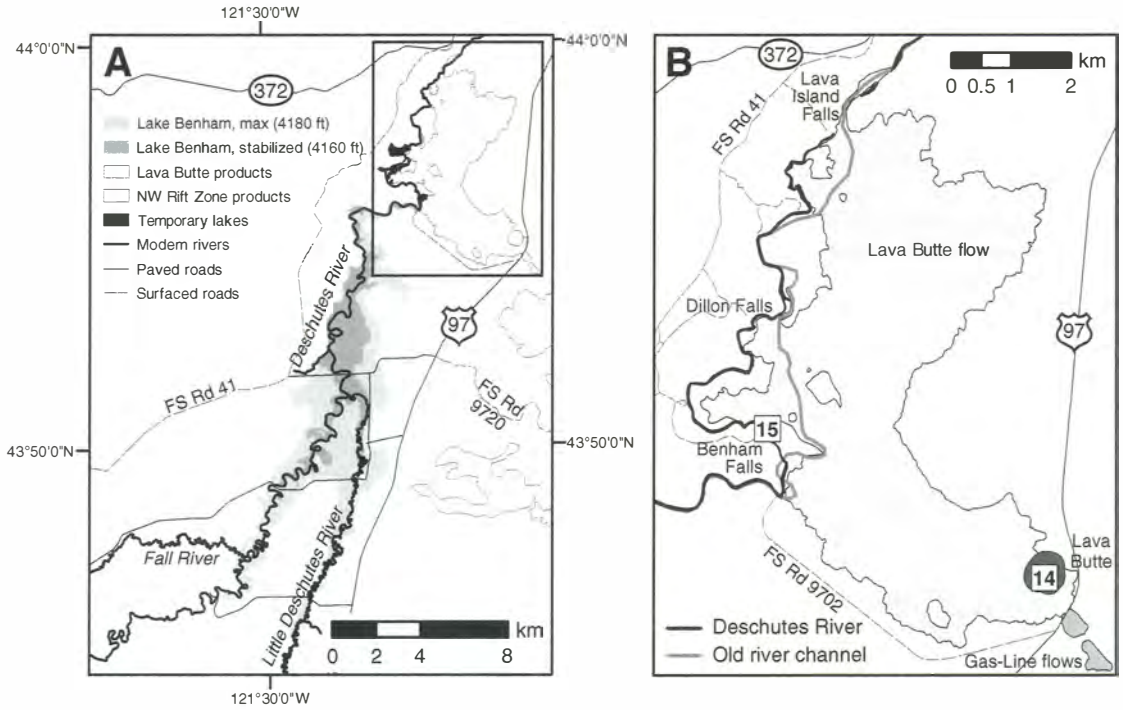

Figure 30. (A) Map showing the extent of Lake Benham, formed when the young (<7000 ^{14}C yr B.P.) lava flow from Lava Butte blocked the ancestral Deschutes River. (B) Enlargement of the Lava Butte flow showing the current and (inferred) ancestral Deschutes channels. Both maps were redrafted from Jensen (2006).

30A). Radiocarbon dates of roots help constrain the timing (and extent) of this lake. Immediately following the eruption, the lake stood at an elevation of 1274 m. By 5890 ^{14}C yr B.P., the lake elevation dropped and stabilized at 1268 m. Plant material from the top of the diatomaceous lake sediments suggests that the lake existed until 1950 ^{14}C yr B.P., at which point the Deschutes River had sufficiently reestablished itself to drain the lake.

Benham Falls provides a good opportunity to examine the gradual erosion of a lava flow dam. Just upstream lies the southernmost incursion by the lava into the river channel (Fig. 30B). At this point the lava was in contact with a soft, and easily eroded, 1.8 Ma rhyolite dome (Fiebelkorn et al., 1983). Where the lava banked up against older (and harder) basalts, channel erosion has been less efficient, as illustrated by the presence of Benham Falls. A series of meadows downstream of Benham Falls suggest that the river gradually reestablished itself, forming a sequence of temporary lakes where the lava flow had invaded its channel. These lakes existed until the river was able to carve a new channel. Alternatively, depending on the timing of lava incursions into the river channel, these meadows may reflect temporary lakes that formed by syneruptive displacement of the river (i.e., before the formation of Lake Benham). Determining the exact timing of lava-river interactions along this stretch of the Deschutes River will require detailed studies of sediments preserved within the meadows.

Following a familiar theme, Benham Falls was investigated as a potential site for power generation or reservoir site for irrigation (U.S. Reclamation Service, 1914). Drill holes employed for site surveys in this area showed that the paleo–Deschutes canyon was 24 m deeper than the current river channel. These studies also concluded that any dam site in the vicinity of Benham Falls would leak badly; dams were subsequently built upstream to form Crane Prairie and Wickiup Reservoirs. Flow of water through the Lava Butte flow is indicated by local springs at the base of the lava flow near Dillon Falls, which suggest that Lake Benham may have been impounded by a leaky, rather than impermeable, lava dam.

Groundwater studies show net transfer of water from the river into the lava flow, driven by the northward-increasing depth to water table in this area as described above. South of Sunriver, the Deschutes River system gains water due to groundwater discharge, and major spring complexes are common. North of Sunriver, the streams lose water to the groundwater system as groundwater levels drop far below stream altitudes. For example, stream gage data from the 1940s–1950s showed that the Deschutes River lost an average of 0.68 m^3/s between Sunriver and Benham Falls. The average loss between Benham Falls and Lava Island, ~12 km downstream, is 2.3 m^3/s. Most of the loss likely occurs where the channel crosses or is adjacent to the lava flows from Lava Butte. This lava is sufficiently young that fractures have not been sealed by sediment, and water easily leaks through the streambed or channel walls and into underlying lava flows.

In stops farther north we will see that conditions are reversed and the regional water table is above river level, causing groundwater to once again discharge to streams. The relation between topography and groundwater level in the upper Deschutes Basin is shown diagrammatically in Figure 31.

Note: The remainder of the discussion for Stop 15 is taken verbatim from Sherrod et al. (2002).

The rate of leakage from the Deschutes River in the Benham Falls area is proportional to the river stage and hence streamflow (Gannett et al., 2001)—the higher the stage, the greater the rate of loss. The groundwater level near the river varies in response to variations in the leakage rate. Continuous-recorder hydrographs show how the water table responds to changes in streamflow (Fig. 32). The stage and discharge in the Deschutes River in this reach are controlled by reservoir operations upstream. Streamflow is highest from April to October as water is routed down from the reservoirs to canal diversions near Bend. The water level in well 19S/11E-16ACC, ~150 m from the river near the Benham Falls parking area, rises and falls rapidly in response to river stage. Abrupt changes in streamflow usually become apparent in the

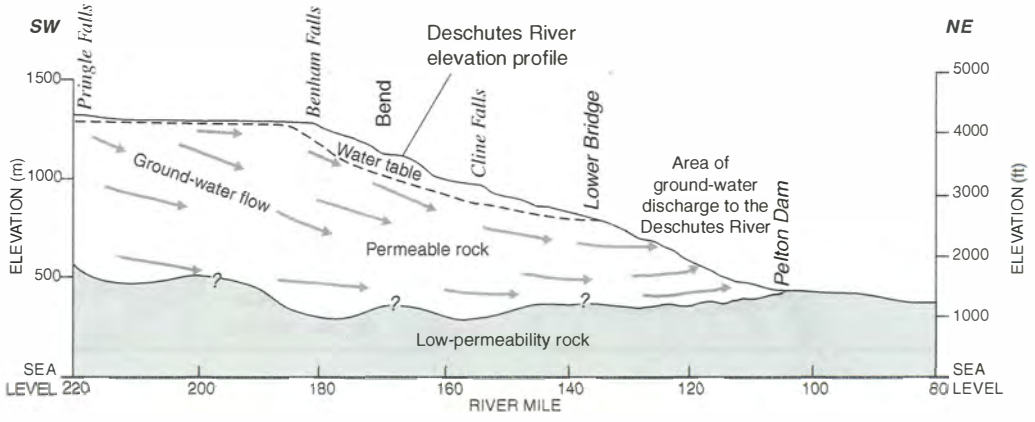

Figure 31. Diagrammatic section showing the effect of geology and topography on groundwater discharge along the Deschutes River from Benham Falls to Pelton Dam. Modified from Gannett et al. (2001).

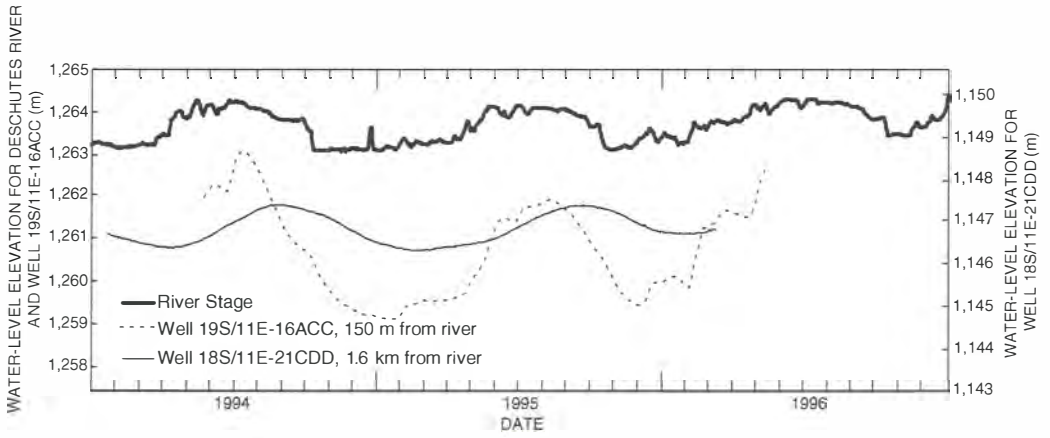

Figure 32. Hydrograph showing the relation between the stage of the Deschutes River at Benham Falls and water levels in wells 150 and 1600 m from the river. Modified from Gannett et al. (2001).

well within a few to several days. These effects are much less pronounced, however, in wells farther from the river. The water level in well 18S/11E-21CDD, ~1.6 km from the river, also fluctuates in response to river stage, but the fluctuations are subdued and the hydrograph is nearly sinusoidal, showing only the slightest inflections in response to abrupt changes in streamflow. In addition, the peaks and troughs in the hydrograph of well 18S/11E-21CDD lag those of well 19S/11E-16ACC by one to two months (Fig. 32).

Lithologic and geophysical logs from wells provide limited stratigraphic information for the Lava Butte area. The driller's log from the well at the Lava Lands visitor center, just south of the butte, describes a more or less monotonous stack of interbedded lava and cinders to a depth of 155 m. The driller's log for a test well east of U.S. Highway 97 shows predominantly lava and cinders to a depth of 91 m underlain by 12 m of tan sandstone in turn underlain by 12 m of white pumice. A gamma log (Fig. 33; Sherrod et al., 2002) indicates that these latter strata are silicic, so we interpret the "sandstone" and pumice to be the Tumalo Tuff and Bend Pumice (described at Stop 17). Although ambiguous, descriptions for the 19.5-m section below the silicic deposits suggest interbedded lava and sediment. At the base of Lava Butte, the water table is at ~1251 m and lies ~122 m below land surface.

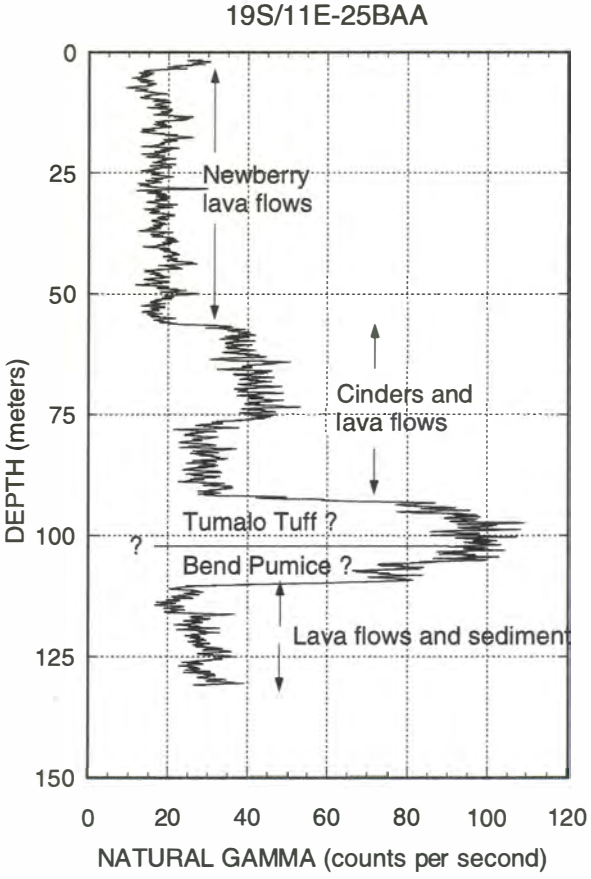

Figure 33. Natural gamma log and inferred stratigraphy in a well east of U.S. Highway 97 near Lava Butte. From Sherrod et al. (2002).

Directions to Stop 16

Return to Highway 97 at Lava Lands Visitor's Center. Drive north 11.5 mi on U.S. Highway 97, which becomes the newly completed Bend Parkway through downtown Bend. Take Exit 137 (Revere Avenue–Downtown) straight through traffic signal onto Division Street. Proceed on Division Street 0.5 mi from traffic signal to Riverview Park's tiny parking area on west side of road. Diversion dam and head gates are seen just north of parking area.

Stop 16. Surface-Water Diversions in Bend

Note: From Sherrod et al. (2002).

At this stop we can see the dam and headgates for diversion into the North Unit and Pilot Butte canals (Fig. 34). The dam, near river mile 165, was constructed in the early 1900s as part of the diversions (K.G. Gorman, 2001, oral commun. 2001). It also once served as a hydropower impoundment. Some of the original power-generating equipment is visible downstream from the dam.

During the irrigation season, water is diverted from the Deschutes River between Lava Butte and Bend into irrigation canals at a rate of ~57 m^3/s (Gannett et al., 2001), equivalent to an average annual rate of ~28 m^3/s. The North Unit and Pilot Butte canals account for roughly one-half the total diversion. Most canals are unlined and leak considerably. Overall transmission losses approach 50% and are even greater where the canals cross fractured Pleistocene lava. Water lost from canals infiltrates and recharges the groundwater system. Although the canals lose large amounts of water, the Deschutes River north of Bend shows little or no loss. The probable reason for the lack of stream leakage is that lava in the stream channel north of Bend is sufficiently old that fractures have been sealed by sediment.

Total canal losses north of Bend approach a mean annual rate of 14 m^3/s, more than 10% of the long-term average recharge from precipitation in the entire upper Deschutes Basin, which is ~108 m^3/s (Gannett et al., 2001). Groundwater flow directions inferred from head maps (Fig. 27) suggest that the lost canal water should flow toward the lower Crooked River. Comparing rates of estimated canal losses with long-term streamflow records confirms that this is the case. Figure 35 shows the estimated annual mean canal losses from 1905 to 1998. Also shown are the August mean flows of the lower Crooked River for the same period. During August, flows of the lower Crooked River are due almost entirely to spring

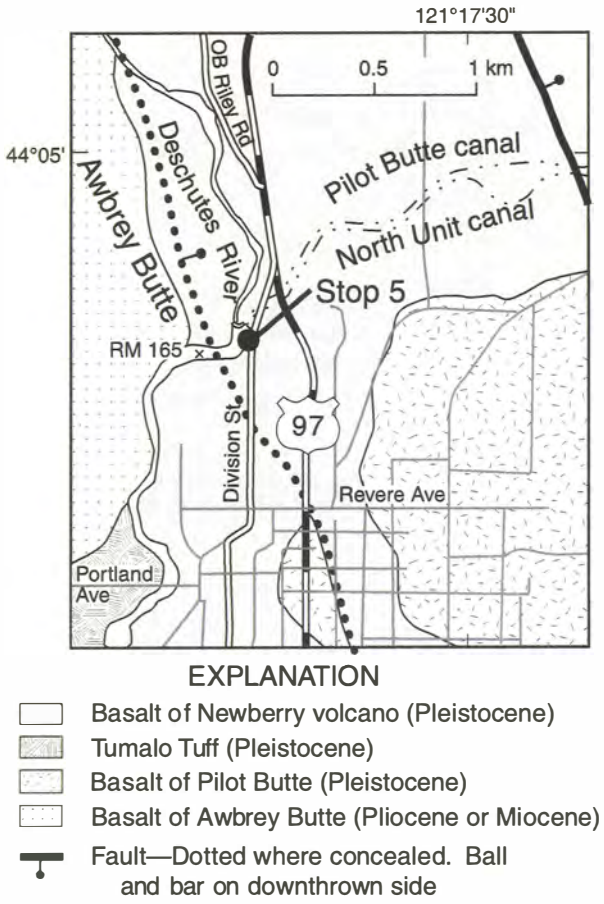

Figure 34. Map showing the Deschutes River diversions for the North Unit and Pilot Butte canals near Bend. From Sherrod et al. (2002).

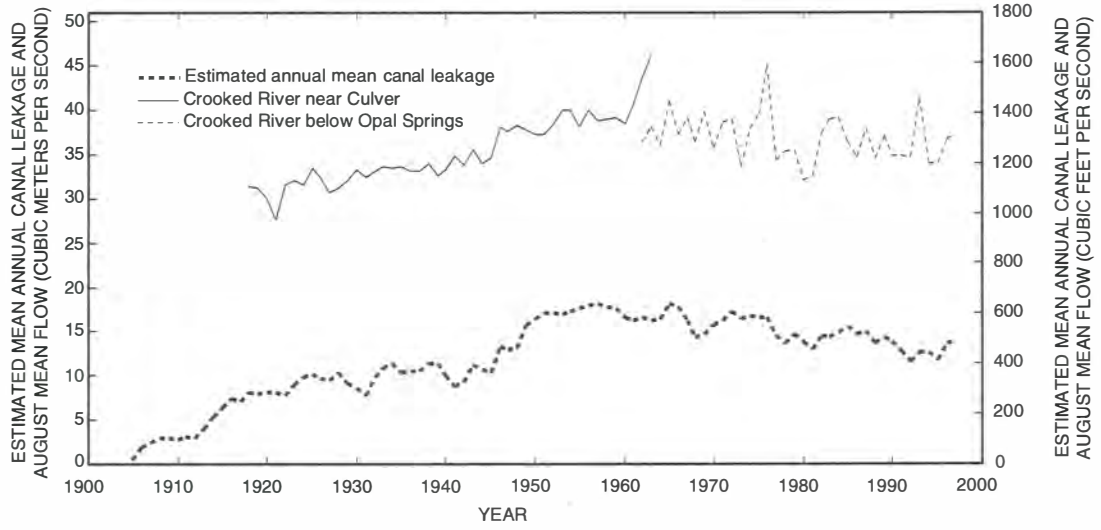

Figure 35. Hydrograph showing estimated canal losses north of Bend and August mean discharge of the Crooked River. Modified from Gannett et al. (2001).

discharge, and variations in August mean flows are a good proxy for variations in groundwater discharge (baseflow). As shown in Figure 35, baseflow to the lower Crooked River increased in a manner similar to the estimated canal losses throughout most of the past century. This relation has implications for water management as efforts to conserve water by lining the canals will result in reduced streamflow in the lower Crooked River.

Many wells in the Bend area have static water levels greater than 200 m below land surface. Some wells, however, have depths to water ranging from 30 to 60 m. Many of these shallower saturated zones are artificially recharged from canal leakage and deep percolation of irrigation water. Historic data are insufficient to determine precisely how much shallow groundwater is canal derived and how much might result from natural stream leakage.

Groundwater levels show varying rates of response to changes in canal flow depending on the permeability of bedrock, as described in detail by Gannett et al. (2001). For example, the static water level in a well 5 km southeast of here, drilled in fractured lava 1 km from the Arnold canal, responds within a matter of days to canal operation (Fig. 36A). In contrast is a well on the north side of Redmond in an area mapped as the 3–4 Ma basalt of Dry River and yields water from underlying sedimentary strata of the Deschutes Formation The water level in this well, 0.4 km west of the Pilot Butte canal, has a greater lag time and more subdued response (Fig. 36B). It begins to respond two months after canal operation begins and peaks one to two months after the canals are shut off for the year.

Directions to Stop 17

Drive north 0.2 mi on Division Street to intersection with U.S. Highway 97 business route. North 0.3 mi to O.B. Riley Road. West 4.1 mi on O.B. Riley Road to Tumalo Reservoir Road, which lies just beyond crossing of Deschutes River. West (left) 0.5 mi on Tumalo Reservoir Road, then park on road shoulder. Stop 17 is prominent exposure of pyroclastic deposits quarried north of road.

Stop 17. Tumalo Reservoir Road—Sisters Fault Zone Outcrop

Note: From Sherrod et al. (2002).

This stop shows in cross section a minor fault of the Sisters fault zone. The quarried exposure shows Bend Pumice (fallout tephra), Tumalo Tuff (pyroclastic flow), and overlying gravel deposits cut by a steep northwest-striking fault with offset less than 4 m, down on the northeast side. Although they were given different names, both deposits were formed from a single eruption ca. 0.4 Ma ago, based on ages obtained by both conventional K-Ar (Sarna-Wojcicki et al., 1989) and step-heating $^{40}Ar/^{39}Ar$ methods (Lanphere et al., 1999). The capping gravel deposit is undated. Thus latest fault motion here is known only to be younger than 0.4 Ma. Exposed in adjacent roadcuts are older deposits, including the underlying Desert Spring Tuff, which is 0.6 Ma in age.

Groundwater levels in this area are elevated slightly due to canal losses and irrigation (Gannett et al., 2001). The water table is

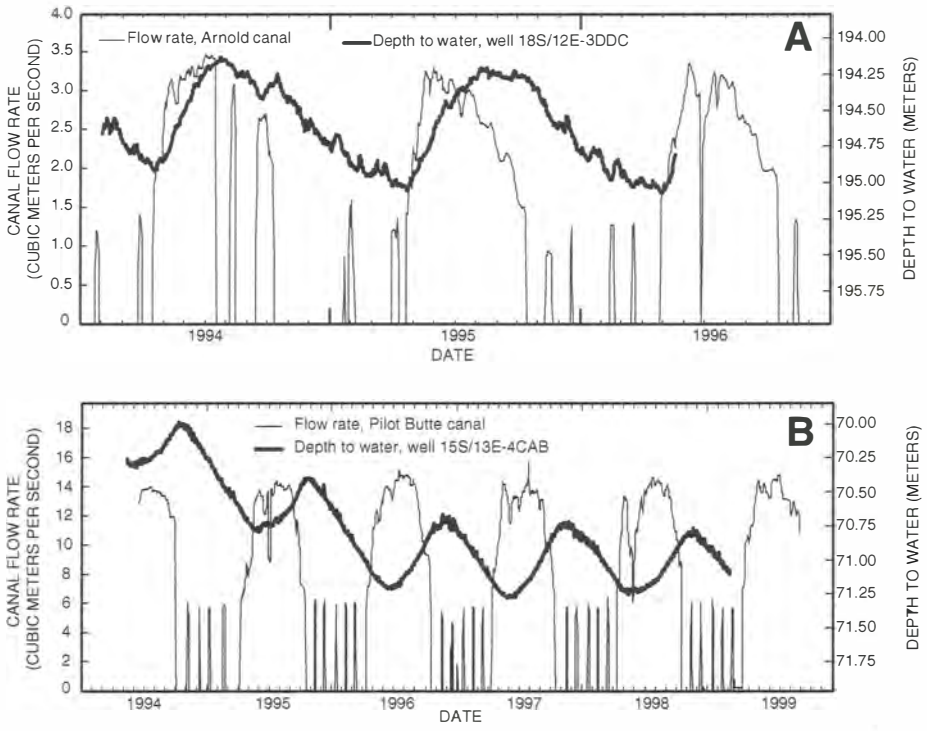

Figure 36. Hydrographs showing the relation between groundwater fluctuations and canal operation. (A) Well and canal water fluctuations in highly permeable late Quaternary lava flows at Bend. (B) Well and canal water fluctuations in early Pliocene and Miocene lava flows and sedimentary strata at Redmond. Modified from Gannett et al. (2001).

at an altitude of ~930 m, and depths to water range from 60 to 120 m depending on land-surface altitude and proximity to the river.

Directions to Stop 18

Return to O.B. Riley Road and continue north ~1 mi to Highway 20. Cross Highway 20 on to Cook Avenue in the town or Tumalo. Proceed north 10.3 mi on Cook Avenue (becomes Cline Falls Highway after a few blocks) to Oregon Highway 126. West (toward Sisters) 3.7 mi on Oregon Highway 126 to Buckhorn Road. North 4.2 mi on Buckhorn Road to Lower Bridge Road. East 1.6 mi to Deschutes River. Park just before crossing the bridge (south side).

Stop 18: Lower Bridge—Where Groundwater Meets the Deschutes River

Note: From Sherrod et al. (2002).

This stop is at the south side of the bridge on the left bank of the Deschutes River. It is about here where the Deschutes River has incised deeply enough to intercept the regional water table. Downstream from this point, the Deschutes River is below the regional water table, resulting in groundwater discharge to the river. Wells in the Lower Bridge area have static water levels coincident with river level.

Synoptic streamflow measurements (measurements gathered nearly simultaneously) (Fig. 37) show that the Deschutes River gains ~11.3 m^3/s from groundwater discharge between Lower Bridge and the stream gage just above Lake Billy Chinook near Culver. About one-quarter of this increase comes from groundwater discharge to the lower 3.2 km of Whychus Creek. Groundwater inflow is not uniform along the stream but emerges preferentially from permeable deposits such as coarse conglomerate and the fractured rhyodacite (Ferns et al., 1996b).

Exposures on the west side of the road provide easy access to ~24 m of the Deschutes Formation sedimentary and volcanic sequence (Fig. 38). In the middle one-third is the tuff of Lower Bridge, ~8.5 m here, a typical thickness. At the top of the exposure is the tuff of McKenzie Canyon. It is only 2.8 m thick, but its top is eroded. The tuff of McKenzie Canyon commonly is 6–10 m thick in this part of the basin. Both units were erupted from vents in the Cascade Range. Neither tuff has been dated, but both were emplaced between ~5.77 and 5.06 Ma on the basis of their position above the basalt of Opal Springs and beneath the basaltic andesite of Steamboat Rock (Table 3). A gamma log from a well ~1.3 km south of this exposure reflects the same stratigraphic section viewed at this stop (Fig. 39). The principal water-bearing unit in the well is the sand and gravel deposit 12–25 m below the tuff of Lower Bridge.

Two Pleistocene stratigraphic units are widespread in the Lower Bridge area and visible from this stop. Unconsolidated earthy white diatomite caps the bluff west of our stop and is also exposed in roadcuts along the highway grade east from here. The diatomite has been mined extensively from the now-abandoned quarry above the bluff. Basalt from Newberry volcano overlies the diatomite in several exposures.

The diatomite was once as thick as 20 m (Moore, 1937). Little of the original deposit remains, however, and the site is now mostly occupied by irregularly heaped overburden and waste from strip mining. Dominant diatom species are Stephanodiscus niagarae (K.E. Lohman in Moore, 1937) and S. excentricus (Smith et al., 1987), indicating a late Pliocene or Pleistocene age (Krebs et al., 1987). Volcanic ash bedded within the deposit has been tentatively correlated with the Loleta ash bed, the distal-fallout equivalent of Bend Pumice (Smith et al., 1987; A.M. Sarna-Wojcicki, 1995, oral commun.), which is thought to be ca. 0.4 Ma in age. An alternative correlation with a 1.9 Ma ash bed found in drill core from a well near Tulelake, California (T-749, 191 m depth; Rieck et al., 1992) is nearly as satisfactory on the basis of statistical comparison coefficients (A.M. Sarna-Wojcicki, 1995, oral commun.).

The age of the main diatomite body is probably middle Pleistocene, because the deposit fills a valley floor whose altitude is only slightly higher than the surface later mantled by basalt of Newberry volcano. Presumably the pre-diatomite erosional stage is only slightly older than the basalt. Although overlain by the basalt of Newberry volcano in roadcuts northeast of Lower Bridge, earlier Newberry lava flows may have dammed the ancestral Deschutes River to create the lake in which the diatomite was deposited (Smith, 1986a).

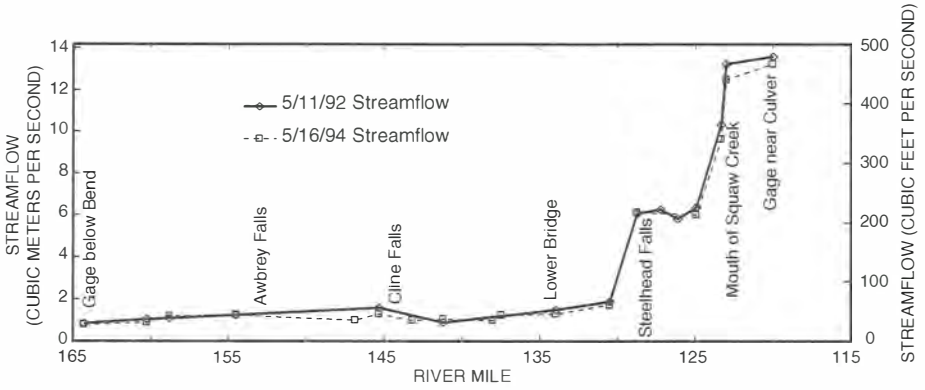

Figure 37. Graph showing gain in flow of the Deschutes River owing to groundwater discharge between river miles 165 and 120, May 1992 and May 1994. Modified from Gannett et al. (2001).

Directions to Stop 19

East 6.2 mi on Lower Bridge Road to U.S. Highway 97. North 2.4 mi on Highway 97 to wayside at Ogden scenic viewpoint. Pull into wayside, and then walk to old highway bridge, which is now a pedestrian walkway.

Stop 19. Peter Skene Ogden Bridge—Canyon-Filling Lava Flows

Note: From Sherrod et al. (2002).

Where U.S. Highway 97 crosses the Crooked River, middle Pleistocene basalt forms most of the canyon walls. These lava flows were erupted from vents on the north flank of Newberry volcano and flowed north across the broad plain extending to Redmond. The lava poured into the ancestral Crooked River canyon 9 km southeast of the Ogden bridge and flowed downstream beyond the bridge at least another 8 km—a distance of more than 55 km from the vent area. Lava flows also entered the Deschutes River and reached to Lake Billy Chinook, at least 65 km from vent.

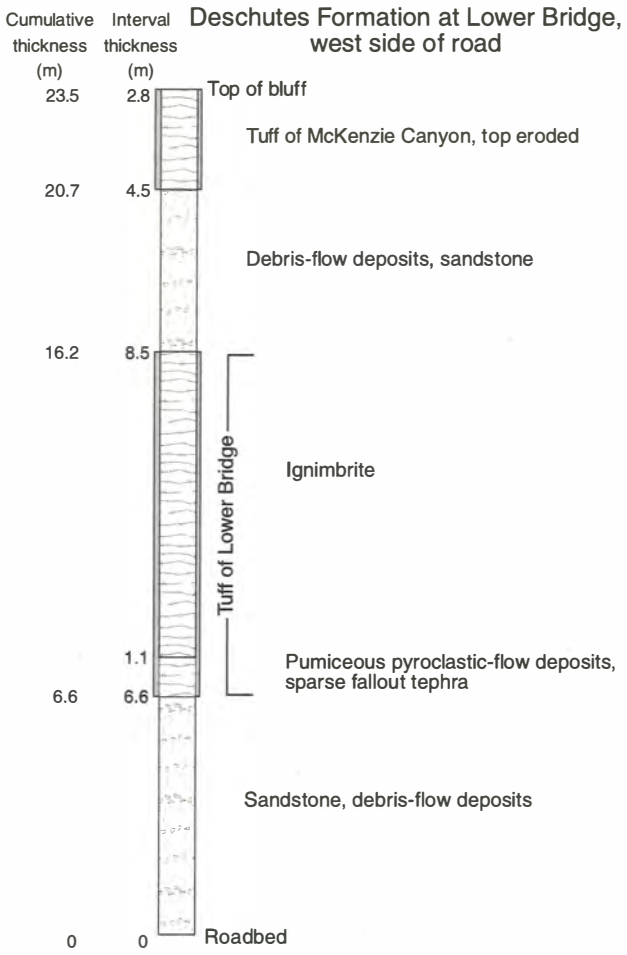

Figure 38. Stratigraphic section of the Lower Bridge area. From Sherrod et al. (2002).

The altitude of the Crooked River at the U.S. Highway 97 crossing is ~750 m. At this level, the Crooked River has incised to the depth of the regional water table. Synoptic streamflow measurements gathered in 1994 (Fig. 40) show the Crooked River gaining ~2 m^3/s from groundwater discharge between Trail Crossing, ~3.2 km upstream from the Highway 97 crossing, to Osborne Canyon, ~7.2 km downstream. Along the 11.2 km reach downstream between Osborne Canyon and the gage above Lake Billy Chinook, the river gains an additional 28 m^3/s, making this reach one of the principal groundwater discharge areas in the basin.

The hills to the east are underlain by southeast-dipping strata of the John Day Formation. They form the upthrown block of the Cyrus Springs fault zone (Smith et al., 1998). Rocks as young as the Prineville Basalt (15.8 Ma) were involved in the deformation, whereas the Deschutes Formation, the next youngest unit preserved, is undeformed. Thus the deformation occurred after early Oligocene and before late Miocene time. The deformation may be entirely middle or earliest late Miocene in age.

Rocks of the John Day Formation have low permeability because the tuffaceous material has devitrified to clay and other minerals. Lava flows within the formation are weathered and contain abundant secondary minerals. The John Day Formation acts as a barrier to regional groundwater flow. It and age-equivalent Cascade Range strata are considered the lower boundary of the regional flow system throughout much of the Deschutes Basin. The overlying middle Miocene Prineville Basalt is locally fractured, contains permeable interflow zones, and is used as a source of water in some places.

Directions to Stop 20

Return south 1.4 mi on U.S. Highway 97 to Wimp Way. West 0.3 mi on Wimp Way, which curves north to Ice Avenue. West 0.2 mi to 43rd Street. North 0.8 mi to a "T" intersection at Chinook Drive. West (then curves more or less north) 3.3 mi to Clubhouse Road. East and southeast 0.4 mi on Clubhouse Road past clubhouse and stores; park near chapel. Walk through parking lot for motel and hike into Crooked River canyon on a road that starts beyond the gate south of the motel parking lot. The road crosses private property. *Check at Crooked River Ranch office for information on access to the road through the gate. Alternatively, check with motel for permission to follow the fence line north to canyon rim, where the road is reached by an easy scramble. Watch for rattlesnakes.*

Stop 20: Crooked River Gorge at Crooked River Ranch

Note: From Sherrod et al. (2002).

This stop includes a walk into the Crooked River canyon on a dirt access road known colloquially as the Hollywood grade. Headworks for a flume system are preserved at the base of the grade. The term "Hollywood" stems from the use of this area

TABLE 3. POTASSIUM-ARGON AND $^{40}AR/^{39}AR$ ISOTOPIC AGES

Age (Ma)	Quality	Geologic unit or geographic location	Latitude (N)	Longitude (W)	Rock type	Material dated	Reference
Volcanic rocks of High Cascades or Basin and Range provinces							
0.093 ± 0.011	+	South Sister, early-erupted lava on northeast flank	44°08.29'	121°43.20'	Dacite	Whole rock	Hill and Duncan, 1990; Hill, 1992
0.61 ± 0.05	+	Gilchrist Butte	43°38.75'	121°39.15'	Basalt	Whole rock	Sherrod and Pickthorn, 1989
*1.19 ± 0.08	+	The Island, intracanyon flows in Crooked River	44°25.96'	121°14.48'	Basalt	Whole rock	Smith, 1986a
1.43 ± 0.33	+	Black Butte, 1 km northeast of summit	44°24.41'	121°37.53'	Basaltic andesite	Whole rock	Hill and Priest, 1992
2.33 ± 0.09	+	Walker Rim (east side, Chemult graben)	43°16.20'	121°44.05'	Basalt	Whole rock	Sherrod and Pickthorn, 1989
3.68 ± 3.3	–	Eaton Butte	43°38.6'	121°41.2'	Basalt	Whole rock	Fiebelkorn et al., 1983
Pliocene basalt and basaltic andesite							
2.9 ± 0.2	+	Summit, Squaw Back Ridge shield volcano	44°28.70'	121°28.59'	Basaltic andesite	Whole rock	Armstrong et al., 1975
*3.56 ± 0.30	+	Basalt of Redmond	44°23.20'	121°13.02'	Basalt	Whole rock	Smith, 1986a
Deschutes Formation							
3.97 ± 0.05	+	Basalt of Round Butte	44°37.29'	121°11.80'	Basalt	Whole rock	Smith, 1986a
4.7 ± 0.1	+	Deschutes Formation lava, near Bull Spring	44°06.63'	121°29.22'	Basaltic andesite	Whole rock	Hill, 1992
4.9 ± 0.4	+	Lava flow at top of Deep Canyon grade	44°17.38'	121°24.80'	Basaltic andesite	Whole rock	Armstrong et al., 1975
*5.06 ± 0.03	+	Basaltic andesite of Steamboat Rock, Deschutes Formation	44°21.45'	121°16.03'	Basaltic andesite	Whole rock	Smith, 1986a; Smith et al., 1987a
*5.31 ± 0.05	o	Basalt of Tetherow Butte	44°32.70'	121°15.07'	Basaltic andesite	Whole rock	Smith, 1986a
*5.43 ± 0.05	o	Basalt of Lower Desert	44°31.05'	121°18.57'	Basalt	Whole rock	Smith, 1986a
*5.77 ± 0.07	+	Basalt of Opal Springs, Deschutes Formation	44°26.11'	121°14.50'	Basalt	Whole rock	Smith, 1986a; Smith et al., 1987a
*6.14 ± 0.06	+	Rhyolite of Cline Buttes, Deschutes Formation	44°15.89'	121°17.50'	Rhyolite	Plagioclase	Sherrod et al., 2004
*6.74 ± 0.20	+	Rhyodacite SW of Steelhead Falls, Deschutes Formation	44°23.21'	121°22.44'	Rhyodacite	Plagioclase	Sherrod et al., 2004
*7.42 ± 0.22	+	Pelton Basalt	44°39.97'	121°12.10'	Basalt	Whole rock	Smith et al., 1987
John Day Formation							
*28.82 ± 0.23	+	Gray Butte rhyolite, basal vitrophyre	44°24.30'	121°06.79'	Rhyolite	Anorthoclase	Smith et al., 1998
28.3 ± 1.0	+	Powell Buttes dome	44°11.86'	120°58.03'	Rhyolite	Anorthoclase	Evans and Brown, 1981
*27.62 ± 0.63	+	West end of Haystack Reservoir, quarry	44°29.87'	121°09.37'	Welded tuff	Sanidine	Smith et al., 1998
*29.57 ± 0.17	+	West end of Haystack Reservoir, quarry	44°29.76'	121°09.36'	Welded tuff	Sanidine	Smith et al., 1998
*29.53 ± 0.09	+	West end of Haystack Reservoir, quarry	44°29.85'	121°09.28'	Hydromagmatic tuff	Sanidine	Smith et al., 1998

Note: Abridged from Sherrod et al. (2004) for ages discussed in the text.

for filming a 1967 motion picture, *The Way West,* starring Kirk Douglas. The destination of this stop is ~2.4 km downstream from the top of the road, where several springs emerge from the canyon walls. Springs occur intermittently from about river mile 13, just below Osborne Canyon, to Opal Springs, about river mile 6.7. These springs issue from the 5.77 Ma basalt of Opal Springs. The Crooked River gains over 28 m^3/s from groundwater discharge through springs in the basalt of Opal Springs in this reach. Most prolific of these is Opal Springs itself, which discharges from the base of the basalt on the east bank of the river. Discharge from this single spring is ~7–9 m^3/s (Stearns, 1931).

Isotope and temperature data (Table 2) indicate that the water from Opal Springs has followed a relatively long, deep flow path (Caldwell, 1997; James et al., 2000). The low tritium content indicates that the water was recharged prior to atmospheric testing of nuclear bombs in the early 1950s. Carbon and helium isotope data indicate that the water of Opal Springs contains a component of magmatic gas not present in many springs higher in the basin, such as those at North Davis Creek. Comparing the temperature of Opal Springs (12 °C) with the mean annual temperature at the altitude of recharge inferred from oxygen isotope measurements indicates considerable geothermal warming (James et al., 2000).

About 170 m of Deschutes Formation strata are exposed across the valley in the area of this stop. At the top is the basalt of Tetherow Butte, a spectacularly jointed sequence of tholeiitic basalt 45–60 m thick. In the lower one-third of the valley wall is the orange-weathering tuff of Osborne Canyon, 20–30 m thick (Fig. 41). At the base of the sequence is the basalt of Opal Springs. The Opal Springs unit is exposed through 28 m, but it continues into the subsurface in this area. The basalt of Opal Springs is as thick as 40 m elsewhere in the basin (Smith, 1986a).

This part of the Deschutes Formation was deposited in less than one million years. The basalt of Opal Springs, at the canyon floor, has an isotopic age of 5.77 ± 0.07 Ma (Table 3). The capping basalt of Tetherow Butte is probably younger than 5.04 Ma. It has an isotopic age of 5.31 ± 0.05 Ma (Table 3), but it possesses normal-polarity, thermal-remanent magnetization. An age younger than 5.04 Ma would agree with the currently accepted paleomagnetic timescale (Fig. 42).

Erosion along the ancestral Crooked River canyon has carved into and removed the basalt of Tetherow Butte and some underlying sedimentary beds from the area of our traverse. Quaternary intracanyon lava flows have invaded and partly refilled the inner canyon, creating the broad flat bench of Crooked River Ranch. The walk down the grade begins stratigraphically in the middle Pleistocene basalt of Newberry volcano, and then passes into sedimentary and volcanic strata of the Deschutes Formation (Fig. 41). The tuff of McKenzie Canyon, which we saw at Stop 19, is present partway down the grade. It is only 1–2 m thick and easily overlooked. Near the base of the grade is the prominent tuff of Osborne Canyon.

Directly beneath the tuff of Osborne Canyon is the basalt of Opal Springs. It comprises two lava-flow sequences, each containing several flows of open-textured olivine basalt. The two flow sequences are separated by 3–6 m of debris-flow deposits and other sedimentary beds. The isotopic age for the basalt of Opal Springs, 5.77 ± 0.07 Ma, came from lava in the lower sequence (Smith, 1986a).

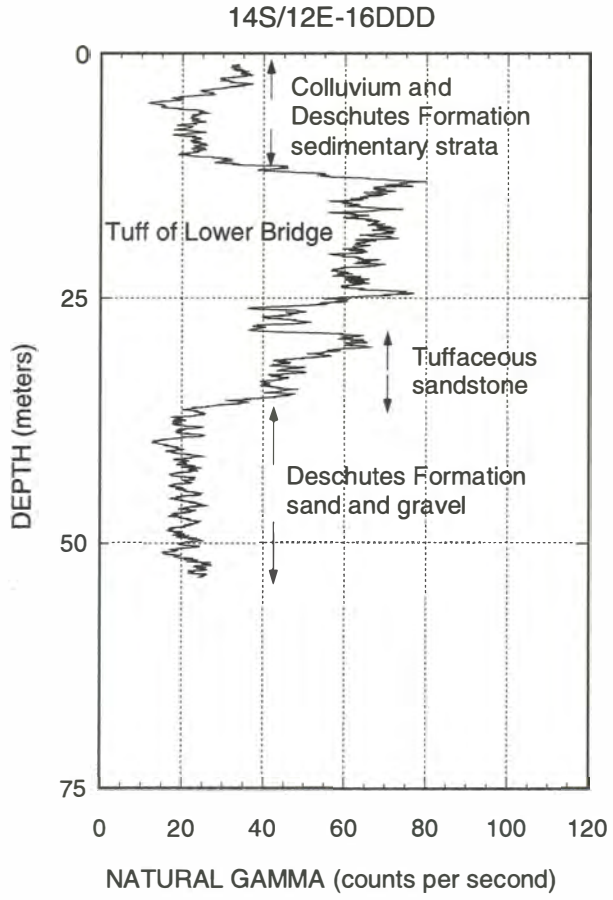

Figure 39. Natural gamma log and inferred stratigraphy in a well near Lower Bridge. From Sherrod et al. (2002).

Both the capping basalt of Newberry volcano and the stream-flooring basalt of Opal Springs possess normal-polarity, thermal-remanent magnetization. A third basalt sequence, with reversed-polarity magnetization, underlies the basalt of Newberry volcano at the base of Hollywood grade. Named the basalt of The Island for a prominent mesa at Cove Palisade State Park, it is lithologically similar to the basalt of Newberry volcano and the basalt of Opal Springs. It has an isotopic age of 1.19 ± 0.08 Ma (whole-rock, $^{40}Ar/^{39}Ar$; Smith, 1986a).

The basalt of The Island has been attributed to Newberry volcano (for example, Peterson et al., 1976; Smith, 1986a; Dill, 1992), but the unit cannot be traced farther south toward Newberry than the area near Crooked River Ranch. Thus, the upstream pathway for the reversed-polarity basalt must now be overlain entirely by normal-polarity basalt of Newberry volcano. An observation that may argue against a Newberry source is that the upper surface of these flows lies roughly at 730 m altitude in most locations (Dill, 1992; Ferns et al., 1996a), which would be unlikely if the lava were flowing downstream along its entire extent. An alternative explanation, therefore, is that the basalt of The Island was erupted from some yet-to-be-found fissure vent downstream from (north of) Crooked River Ranch and backed up along the Crooked River (Sherrod et al., 2004).

Directions to Stop 21

Return to U.S. Highway 97 by retracing route from Stop 10. North 8.5 mi on Highway 97 to Culver Road. East, then north, 2.6 mi on Culver Road to C Street in town of Culver. Signs from here help by pointing route toward The Cove Palisades State Park. West 1.0 mi on C Street to Feather Drive. North 0.9 mi on Feather Drive to Fisch Lane. West 0.5 mi on Fisch to where it turns north

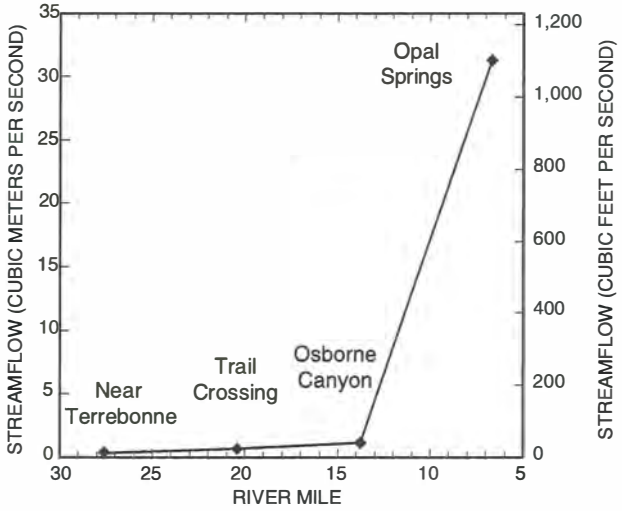

Figure 40. Graph showing gain in flow of the lower Crooked River owing to groundwater discharge between river miles 28 and 7, July 1994. Modified from Gannett et al. (2001).

and becomes Frazier. Follow Frazier 0.5 mi to intersection with Jordan Road. West on Jordan Road 0.3 mi to Mountainview (look for the sign to "view points"). North on Mountainview, following it 2.1 mi along rim of Crooked River canyon to third scenic view point on left. Failure to turn onto Mountainview will result in a geologically rewarding drive into Cove Palisades State Park.

Stop 21. Lake Billy Chinook Overlook

Note: From Sherrod et al. (2002).

Stop 21 provides a view of the Crooked and Deschutes river canyons just upstream of their confluence. The reservoir, Lake Billy Chinook, is impounded behind Round Butte Dam, which was completed in 1964. Our east-rim overlook is on the ca. 5 Ma basalt of Tetherow Butte (Smith, 1986a). Sedimentary rocks of the Deschutes Formation form most of the canyon walls. The far rim (west rim of Deschutes River canyon) is capped by the basalt of Lower Desert (Smith, 1986a). The basalt of Lower Desert has normal-polarity magnetization. Its isotopic age is 5.43 ± 0.05 Ma (Table 3), but its magnetization suggests that it, too, is ca. 5 Ma in age (Fig. 42). The narrow flat-topped ridge separating the Crooked and Deschutes Rivers is The Island, an erosional remnant of a reversely polarized 1.19 Ma intracanyon lava flow, the basalt of The Island. Our viewpoint rim is at an altitude of 786 m. The pool altitude is 593 m, and the canyon floor, now flooded, is ~488 m. A photograph taken from this same spot in August 1925 by Harold T. Stearns (Fig. 43A) provides a glimpse of the pre-reservoir exposures. In Figure 43B, the prominent lava flows at the base of the canyon belong to the 7.42 Ma Pelton Basalt Member, the lowest lava-flow member of the Deschutes Formation (Stearns, 1931; Smith, 1986a).

The Pelton Basalt Member is considered to be the base of the Deschutes Formation as defined by Smith (1986a). It comprises several lava flows of olivine tholeiite, some with thin sedimentary interbeds (Smith, 1986a). A dated flow within the Pelton Basalt Member has an age of 7.42 ± 0.22 Ma (Table 3). The Pelton Basalt is exposed today as far south as Round Butte Dam and was mapped another 6.4 km southward from the mouth of the Crooked River prior to impoundment of Lake Billy Chinook (Stearns, 1931). It is as thick as 30 m near Pelton Dam (Smith, 1987b).

As is the case for the basalt of Opal Springs, considerable groundwater discharges from springs in the Pelton Basalt Member. Stearns (1931) observed that the Pelton Basalt is the stratum from which springs issue in the lower Crooked River below about river mile 4, and along the Deschutes from its confluence with the

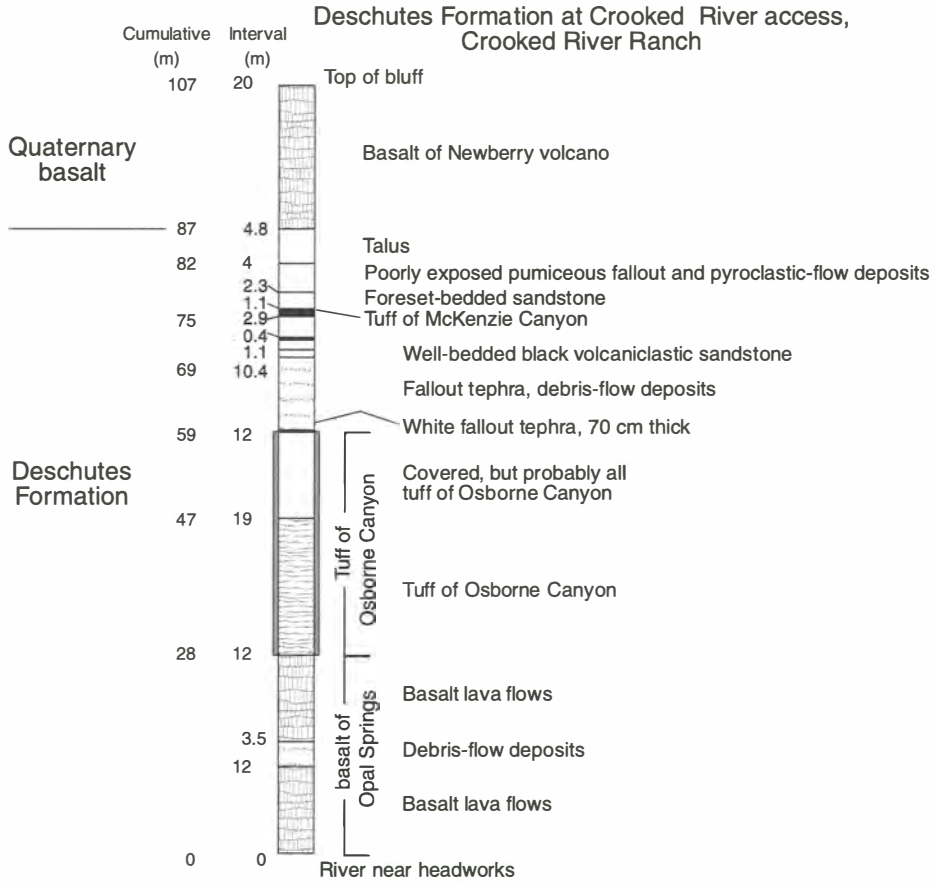

Figure 41. Stratigraphic section exposed along Hollywood grade in the Crooked River canyon near Crooked River Ranch. From Sherrod et al. (2002).

Crooked River to below the confluence with the Metolius River. He noted a large spring issuing from the Pelton Basalt in the forebay of the power plant that once existed ~1.6 km upstream of this point. He also documented a line of springs extending 1.2 km along the west bank of the Deschutes River, ~0.8 km upstream from the Metolius River, with an estimated discharge between 2.3 and 2.8 m^3/s. Groundwater discharge to Lake Billy Chinook is estimated from stream-gage data to be ~12 m^3/s, most probably from the Pelton Basalt (Gannett et al., 2001).

The Pelton Basalt Member extends in the subsurface south beyond its now-submerged exposure in the canyon. Wells drilled at river level near Opal Springs (river mile 6.7) penetrated the Pelton Basalt at a depth of ~110 m. The Pelton Basalt has proved to be a productive aquifer at this location. Wells encountered artesian pressures in the Pelton Basalt of ~50 psi at land surface and artesian flow rates up to 0.32 m^3/s (5000 gallons per minute).

The Pelton Basalt Member is the lowest sequence of lava in the Deschutes Formation, and although Smith (1987a, 1987b) maps a thin section of Deschutes Formation sediment underlying it, the Pelton Basalt is effectively the base of the permeable section in the Deschutes Formation. The Deschutes Formation contact with underlying units is exposed ~8 km north of this stop. By that point, most of the groundwater flowing from the upper basin in the Deschutes Formation has discharged to the river system. Depending on location, the Deschutes Formation may be seen in unconformable contact with the underlying middle Miocene Simtustus Formation or the upper Oligocene–lower Miocene John Day Formation. Mapping by Smith (1987a, 1987b) shows that the Simtustus Formation and Prineville Basalt typically separate the Deschutes and John Day Formations in the Deschutes River canyon. West of the canyon, the Deschutes Formation lies directly on the John Day Formation in many places.

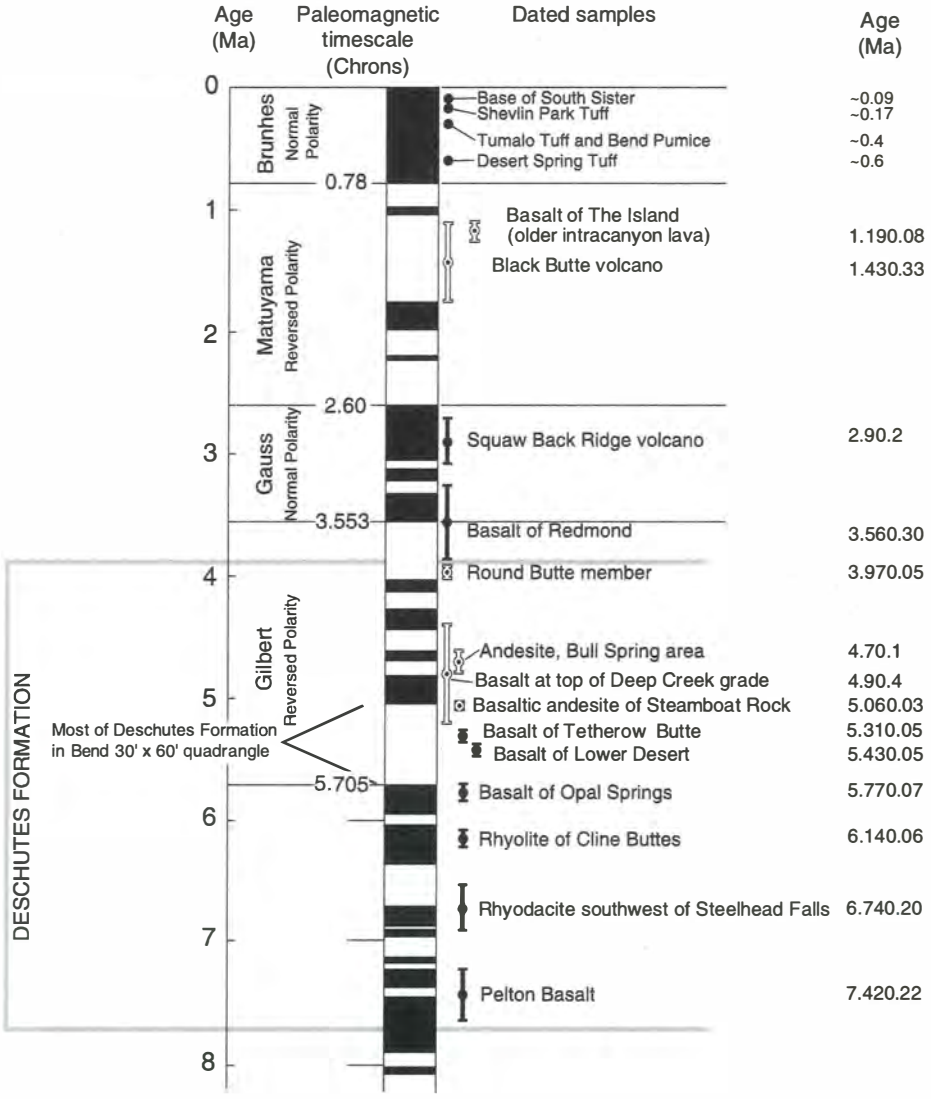

Figure 42. Correlation of selected dated samples with paleomagnetic timescale. Patterns show remanent magnetization: dark fill—normal polarity; white fill—reversed polarity. Bars showing age and standard deviation are similarly patterned. See Table 3 for references to age data. Remanent magnetization determined using portable fluxgate magnetometer. Timescale from Cande and Kent (1992). Figure from Sherrod et al. (2002).

The Simtustus Formation is a sequence of middle Miocene volcanogenic sandstone, mudstone, and tuff conformable on and interbedded with lava of the Prineville Basalt (Smith, 1986b). The Simtustus Formation, which is as thick as 65 m, was deposited across an area almost 20 km wide. Deposition was in response to drainage-system disruption by lava flows of the Columbia River Basalt Group and the Prineville Basalt (Smith, 1986b). The Simtustus Formation is exposed in areas ranging from the Deschutes River canyon to east of Gateway. Its hydrologic characteristics are unknown. Because of its location, limited areal extent, and relative thinness, it is thought to be a hydrologically insignificant stratigraphic unit.

The Prineville Basalt is a sequence of relatively evolved lava flows exposed sporadically across north-central Oregon. Of middle Miocene age, it includes flows with both normal- and reversed-polarity magnetization that are thought to have erupted during a short time period ca. 15.8 Ma when Earth's magnetic field was changing polarity from reversed to normal (Hooper et al., 1993). In the Deschutes Basin, the Prineville Basalt is as thick as 200 m. It is exposed east of Powell Buttes, east of Smith Rock, and along the Deschutes River from Pelton Dam downstream toward Cow Canyon, 20 km northeast of Gateway (Smith, 1986a). The Prineville Basalt may underlie the Deschutes Formation in much of the eastern half of the basin. Stratigraphic separation between the two formations is relatively small, depending on the thickness of intervening middle Miocene strata of the Simtustus Formation.

The hydrologic characteristics of the Prineville Basalt are poorly known. It is generally less permeable than the Deschutes Formation, and we know of no published reports of major springs issuing from the unit. It is, however, used locally as a source of water from domestic wells and a few irrigation wells.

About 13 km north of this location, just below Pelton Dam, the John Day Formation is exposed in the Deschutes River canyon. The John Day Formation in this area consists primarily of light-colored tuff, lapillistone, fine-grained volcanic sandstone, and mudstone (Smith, 1987a, 1987b). The John Day Formation has very low permeability and is considered the basement of the regional groundwater flow system (Sceva, 1968; Gannett et al., 2001). In contrast to the upper basin, little groundwater discharges to the Deschutes River downstream from the point where it intersects the John Day Formation. The John Day Formation can be observed at optional Stop 22.

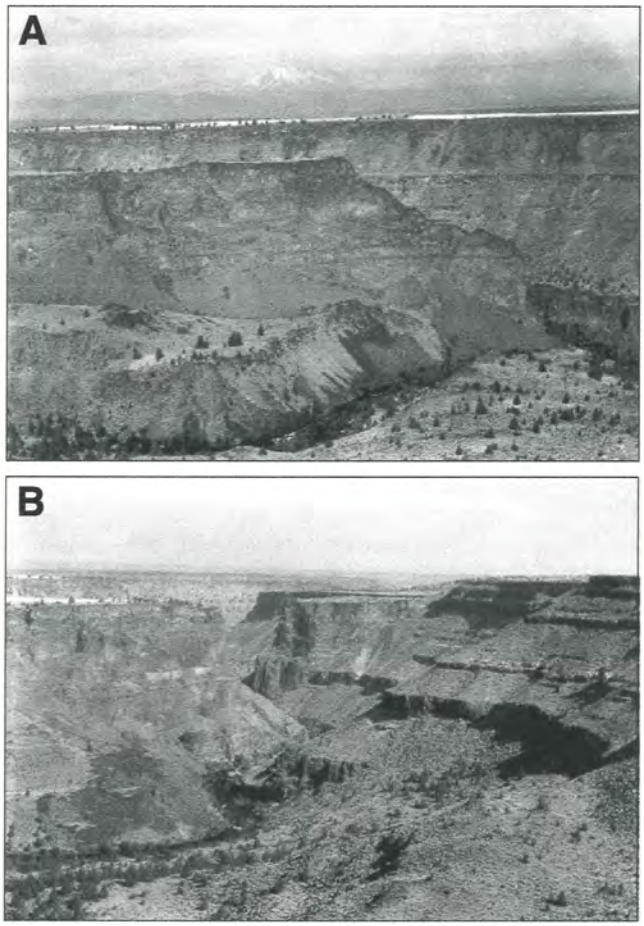

Figure 43. Photographs of the Crooked and Deschutes River canyons from the SE¼ sec. 35, T. 11 S., R. 12 E., taken by H.T. Stearns, August 1925, prior to inundation by Lake Billy Chinook (Stop 11). (A) View west across Crooked River canyon to The Island and, beyond it, the west rim of Deschutes River canyon. Deschutes-Crooked confluence is at right side of photograph in near ground. Mount Jefferson centered in background 45 km west-northwest. (B) View north (downstream) into Deschutes River canyon. Deschutes-Crooked confluence is at lower left edge of photograph. From Sherrod et al. (2002).

Directions to Optional Stop 22

Continue north on Mountainview ~2.2 mi to an intersection. Turn left and continue north on Mountainview 2.6 mi to a "T" intersection. Turn right on Belmont Lane and travel east 1.5 mi to Elk Drive. Left (north) on Elk Drive for 2.8 mi, where it turns left down into the canyon and becomes Pelton Dam Road. Follow Pelton Dam Road 6.8 mi north to its intersection with U.S. Highway 26. Turn left (north) on Highway 26 and go ~1.5 mi to where the canyon narrows. This is the stop. Highway 26 lacks pullouts in the area, and road shoulder is narrow. Use extreme caution, if disembarking to look at outcrops. A wayside and boat ramp ~0.7 mi north of this location provides an opportunity to examine the river.

Optional Stop 22. Deschutes River Canyon near Warm Springs

Note: From Sherrod et al. (2002).

At this location the John Day Formation forms the lower canyon walls on either side of the Deschutes River. These strata have limited permeability. The permeable strata of the Deschutes Formation are above the river at this point and thin abruptly northward. Virtually all of the regional groundwater flow has discharged to the Deschutes River and its tributaries upstream of

this point. During the summer months, virtually the entire flow of the Deschutes River at this location comes from groundwater discharge. Year-round, ~90% of the mean discharge of the Deschutes River here is attributable to groundwater. In the 160 km between here and the mouth of the river, the Deschutes gains very little water from groundwater discharge, and increases in flow are primarily from tributary streams.

ACKNOWLEDGMENTS

KVC acknowledges support from National Science Foundation grants EAR-207601 and EAR-207811. KVC and NID also wish to thank Rick Conrey, Nick Deardorff, Emily Johnson, Colin Long, and Daniele McKay for allowing us to use their unpublished data. We appreciate the help of NCALM, the Oregon LiDAR Consortium and EWEB for acquisition of LiDAR data along the upper McKenzie River. Much of the Deschutes Basin part of this guide was taken with little or no modification from an earlier guide one of us (MG) coauthored with Dave Sherrod (USGS) and Ken Lite (Oregon Water Resources Department), we gratefully acknowledge their generosity and immense contribution to this guide, as well as their substantial role in developing the present understanding of the geology and hydrology of the Cascade Range and central Oregon. In particular, we would like to acknowledge D. Sherrod for his thorough review of a first draft. This guide also benefitted from years of discussions with many others working in the region including Larry Chitwood, Kyle Gorman, Jonathan La Marche, Bob Main, and Rick Conrey. Finally, we give grateful thanks to Sarah Lewis for extensive and gracious assistance with field trip planning and manuscript preparation.

REFERENCES CITED

Allen, J.E., 1966. The Cascade Range volcanic-tectonic depression of Oregon. *in* Transactions of the Lunar Geological Field Conference, Bend, Oregon, August 1965: Oregon Department of Mineral Industries. p. 21–23.

Armstrong, R.L., Taylor, E.M., Hales, P.O., and Parker, D.J., 1975. K-Ar dates for volcanic rocks. central Cascade Range of Oregon: Isochron-West, no. 13, p. 5–10.

Blackwell, D.D., Bowen, R.G., Hull, D.A., Riccio, H., and Steele, J.L., 1982, Heat flow, arc volcanism, and subduction in northern Oregon: Journal of Geophysical Research, v. 87, no. B10, p. 8735–8754, doi: 10.1029/JB087iB10p08735.

Caldwell, R.R., 1997, Chemical study of regional ground-water flow and ground-water/surface-water interaction in the upper Deschutes Basin, Oregon: U.S. Geological Survey Water-Resources Investigations Report 97-4233, 49 p.

Cande, S.C., and Kent, D.V., 1992, A new geomagnetic polarity time scale for the Late Cretaceous and Cenozoic: Journal of Geophysical Research, v. 97, no. B10, p. 13,917–13,951, doi: 10.1029/92JB01202.

Champion, D.E., 1980. Holocene geomagnetic secular variation in the western United States: U.S. Geological Survey Open-File Report 80-824, 314 p.

Chitwood, L.A., Jensen, R.A., and Groh, E.A., 1977, The age of Lava Butte: Ore Bin, v. 39, no. 10, p. 157–164.

Conrey, R.M., Taylor, E.M., Donnelly-Nolan, J.M., and Sherrod, D.R., 2002, North-central Oregon Cascades: Exploring petrologic and tectonic intimacy in a propagating intra-arc rift, *in* Moore, G.W., ed., Field Guide to Geologic Processes in Cascadia: Oregon Department of Geology and Mineral Industries Special Paper 36, p. 47–90.

Dill, T.E., 1992, Stratigraphy of the Neogene volcanic rocks along the lower Metolius River, Jefferson County, central Oregon [M.S. thesis]: Corvallis, Oregon State University, 343 p.

Dreher, D.M., 2004, Effects of input and redistribution processes on in-stream wood abundance and arrangement in Lookout Creek, western Cascades Range, Oregon [M.S. thesis]: Corvallis, Oregon, Oregon State University, 143 p.

Evans, S.H., and Brown, F.H., 1981. Summary of potassium/argon dating—1981: U.S. Department of Energy, Division of Geothermal Energy DE-AC07-80-ID-12079-45, 29 p.

Faustini, J.M., 2001, Stream channel response to peak flows in a fifth-order mountain watershed [Ph.D. thesis]: Corvallis, Oregon, Oregon State University, 339 p.

Ferns, M.L., Stensland, D.E., and Smith, G.A., 1996a, Geologic map of the Steelhead Falls quadrangle, Deschutes and Jefferson Counties, Oregon: Oregon Department and Geology and Mineral Industries Geological Map Series GMS-101, scale 1:24,000.

Ferns, M.L., Lite, K.E., Jr., and Clark, M.D., 1996b, Lithologic controls on groundwater discharge to the Deschutes River between Lower Bridge and Lake Billy Chinook, central Oregon: Geological Society of America Abstracts with Programs, v. 28, no. 5, p. 65.

Fiebelkorn, R.B., Walker, G.W., MacLeod, N.S., McKee, E.H., and Smith, J.G., 1983, Index to K-Ar age determinations for the State of Oregon: Isochron-West, no. 37, p. 3–60.

Fisher, R.V., and Schmincke, H.-U., 1984, Pyroclastic Rocks: Springer-Verlag: Berlin, 472 p.

Gannett, M.W., and Lite, K.E., Jr., 2004, Simulation of regional ground-water flow in the upper Deschutes Basin, Oregon: U.S. Geological Survey Water-Resources Investigations Report 03-4195, 84 p.

Gannett, M.W., Lite, K.E., Jr., Morgan, D.S., and Collins, C.A., 2001, Groundwater hydrology of the upper Deschutes Basin, Oregon: U.S. Geological Survey Water Resources Investigation Report 00-4162, 77 p.

Gannett, M.W., Manga, M., and Lite, K.E., Jr., 2003, Groundwater hydrology of the upper Deschutes Basin and its influence on streamflow, *in* O'Connor, J.E., and Grant, G.E. eds., A Peculiar River—Geology, Geomorphology, and Hydrology of the Deschutes River, Oregon: American Geophysical Union: Water Science and Application, v. 7, p. 31–49.

Grant, G.E., 1997, A geomorphic basis for interpreting the hydrologic behavior of large river basins, *in* Laenan, A., and Dunnette, D., eds., River Quality, Dynamics and Restoration: New York, CRC Press, p. 105–116.

Grant, G.E., and Swanson, F.J., 1995, Morphology and processes of valley floors in mountain streams, western Cascades, Oregon, *in* Costa, J.E., et al., eds., Natural and Anthropogenic Influences in Fluvial Geomorphology: the Wolman Volume: American Geophysical Union, Geophysical Monograph 89, p. 83–101.

Grant, G.E., Swanson, F.J., and Wolman, M.G., 1990, Pattern and origin of stepped-bed morphology in high-gradient streams, Western Cascades, Oregon: Geological Society of America Bulletin, v. 102, p. 340–352, doi:10.1130/0016-7606(1990)102<0340:PAOOSB>2.3.CO;2.

Hildreth, W., 2007, Quaternary magmatism in the Cascades: Geologic perspectives. U.S. Geological Survey Professional Paper 1744, 136 p.

Hill, B.E., 1992, Petrogenesis of compositionally distinct silicic volcanoes in the Three Sisters region of the Oregon Cascade Range: The effects of crustal extension on the development of continental arc silicic magmatism [Ph.D. thesis]: Corvallis, Oregon State University, 235 p.

Hill, B.E., and Duncan, R.A., 1990, The timing and significance of silicic magmatism in the Three Sisters region of the Oregon High Cascades: Eos (Transactions, American Geophysical Union), v. 71, no. 43, p. 1614.

Hill, B.E., and Priest, G.R., 1992, Geologic setting of the Santiam Pass area, central Cascade Range, Oregon, *in* Hill, B.E., ed., Geology and Geothermal Resources of the Santiam Pass Area of the Oregon Cascade Range, Deschutes, Jefferson, and Linn Counties, Oregon: Oregon Department of Geology and Mineral Industries Open-File Report O-92-3, p. 5–18.

Hooper, P.R., Steele, W.K., Conrey, R.M., Smith, G.A., Anderson, J.L., Bailey, D.G., Beeson, M.H., Tolan, T.L., and Urbanczyk, K.M., 1993, The Prineville Basalt, north-central Oregon: Oregon Geology, v. 55, no. 1, p. 3–12.

Hughes, S.S., and Taylor, E.M., 1986, Geochemistry, petrogenesis, and tectonic implications of central High Cascade mafic platform lavas: Geological Society of America Bulletin, v. 97, p. 1024–1036, doi: 10.1130/0016-7606(1986)97<1024:GPATIO>2.0.CO;2.

Ingebritsen, S.E., Sherrod, D.R., and Mariner, R.H., 1992, Rates and patterns of groundwater flow in the Cascade Range volcanic arc, and the effect on subsurface temperatures: Journal of Geophysical Research, v. 97, p. 4599–4627.

Ingebritsen, S.E., Mariner, R.H., and Sherrod, D.R., 1994, Hydrothermal systems of the Cascade Range, north-central Oregon: U.S. Geological Survey Professional Paper 1044-L, 86 p.

James, E.R., Manga, M., and Rose, T.P., 1999, CO_2 degassing in the Oregon Cascades: Geology, v. 27, no. 9, p. 823–826, doi: 10.1130/0091-7613(1999)027<0823:CDITOC>2.3.CO;2.

James, E.R., Manga, M., Rose, T.P., and Hudson, G.B., 2000, The use of temperature and the isotopes of O, H, C, and noble gases to determine the pattern and spatial extent of groundwater flow: Amsterdam, Journal of Hydrology, v. 237, p. 100–112, doi: 10.1016/S0022-1694(00)00303-6.

Jefferson, A., and Grant, G., 2003, Recharge areas and discharge of groundwater in a young volcanic landscape, McKenzie River, Oregon: Geological Society of America Abstracts with Programs, v. 35, no. 6, p. 373.

Jefferson, A., Grant, G., and Rose, T., 2006, Influence of volcanic history on groundwater patterns on the westslope of the Oregon High Cascades: Water Resources Research, v. 42, W12411, 15 p, doi: 10.1029/2005WR004812.

Jefferson, A., Grant, G., and Lewis, S., 2007, A river runs underneath it: Geological control of spring and channel systems and management implications, Cascade Range, Oregon, *in* Furniss, M.J., Clifton, C.F., and Ronnenberg, K.L., eds., Advancing the Fundamental Sciences: Proceedings of the Forest Service National Earth Sciences Conference: Portland, Oregon, PNW-GTR-689: U.S. Department of Agriculture, Forest Service, Pacific Northwest Research Station, p. 391–400.

Jefferson, A., Nolin, A., Lewis, S., and Tague, C., 2008, Hydrogeologic controls on streamflow sensitivity to climatic variability: Hydrological Processes, v. 22, p. 4371–4385, doi: 10.1002/hyp.7041.

Jensen, R., 2006, Roadside guide to the geology and history of Newberry Volcano: Bend, The Press Pros, 182 p.

Johnson, D.M., Petersen, R.R., Lycan, D.R., and Sweet, J.W., 1985, Atlas of Oregon lakes: Corvallis, Oregon State University Press, 317 p.

Johnson, E.R., Wallace, P.J., Cashman, K.V., Delgado Granados, H., and Kent, A.J.R., 2008, Magmatic volatile contents and degassing-induced crystallization at Volcán Jorullo, Mexico: Implications for melt evolution and the plumbing systems of monogenetic volcanoes: Earth and Planetary Science Letters, v. 269, p. 478–486, doi: 10.1016/j.epsl.2008.03.004.

Krebs, W.N., Bradbury, J.P., and Theriot, E., 1987, Neogene and Quaternary lacustrine diatom biochronology, western U.S.A: Palaios, v. 2, no. 5, p. 505–513, doi: 10.2307/3514621.

Lanphere, M.A., Champion, D.E., Christiansen, R.L., Donnelly-Nolan, J.M., Fleck, R.J., Sarna-Wojcicki, A.M., Obradovich, J.D., and Izett, G.A., 1999, Evolution of tephra dating in the western United States: Geological Society of America Abstracts with Programs, v. 31, no. 6, p. A73.

Lescinsky, D.T., and Fink, J.H., 2000, Lava and ice interaction at stratovolcanoes: Use of characteristic features to determine past glacial extents and future volcanic hazards: Journal of Geophysical Research, v. 105, p. 23,711–23,726, doi: 10.1029/2000JB900214.

Licciardi, J.M., Kurz, M.D., Clark, P.U., and Brook, E.J., 1999, Calibration of cosmogenic ^{3}He production rates from Holocene lava flows in Oregon, USA, and effects of the Earth's magnetic field: Earth and Planetary Science Letters, v. 172, p. 261–271, doi: 10.1016/S0012-821X(99)00204-6.

Lite, K.E., Jr., and Gannett, M.W., 2002, Geologic framework of the regional ground-water flow system in the Upper Deschutes Basin, Oregon: U.S. Geological Survey Water-Resources Investigations Report 02-4015, 44 p.

Luhr, J.F., and Simkin, T., 1993, Parícutin: The volcano born in a Mexican cornfield: Phoenix, Arizona, Geoscience Press, 427 p.

Lund, E.H., 1977, Geology and hydrology of the Lost Creek glacial trough: The Ore Bin, v. 39, no. 9, p. 141–156.

MacLeod, N.S., Sherrod, D.R., Chitwood, L.A., and Jensen, R.A., 1995, Geologic map of Newberry volcano, Deschutes, Klamath, and Lake Counties, Oregon: U.S. Geological Survey Miscellaneous Investigations Series Map I-2215, scales 1:62,500 and 1:24,000.

Manga, M., 1996, Hydrology of spring-dominated streams in the Oregon Cascades: Water Resources Research, v. 32, no. 8, p. 2435–2440, doi: 10.1029/96WR01238.

Meinzer, O.C., 1927, Large springs in the United States: U.S. Geological Survey Water-Supply Paper 557, 94 p.

Moore, B.N., 1937, Nonmetallic mineral resources of eastern Oregon: U.S. Geological Survey Bulletin 875, 180 p.

Mote, P.W., 2003, Trends in snow water equivalent in the Pacific Northwest and their climatic causes: Geophysical Research Letters: v. 30, no. 12, p. 1601, doi: 10.1029/2003GL017258.

Mote, P.W., Hamlet, A.F., Clark, M., and Lettenmaier, D.P., 2005, Declining mountain snowpack in western North America: Bulletin of the American Meteorological Society, v. 86, no. 1, p. 39–49, doi: 10.1175/BAMS-86-1-39.

Nakamura, F., and Swanson, F.J. 1993, Effects of coarse woody debris on morphology and sediment storage of a mountain stream system in western Oregon: Earth Surface Processes and Landforms, v. 18, p. 43–61.

Nolin, A.W., and Daly, C., 2006, Mapping "at-risk" snow in the Pacific Northwest, U.S.A.: Journal of Hydrometeorology, v. 7, p. 1164–1173, doi: 10.1175/JHM543.1.

O'Connor, J.E., Sarna-Wojcicki, A., Wozniak, K.C., Polette, D.J., and Fleck, R.J., 2001a, Origin, extent, and thickness of Quaternary geologic units in the Willamette Valley, Oregon: U.S. Geological Survey Professional Paper 1620, 52 p.

O'Connor, J.E., Hardison, J.H., III, and Costa, J.E., 2001b, Debris flows from failures of Neoglacial-age moraine dams in the Three Sisters and Mount Jefferson Wilderness areas, Oregon: U.S. Geological Survey Professional Paper 1606, 93 p.

Peterson, N.V., Groh, E.A., Taylor, E.M., and Stensland, D.E., 1976, Geology and mineral resources of Deschutes County, Oregon: Oregon Department of Geology and Mineral Industries Bulletin 89, 66 p.

Pioli, L., Erlund, E., Johnson, E., Cashman, K., Wallace, P., Rosi, M., and Delgado Granados, H., 2008, Explosive dynamics of violent Strombolian eruptions: The eruption of Parícutin volcano 1943–1952 (Mexico): Earth and Planetary Science Letters, v. 271, p. 359–368, doi: 10.1016/j.epsl.2008.04.026.

Redmond, K.T., 1990, Crater Lake climate and lake level variability, *in* Drake, E.T., Larson, G.L., Dymond, J., and Collier, R., eds., Crater Lake: An Ecosystem Study: San Francisco, California, American Association for the Advancement of Science, p. 127–141.

Rieck, H.J., Sarna-Wojcicki, A.M., Meyer, C.E., and Adam, D.P., 1992, Magnetostratigraphy and tephrochronology of an upper Pliocene to Holocene record in lake sediments at Tulelake, northern California: Geological Society of America Bulletin, v. 104, no. 4, p. 409–428, doi: 10.1130/0016-7606(1992)104<0409:MATOAU>2.3.CO;2.

Russell, I.C., 1905, Geology and water resources of central Oregon: U.S. Geological Survey Bulletin 252, 138 p.

Saar, M.O., and Manga, M., 2004, Depth dependence of permeability in the Oregon Cascades inferred from hydrogeologic, thermal, seismic, and magmatic modeling constraints: Journal of Geophysical Research, v. 109, 19 p. B04204, doi: 10.1029/2003JB002855.

Sarna-Wojcicki, A.M., Meyer, C.E., Nakata, J.K., Scott, W.E., Hill, B.E., Slate, J.L., and Russell, P.C., 1989, Age and correlation of mid-Quaternary ash beds and tuffs in the vicinity of Bend, Oregon, *in* Scott, W.E., Gardner, C.A., and Sarna-Wojcicki, A.M., eds., Guidebook for Field Trip to the Mount Bachelor–South Sister–Bend area, central Oregon High Cascades: U.S. Geological Survey Open-File Report 89-645, p. 55–62.

Sceva, J.E., 1968, Liquid waste disposal in the lava terrane of central Oregon: U.S. Department of the Interior, Federal Water Pollution Control Administration, Technical Projects Branch Report No. FR-4, 66 p.

Schick, J.D., 1994, Origin of compositional variability of the lavas at Collier Cone, High Cascades, Oregon: Eugene, University of Oregon, 142 p.

Schmidt, M.E., and Grunder, A.L., 2009, The evolution of North Sister: A volcano shaped by extension and ice in the central Oregon Cascade arc: Geological Society of America Bulletin, v. 121, p. 643–662, doi: 10.1130/B26442.1.

Scott, W.E., 1977, Quaternary glaciation and volcanism, Metolius River area, Oregon: Geological Society of America Bulletin, v. 88, p. 113–124, doi: 10.1130/0016-7606(1977)88<113:QGAVMR>2.0.CO;2.

Scott, W.E., 1987, Holocene rhyodacite eruptions on the flanks of South Sister volcano, Oregon, in Fink, J.H., ed., The emplacement of silicic domes and lava flows: Geological Society of America Special Paper 212, p. 35–53.

Scott, W.E., 1990, Temporal relations between eruptions of the Mount Bachelor volcanic chain and fluctuations of late Quaternary glaciers: Oregon Geology, v. 52, p. 114–117.

Scott, W.E., and Gardner, C.A., 1992, Geologic map of the Mount Bachelor volcanic chain and surrounding area, Cascade Range, Oregon: U.S. Geological Survey Miscellaneous Investigations Map I-1967, scale 1:50,000.

Sherrod, D.R., 1986, Geology, petrology, and volcanic history of a portion of the Cascade Range between latitudes 43–44 degrees N, central Oregon, U.S.A. [Ph.D. thesis]: Santa Barbara, University of California, Santa Barbara.

Sherrod, D.R., and Pickthorn, L.G., 1989, Some notes on the Neogene structural evolution of the Cascade Range in Oregon, *in* Muffler, L.J.P., Weaver, C.S., and Blackwell, D.D., eds., Geology, Geophysics, and Tectonic

Setting of the Cascade Range: U.S. Geological Survey Open-File Report 89-178, p. 351–368.

Sherrod, D.R., and Smith, J.G., 1990, Quaternary extrusion rates of the Cascade Range, northwestern United States and southern British Columbia: Journal of Geophysical Research, v. 95, no. 19, p. 465–474.

Sherrod, D.R., Gannett, M.W., and Lite, K.E., Jr., 2002, Hydrogeology of the upper Deschutes Basin, central Oregon—A young basin adjacent to the Cascade volcanic arc, *in* Moore, G.E., ed., Field Guide to Geologic Processes in Cascadia: Oregon Department of Geology and Mineral Industries Special Paper 36, p. 109–144.

Sherrod, D.R., Taylor, E.M., Ferns, M.L., Scott, W.E., Conrey, R.M., and Smith, G.A., 2004, Geologic map of the Bend 30- by 60-minute quadrangle, central Oregon: U.S. Geological Survey Miscellaneous Investigations Map I-2683, scale 1:100,000.

Smith, G.A., 1986a, Stratigraphy, sedimentology, and petrology of Neogene rocks in the Deschutes Basin, central Oregon: A record of continental-margin volcanism and its influence on fluvial sedimentation in an arc-adjacent basin [Ph.D. thesis]: Corvallis, Oregon State University, 467 p.

Smith, G.A., 1986b, Simtustus Formation: paleogeographic and stratigraphic significance of a newly defined Miocene unit in the Deschutes Basin, central Oregon: Oregon Geology, v. 48, no. 6, p. 63–72.

Smith, G.A., 1987a, Geologic map of the Seekseequa Junction and a portion of the Metolius Bench quadrangles, Jefferson County, Oregon: Oregon Department of Geology and Mineral Industries Geological Map Series GMS-44, scale 1:24,000.

Smith, G.A., 1987b, Geologic map of the Madras West and Madras East quadrangles, Jefferson County, Oregon: Oregon Department of Geology and Mineral Industries Geological Map Series GMS-45, scale 1:24,000.

Smith, G.A., Snee, L.W., and Taylor, E.M., 1987, Stratigraphic, sedimentologic, and petrologic record of late Miocene subsidence of the central Oregon High Cascades: Geology, v. 15, no. 5, p. 389–392, doi: 10.1130/0091-7613(1987)15<389:SSAPRO>2.0.CO;2.

Smith, G.A., Manchester, S.R., Ashwill, M., McIntosh, W.C., and Conrey, R.M., 1998, Late Eocene–early Oligocene tectonism, volcanism, and floristic change near Gray Butte, central Oregon: Geological Society of America Bulletin, v. 110, no. 6, p. 759–778, doi: 10.1130/0016-7606(1998)110<0759:LEEOTV>2.3.CO;2.

Stearns, H.T., 1929, Geology and water resources of the upper McKenzie Valley, Oregon: U.S. Geological Survey Water-Supply Paper 597-D, 20 p.

Stearns, H.T., 1931, Geology and water resources of the middle Deschutes River basin, Oregon: U.S. Geological Survey Water-Supply Paper, v. 637-D, p. 125–212.

Strong, M., and Wolff, J., 2003, Compositional variations within scoria cones: Geology, v. 31, p. 143–146, doi: 10.1130/0091-7613(2003)031<0143:CVWSC>2.0.CO;2.

Swanson, F.J., and Jones, J.A., 2002, Geomorphology and hydrology of the H.J. Andrews Experimental Forest, Blue River, Oregon, *in* Moore, G.W., ed., Field guide to geologic processes in Cascadia: field trips to accompany the 98th annual meeting of the Cordilleran section of the Geological Society of America, Corvallis, Oregon: Portland, Oregon, Oregon Department of Geology and Mineral Industries Special Paper 36, p. 288–314.

Tague, C., and Grant, G.E., 2004, A geological framework for interpreting the low flow regimes of Cascade streams, Willamette River Basin, Oregon: Water Resources Research, v. 40, no. W04303, doi: 10.1029/2003WR002629.

Tague, C., and Grant, G.E., 2009, Groundwater dynamics mediate low flow response to global warming in snow-dominated alpine regions: Water Resources Research, v. 45, W07421, doi: 10.1029/2008WR007179.

Tague, C., Farrell, M., Grant, G., Choate, J., and Jefferson, A., 2008, Deep groundwater mediates streamflow response to climate warming in the Oregon Cascades: Climatic Change, v. 86, p. 189–210, doi: 10.1007/s10584-007-9294-8.

Taylor, E.M., 1965, Recent volcanism between Three Fingered Jack and North Sister, Oregon Cascade range: The Ore Bin, v. 27, p. 121–147.

Taylor, E.M., 1968, Roadside Geology, Santiam and McKenzie Pass Highways, Oregon, *in* Dole, H.M., ed., Andesite Conference Guidebook: Portland, Oregon, Department of Geology and Mineral Industries, p. 3–33.

Taylor, E.M., 1981, Central High Cascade roadside geology, *in* Johnston, D.A., and Donnelly-Nolan, J.M., eds., Guides to some volcanic terranes in Washington, Idaho, Oregon, and northern California: U.S. Geological Survey Circular 838, p. 55–83.

Taylor, E.M., 1990, Sand Mountain, Oregon and Belknap, Oregon, *in* Wood, C.A., and Kienle, J., eds., Volcanoes of North America (United States and Canada): Cambridge, Cambridge University Press, p. 180–183.

Taylor, E.M., and Ferns, M.L., 1994, Geology and mineral resource map of the Tumalo Dam quadrangle, Deschutes County, Oregon: Oregon Department of Geology and Mineral Industries Geological Map Series GMS-81, scale 1:24,000.

U.S. Reclamation Service, 1914, Deschutes Project: Oregon Cooperative Work, Department of the Interior, U.S. Reclamation Service [now Bureau of Reclamation] in cooperation with the State of Oregon, folio including 147 p. text and 79 sheets.

Walker, G.P.L., 1973, Explosive volcanic eruptions—A new classification scheme: International Journal of Earth Sciences, v. 62, no. 2, p. 431–446, doi: 10.1007/BF01840108.

Walker, G.W., and MacLeod, N.S., 1991, Geologic map of Oregon: U.S. Geological Survey, 2 sheets, 1:500,000 scale.

Whiting, P.J., and Moog, D.B., 2001, The geometric, sedimentologic, and hydrologic attributes of spring-dominated channels in volcanic areas: Geomorphology, v. 39, p. 131–149, doi: 10.1016/S0169-555X(00)00103-3.

Whiting, P.J., and Stamm, J., 1995, The hydrology and form of spring-dominated channels: Geomorphology, v. 12, p. 223–240.

Wilcox, R.E., 1954, Petrology of Paricutin Volcano Mexico: U.S. Geological Survey Bulletin, 965-C, p. 281–353.

Williams, H., 1976, The ancient volcanoes of Oregon: Condon Lectures: Eugene, University of Oregon Press, 70 p.

Winch, M.T., 1984–1985, Tumalo—Thirsty land: Oregon Historical Quarterly, v. 85, no. 4, p. 341–374; v. 86, no. 1, p. 47–79, no. 2, p. 153–182, no. 3, p. 269–297.

Manuscript Accepted by the Society 22 July 2009

Printed in the USA